KINETIC THEORY OF THE SPATIAL AND SPECTRAL COUPLING OF THE REACTOR NEUTRON FIELD

By
ROBERT GIFFORD COCKRELL

A DISSERTATION PRESENTED TO THE GRADUATE COUNCIL OF
THE UNIVERSITY OF FLORIDA
IN PARTIAL FULFILLMENT OF THE REQUIREMENTS FOR THE
DEGREE OF DOCTOR OF PHILOSOPHY

UNIVERSITY OF FLORIDA
August, 1965

To Mike, David and Donny

ACKNOWLEDGMENT

The author expresses his sincere appreciation to his teachers and fellow students for their encouragement and assistance during the preparation of this dissertation.

Appreciation is extended to the members of the author's graduate committee for their guidance. In particular the author is grateful for having studied under the direction of a very remarkable gentleman, Dr. R. B. Perez, the chairman of his graduate committee. The author also appreciates the assistance of Dr. M. J. Ohanian who unofficially assumed the duties of chairman for two months during the absence of Dr. Perez.

Mr. A. F. Henry and Mr. S. Kaplan of the Bettis Atomic Power Laboratory made several very useful comments regarding the theory presented in this dissertation, and Mr. C. W. Nestor, Jr. of Oak Ridge National Laboratory aided the author by assisting with computer calculations performed on the CDC-1604 computer at ORNL.

Several institutions gave financial assistance for the development of this work. The author was granted an Atomic Energy Commission Special Fellowship in Nuclear Science and Engineering during three years of graduate school. Five hours of time on the CDC-1604 computer at ORNL was granted by the Mathematics Division of ORNL.

Most of the computations were performed on the University of Florida IBM-709 computer. Approximately one-third of the work was supported by the Computing Center.

The author appreciates the invaluable assistance of Miss Barbara Gyles and gives all the credit for the very neat and orderly appearance of the thesis to her. The excellent drawings were executed by Mr. Dick Schoessow.

Without the assistance and companionship of his wife, Bobbye, the author would have found this work much more trying. He is truly grateful.

TABLE OF CONTENTS

Page

ACKNOWLEDGMENTS iii

LIST OF TABLES vi

LIST OF FIGURES viii

ABSTRACT. ix

Chapter

I. INTRODUCTION 1

II. THEORY 7

III. MULTIGROUP DIFFUSION THEORY FORMULATION OF COUPLED KINETICS PARAMETERS 51

IV. SPACE-TIME ANALYSIS OF THE PULSED NEUTRON-BEAM EXPERIMENT IN A REACTOR WITH WEAKLY COUPLED FUEL REGIONS 63

V. A DISCUSSION OF COMPUTER CALCULATIONS AND A SUMMARY OF THE RESULTS 89

VI. SUMMARY AND CONCLUSIONS 139

APPENDIX 144

LIST OF REFERENCES 156

BIOGRAPHICAL SKETCH 161

LIST OF TABLES

Table Page

1. Summary of Results 83

2. Thermal Neutron Parameters as Determined From Various Die-Away Experiments in Graphite 86

3. Buckling Values Used in Group Constant Calculations 110

4. Group-Dependent Values of the Transverse Buckling Obtained From the TWENTY GRAND Computations 120

5. Values of the Decay Constant for the Prompt Neutron Die-Away 122

6. Kinetics Parameters for a 2-Region and a 3-Region Representation of the UFTR 123

7. Kinetics Parameters for a 2-Region, 2-Group Representation of the UFTR 124

8. Kinetics Parameters for a 3-Region, 2-Group Representation of the UFTR 125

9. Recommended Buckling Values for Future Calculations 128

10. Denominator of the Expression on the Right-Hand Side of Equation (5.34) . . 135

A-1. Atom Densities for the UFTR (Tho 61) With 20 Per Cent U-235 Fuel 145

A-2. Group Boundaries by Energy and by Lethargy 146

A-3. Values of the Diffusion Constant for 18 Groups 147

LIST OF TABLES (continued)

Table Page

A-4. Values of the Absorption Cross-Section for 18 Groups 148

A-5. Values of Nu*Sigma Fission and Chi for 18 Groups 149

A-6. Values of the Total Scattering Cross-Section for 18 Groups 150

A-7. Average Inverse Speed for 18 Groups 154

A-8. Average Energy for 18 Groups 155

LIST OF FIGURES

Figure Page

1. One-Dimensional Representation of a Reactor With Two Coupled Fuel Regions 65

2. Flow Diagram of Several of the Computer Codes Used in the Theoretical Computations 96

3. Schematic Drawing of the University of Florida Training Reactor 108

4. Group 1 Flux as Computed by the TWENTY GRAND Code 115

5. Group 2 Flux as Computed by the TWENTY GRAND Code 116

6. Group 3 Flux as Computed by the TWENTY GRAND Code 117

7. Group 4 (Thermal) Flux as Computed by the TWENTY GRAND Code 118

8. Flux and Adjoint Flux for the Thermal Group as Computed by SAIM 130

9. Flux and Adjoint Flux Summed Over the Groups Above Thermal as Computed by SAIM . 131

10. Adjoint Weighted Flux for the Thermal Group 132

11. Adjoint Weighted Flux for the Neutrons Above Thermal 133

12. Flux in the UFTR as Computed by the SAIM Code; ϕ_i is the Flux Due to Neutrons Born in the i-th Region 137

Abstract of Dissertation Presented to the Graduate Council
in Partial Fulfillment of the Requirements for
the Degree of Doctor of Philosophy

KINETIC THEORY OF THE SPATIAL AND SPECTRAL COUPLING OF THE REACTOR NEUTRON FIELD

By

Robert Gifford Cockrell

August, 1965

Chairman: Dr. Rafael B. Perez
Major Department: Nuclear Engineering

A semidirect variational method is used to reduce the integro-differential form of the general Boltzmann neutron transport equation to a coupled set of first order ordinary time-dependent differential equations. The independent variables in this set of coupled equations are the amplitudes of the neutron flux within each arbitrarily specified spatial region of the core and/or within each arbitrarily specified energy group of the neutron spectrum.

A study is made to determine the accuracy of point-model kinetic theory in the prediction of the fundamental prompt neutron decay constant. The results of the study indicate that even the 1-point-model kinetics equation predicts the decay constant to within a few per cent of the exact value.

The results of flux calculations for the University of Florida Training Reactor are presented. The results include a set of 18-group cross-sections and graphs of 1- and 2-dimensional calculations of the flux. On the basis of 18-group, 1-dimensional flux calculations the effective delayed neutron fraction is 0.00703 and the mean prompt neutron generation time is 247.5 microseconds. Comparisons of theoretical calculations with experimental measurements show good agreement.

In connection with this work several computer codes were developed for use on the University of Florida IBM-709 computer. A brief discussion of these codes is given.

The coupled point-model representation of the reactor neutron field should find its greatest applicability in the study of transients and of the propagation of perturbations in a reactor with weakly coupled fuel regions.

CHAPTER I

INTRODUCTION

In a paper published in the Proceedings of the Second Geneva Conference J. C. Stewart made the observation that "in the analysis of certain types of critical multiplying systems, one fruitful approach to the determination of gross flux distributions lies in regarding the system as made up of several subcritical regions whose mutual interaction is sufficient to render the system as a whole critical" (Ste 58). The theory developed by Stewart was in terms of the coupling between regions containing fissile material. Stewart considered only the time-independent problem, but in the same proceedings R. Avery presented his "Theory of Coupled Reactors" (Ave 58a) in which he formulated a method for studying the kinetics of coupled reactors, where the term "coupled" is taken to mean that in each region of the reactor some of the fission neutrons are emitted in fissions induced by neutrons born in other regions.

Avery's theory presents a nodal approach to studying space-dependent kinetics problems. His method treats the system in terms of integral parameters which explicitly characterize the individual regions and the coupling between them. Avery used his theory of coupled reactors to predict the kinetic behavior of fast-thermal coupled systems (Ave 58b).

After studying Avery's work, the idea occurred to the author that his theory might also be useful for studying the kinetic behavior of the University of Florida Training Reactor (UFTR) which is an Argonaut-type reactor with a two-slab loading (Len 56, Dun 58). Experimentally, it has been found that a system of this type exibits a singly exponential stable period when off critical, but that there is a tendency for independent behavior of the two slabs (Bal 59). When an attempt was made to apply Avery's theory to the study of the kinetics of the UFTR several problems arose which resulted in an abandonment of the attempt. Three of the most serious problems are summarized below:

(1) The dependent variable in Avery's formulation is not a directly measurable quantity.

(2) The set of equations describing the kinetic behavior of the coupled system was formulated on the basis of physical arguments and is not derivable from first principles.

(3) The system may only be divided into regions which contain fissile material.

A further search of the literature revealed some notable work by Dougherty and Shen (Dou 61). In this work a semidirect variational method (Hil 52) is used to reduce the space- and time-dependent neutron diffusion equation to a consistent set of ordinary differential equations. In this analysis the neutron flux is expanded in a set of nonorthogonal space modes with time-dependent coefficients. This method is more properly termed a modal, as opposed to nodal, representation because the time-dependent parameters are modal amplitudes rather than nodal amplitudes. There is also a restriction in this approach. Each mode is defined according to the region where the neutrons represented by that mode originated. Each mode extends over all regions of the reactor. Since it is the response to local disturbances, either spatial or spectral, that is of interest in coupled systems, a method is needed for describing the coupling between configuration regions and energy groups in addition to the coupling between modes.

A method that has been widely used (Boy 64; Sea 64) to study the coupling between the fuel regions of weakly coupled cores is based on Baldwin's "Kinetics of a Reactor Composed of Two Loosely Coupled Cores" (Bal 59). In this method the two regions of the core are treated as separate subcritical assemblies with a small interaction. The interaction between the two regions is expressed very simply by a term containing a factor ε that gives the fraction of the flux in a given region at a time t that was in the other region at a time $t-\tau$, where τ is the delay time. The heuristic nature of this formulation has served to satisfy the needs of the experimentalist, but the ad hoc way in which the parameters ε and τ are introduced places limitations on the extension of this work to more complicated systems and makes ε and τ difficult to predict theoretically even for this simple system.

A more general nodal technique has been formulated by Kaplan, _et al_. (Kap 62). This technique consists of dividing the reactor volume into subregions in each of which the time behavior of some average flux is determined. Nodal equations are obtained by integrating the diffusion equations over each node.

All of the methods discussed above contain some useful features, but each contains undesirable restrictions. One notable restriction that has not yet been mentioned is that none of these methods allow a nodal representation of the energy-dependence as well as the space-dependence of the reactor neutron field. In the work presented in this dissertation a semidirect variational method is used to reduce the space-, energy-, angle-, and time-dependent integro-differential form of the Boltzmann neutron transport equation to a coupled set of ordinary first order time-dependent differential equations. This nodal representation of the neutron field is so general as to include the coupling between spatial regions and/or energy groups, and the flux used to compute the coupling parameters may be represented by any number of eigenmodes. All parameters appearing in this formulation are mathematically defined and are free from ad hoc restrictions. In its simplest form this formulation yields the familiar 1-point-model kinetics equation. For a system represented by one region, one group and several properly defined eigenmodes (see Chapter III), this formulation is equivalent to that of Dougherty and Shen (Dou 61); and for a system represented by one mode, one group, and several regions, this formulation is equivalent to that of Kaplan, et al. (Kap 62).

To facilitate the utilization of the general coupled kinetics formulation presented in Chapter II, the coupling parameters are given in terms of multigroup diffusion theory in Chapter III. In Chapter IV an analytic study of the space-dependent kinetics of a weakly coupled reactor is performed in order to compare values of the prompt neutron decay constant predicted by a space-time representation, a coupled 3-point representation, and a 1-point representation.

Chapter V presents a summary of the computer codes that were used to perform a computation of the group constants, flux, coupling parameters, and prompt neutron decay constant for the UFTR. Chapter V and the Appendix contain tables and graphs of reactor physics parameters for the UFTR.

CHAPTER II

THEORY

Introduction

A semidirect variational method (Hil 52) is used to derive a set of first-order ordinary differential equations, which describe the kinetics of a coupled-core reactor, from the integro-differential form of the general Boltzmann neutron transport equation (Wei 58). The independent variables in this set of coupled equations are the amplitudes of the neutron flux within each spatial region of the core and/or within each energy group of the neutron spectrum.

The equations developed in this chapter should be very useful for studying the kinetic behavior of cores with weakly coupled regions. To aid in the exposition of the theory a space- and energy-dependent transfer function is derived for a time varying localized perturbation.

The Most Fundamental Space-, Energy-, and Angular-Dependent Reactor Kinetics Equation

In terms of macroscopic phenomena the fundamental expression describing the kinetics of the reactor neutron field is the Boltzmann neutron transport equation. This equation describes the kinetics of the neutron field within each elemental volume of phase space. In terms of notation similar to that used by Weinberg and Wigner (Wei 58) the space-, angle-, energy-, and time-dependent integro-differential form of the neutron transport equation is given by:

$$\frac{1}{v(E)}\frac{\partial}{\partial t}\psi(\vec{r},E,\vec{\Omega},t) = \left\{\chi(E) - \sum_{i=1}^{D} \beta_i f_i\right\} P\psi(\vec{r},E',\vec{\Omega}',t) \; +$$

$$\sum_{i=1}^{D} \lambda_i f_i(E)\; c_i(\vec{r},t) + s(\vec{r},E,\vec{\Omega},t) \; +$$

$$T\psi(\vec{r},E',\vec{\Omega}',t) - \Omega\cdot\nabla\psi(\vec{r},E,\vec{\Omega},t) \; -$$

$$\Sigma_T(\vec{r},E)\;\psi(\vec{r},E,\vec{\Omega},t) \qquad (2.1)$$

The distribution of the precursor concentration, $c_i(\vec{r},t)$, for the i-th precursor group is described by:

$$\frac{\partial}{\partial t} c_i(\vec{r},t) = \beta_i P\psi(\vec{r},E',\vec{\Omega}',t) - \lambda_i c_i(\vec{r},t)$$

$$i = 1,2,\cdots,D \qquad (2.2)$$

The symbols are defined as follows:

$\psi(\vec{r},E,\vec{\Omega},t)$ = the angular flux (the number of neutrons per unit area per unit time per unit solid angle per unit energy in the volume element $d\vec{r}$ about $\vec{r}$, traveling within the solid angle $d\vec{\Omega}$ in the direction $\vec{\Omega}$, and having an energy in the range dE containing E at time t)

$$P\psi(\vec{r},E',\vec{\Omega}',t) = \int_{E'} dE' \int_{\vec{\Omega}'} d\vec{\Omega}' \; \nu(E')\Sigma_f(\vec{r},E')\psi(\vec{r},E',\vec{\Omega}',t)$$

$$T\psi(\vec{r},E',\vec{\Omega}',t) = \int_{E'} dE' \int_{\vec{\Omega}'} d\vec{\Omega}' \; \Sigma_S(\vec{r},E'\rightarrow E,\vec{\Omega}'\rightarrow\vec{\Omega})\psi(\vec{r},E',\vec{\Omega}',t)$$

$\Sigma_f(\vec{r},E)$ = the macroscopic fission cross-section for neutrons at position $\vec{r}$ with energy E

$\nu(E)$ = the mean number of neutrons resulting from a fission caused by a neutron with the energy E

$\Sigma_S(\vec{r},E'\rightarrow E,\vec{\Omega}'\rightarrow\vec{\Omega})$ = the macroscopic scattering cross-section at position $\vec{r}$ for changing the energy and direction $E',\vec{\Omega}'$ into an energy and direction range dE, $d\vec{\Omega}$ about $E,\vec{\Omega}$

$\chi(E)$ = the fission spectrum for all neutrons, both prompt and delayed

$f_i(E)$ = the energy frequency function, or spectrum, of the neutrons emitted by the i-th precursor group

$\Sigma_T(\vec{r},E)$ = the total macroscopic collision cross-section for neutrons at position $\vec{r}$ with energy E

$c_i(\vec{r},t)$ = the concentration of the i-th precursor group at point $\vec{r}$ and time t

λ_i = the decay constant of the i-th precursor group

β_i = the fraction of fission neutrons that are emitted by the i-th precursor group

$\vec{\Omega}\cdot\nabla$ = the leakage operator (operates on $\psi(\vec{r},E,\vec{\Omega},t)$ to give the rate of change of the angular flux with respect to space variable $\vec{r}$ in the direction $\vec{\Omega}$)

$s(r,E,\vec{\Omega},t)$ = the number of neutrons (per unit time per unit energy per unit solid angle per unit volume at $\vec{r}$,E, and $\vec{\Omega}$) at time t from an external source

Implicit in the formulation of Eqs. (2.1) and (2.2) is the assumption that the precursors do not diffuse, which limits this treatment to fixed fuel reactors. It appears that Eqs. (2.1) and (2.2) are also limited to reactors with only one fissile isotope; however, reactors with several fissile isotopes are included if the production operator is written in the form:

$$\chi(E)P\psi(\vec{r},E',\vec{\Omega}',t) = \sum_j \chi^j(E) \int_{E'} dE' \int_{\vec{\Omega}'} d\vec{\Omega}' \, \nu^j(E') \cdot$$

$$\Sigma_f^j(\vec{r},E')\psi(\vec{r},E',\vec{\Omega}',t)$$

and

$$\beta_i f_i(E)P\psi(\vec{r},E',\vec{\Omega}',t) = \sum_j \beta_i^j f_i^j(E) \int_{E'} dE' \int_{\vec{\Omega}'} d\Omega' \nu^j(E') \cdot$$

$$\Sigma_f^j(\vec{r},E')\psi(\vec{r},E',\vec{\Omega}',t)$$

where j refers to some j-th fissile isotope, and the i-th precursor group is assumed to be the same for all species.

The boundary conditions for Eqs. (21.) and (2.2) are the usual ones (Meg 60) but are stated here for later reference:

(1) The flux, and likewise the precursor concentrations, must be finite and nonnegative for all points in phase space except possibly at a finite number of source points

(2) The flux $\psi(\vec{r}+\epsilon\vec{\Omega},E,\vec{\Omega},t)$ must be a continuous function of ϵ for all values of $\vec{\Omega}$, E, and t

(3) At a vacuum interface (the outermost boundary of a system) there must be no neutrons returning to the reactor from any direction in the vacuum

Because of the complexity of Eqs. (2.1) and (2.2) the problems for which exact solutions may be found are few in number and apply to ideal systems. In order to analyze problems that arise in practice it is necessary to make simplifying assumptions. In the study of reactor kinetics one such assumption is that the neutron field has the same time-dependence in each elemental volume of phase space for all values of $\vec{r},E,\vec{\Omega}$. This assumption permits one to write the function representing the angular flux in a separated form as follows:

$$\psi(\vec{r},E,\vec{\Omega},t) = \phi(\vec{r},E,\vec{\Omega})T(t) \qquad (2.3)$$

There are many methods, both numerical and analytical for obtaining approximate solutions to the steady state flux, $\phi(\vec{r},E,\vec{\Omega})$. The steady state flux along with its adjoint $\phi^{\dagger}(\vec{r},E,\vec{\Omega})$ is then used to reduce the transport equation to a first order ordinary differential equation with $T(t)$ as the dependent variable. This equation is the familiar point-model reactor kinetics equation (Shu 61). The derivation of the point-model equation is discussed in great detail by Henry (Hen 55) and therefore will not be given here. In the derivation of the coupled kinetics equations given in the next section the assumption of separability is less restrictive since it only requires the separability of time and phase space over a subspace of the domain containing the reactor neutron field.

Derivation of the Coupled Kinetics Equations

The derivation which follows is based on a semi-direct variational method (Hil 52). This method consists of varying the functional after substituting and integrating the trial functions over the domain of all but a single variable. It is assumed that the distribution of the angular flux is known at steady state. The purpose of using the variational method is to determine the "best" approximating function for the time-dependence of the flux. By definition the "best" approximating function is that trial function which makes the functional a minimum. A problem arises regarding the minimizing of the functional because the variational principle is not a maximum or minimum principle but rather it is an extremum principle. Sometimes it is possible to study the second-order variation of the functional to determine if the trial function produces a maximum or a minimum, but this approach is extremely difficult for very complicated problems. This fact, however, is of no importance as regards the derivation of the equations of motion, since only the extremum condition is used (Lan 60). Usually, it is possible to tell from the physical situation whether the extremum is a maximum or a minimum.

In the derivation which follows it should be noted that the presentation will be entirely formal; any questions of existence or uniqueness are assumed to be resolved on the basis of physical considerations. Selengut's "Variational Analysis of Multi-Dimensional Systems" (Sel 59) is an excellent reference for a more detailed discussion of the variational principle as applied to reactor physics.

Equations (2.1) and (2.2) may be written in the form (Per 62):

$$H\vec{\Psi} = V^{-1} \frac{\partial}{\partial t} \vec{\Psi} - \vec{S} \qquad (2.4)$$

where

$$\tilde{\vec{\Psi}} = [\psi(\vec{r},E,\vec{\Omega},t)\;\; c_1(\vec{r},t)\;\cdots\; c_i(\vec{r},t)\;\cdots\; c_D(\vec{r},t)] \tag{2.5}$$

$$\tilde{\vec{S}} = [s(\vec{r},E,\vec{\Omega},t)\quad 0\quad \cdots\quad 0\quad \cdots\quad 0\quad]\,. \tag{2.6}$$

The symbol "~" indicates the transpose of the vector.

$$H = \left|\begin{array}{cc} \{\chi(E) - \sum_{i=1}^{D} \beta_i f_i\}\frac{P}{\lambda} + T - \vec{\Omega}\cdot\nabla - \Sigma_T & \lambda_1 f_1 \cdots \lambda_i f_i \cdots \lambda_D f_D \\ \beta_1 f_1 P/\lambda & -\lambda_1 f_1 \cdots\; 0\; \cdots\; 0 \\ \vdots & \\ \beta_D f_D P/\lambda & 0\; \cdots\; 0\; \cdots -\lambda_D f_D \end{array}\right| \tag{2.7}$$

The parameter λ has been inserted in the matrix represented by H to insure the existence of a solution for the homogeneous case. In general there is an infinite set of the eigenvalues represented by λ with a corresponding set of eigenfunctions.

The symbol V^{-1} represents the diagonal matrix given by

$$V^{-1} = \text{diag}\,[\,\frac{1}{v}\;\; f_1 \cdots\; f_i \cdots\; f_D] \tag{2.8}$$

The Lagrangian formulation of a variational principle for the equation given by Eq. (2.4) is:

$$L(\vec{\Psi}^{\dagger},\vec{\Psi}) = \int_{0}^{\infty} dt \int_{R} d\vec{r} \int_{E} dE \int_{\vec{\Omega}} d\vec{\Omega}\vec{\Psi}^{\dagger} \, [V^{-1} \frac{\partial}{\partial t} \vec{\Psi}-H\vec{\Psi}-\vec{S}] \tag{2.9}$$

where

$$\vec{\Psi}^{\dagger} = [\Psi^{\dagger}(\vec{r},E,\Omega,t) \;\; c_{1}^{\dagger}(\vec{r},E,t) \cdots c_{i}^{\dagger}(\vec{r},E,t) \cdots c_{D}^{\dagger}(\vec{r},E,t)$$

The condition that the first variation of the functional $L(\vec{\Psi}^{\dagger},\vec{\Psi})$ be an extremum with respect to small variations in the functions $\vec{\Psi}^{\dagger}$ and $\vec{\Psi}$ yields an expression for the weighting function as follows:

$$\delta L(\delta\vec{\Psi}^{\dagger},\delta\vec{\Psi}) = \int_{0}^{\infty} dt \int_{R} d\vec{r} \int_{E} dE \int_{\vec{\Omega}} d\vec{\Omega} \, \Big\{\delta\vec{\Psi}^{\dagger} \, [V^{-1} \frac{\partial}{\partial t} \vec{\Psi}-H\vec{\Psi}-\vec{S}] \; +$$

$$\vec{\Psi}^{\dagger}[V^{-1} \frac{\partial}{\partial t} \delta\vec{\Psi} - H\delta\vec{\Psi}]\Big\} \tag{2.10}$$

By definition of the adjoint operator (Sel 59) the last term in Eq. (2.10) may be rearranged to yield

$$(\vec{\Psi}^{\dagger},H\delta\vec{\Psi}) = (\delta\vec{\Psi},\tilde{H}^{\dagger}\tilde{\vec{\Psi}}^{\dagger}) \tag{2.11}$$

where $H^{\dagger}$ is the adjoint of the matrix H. The parenthesis notation indicates integration over phase space. The adjoint operator $H^{\dagger}$ is given by:

$$H^{\dagger} = \begin{vmatrix} \left[\left\{\chi(E) - \sum_{i=1}^{D} \beta_i f_i\right\} \frac{P}{\lambda}\right]^{\dagger} + T^{\dagger} + \vec{\Omega}\cdot\nabla - \Sigma_T & [\beta_1 f_1 P/\lambda]^{\dagger} & \cdots & [\beta_D f_D P/\lambda]^{\dagger} \\ \lambda_1 f_1 & -\lambda_1 f_1 & 0 \cdots & 0 \\ \vdots & \vdots & & \vdots \\ \lambda_D f_D & 0 & 0 \cdots & -\lambda_D f_D \end{vmatrix} \tag{2.12}$$

where

$$\left[\left\{\chi(E) - \sum_{i=1}^{D} \beta_i f_i(E)\right\} \frac{P}{\lambda}\right]^{\dagger} \psi^{\dagger} = \frac{\nu(E)\,\Sigma_f(\vec{r},E)}{\lambda} \int dE' \int d\vec{\Omega}' \cdot \left\{\chi(E') - \sum_{i=1}^{D} \beta_i f_i(E')\right\} \psi^{\dagger}(\vec{r},E',\vec{\Omega}',t) \tag{2.13}$$

and

$$T^{\dagger}\psi^{\dagger}(\vec{r},E',\vec{\Omega}',t) = \int_{E'} dE' \int_{\vec{\Omega}'} d\Omega' \; \Sigma_s(\vec{r},E\rightarrow E',\vec{\Omega}\rightarrow\vec{\Omega}')\,\psi^{\dagger}(\vec{r},E',\vec{\Omega}',t)$$

An integration by parts of the next to last term of Eq. (2.10) yields:

$$\int_0^\infty dt \int_R d\vec{r} \int_E dE \int_{\vec{\Omega}} d\vec{\Omega}\ \vec{\Psi}^\dagger\ V^{-1} \frac{\partial}{\partial t} \delta\vec{\Psi} = \int_R d\vec{r} \int_E dE \int_{\vec{\Omega}} d\vec{\Omega} \ \cdot$$

$$[\vec{\Psi}^\dagger V^{-1} \delta\vec{\Psi}]_{t=0}^{\infty} \quad - \quad (\delta\tilde{\vec{\Psi}},\ V^{-1} \frac{\partial}{\partial t} \bar{\vec{\Psi}}^\dagger) \tag{2.14}$$

The requirement that the first variation of $\vec{\Psi}$ vanish at the end points of the time domain causes the first term on the right hand side of Eq. (2.14) to vanish. Inserting Eqs. (2.11) and (2.14) into Eq. (2.10) yields):

$$\delta L(\delta\vec{\Psi}^\dagger, \delta\vec{\Psi}) = \int_0^\infty dt \int_R d\vec{r} \int_E dE \int_{\vec{\Omega}} d\vec{\Omega}\ \{\delta\vec{\Psi}^\dagger\ [V^{-1} \frac{\partial}{\partial t} \vec{\Psi} - H\vec{\Psi} - \vec{S}]\ -$$

$$\delta\ \vec{\Psi}\ [V^{-1} \frac{\partial}{\partial t} \bar{\vec{\Psi}}^\dagger + \bar{H}^\dagger \tilde{\vec{\Psi}}^\dagger]\} \tag{2.15}$$

The condition for an extremum is that

$$\delta L(\delta\vec{\Psi}^\dagger, \delta\vec{\Psi}) \ = \ 0$$

which requires that the integrand of Eq. (2.15) be zero. Since the variations $\delta\vec{\Psi}^\dagger$ and $\delta\vec{\Psi}$ are arbitrary and in general are not equal to zero except at the boundaries of the phase space spanning the reactor neutron field, then the coefficients of $\delta\vec{\Psi}^\dagger$ and $\delta\vec{\Psi}$ must vanish. This requirement yields Eq. (2.14) and Eq. (2.16). Equation (2.4) is repeated here for convenience.

$$H\vec{\Psi} = V^{-1}\frac{\partial}{\partial t}\vec{\Psi} - \vec{S} \tag{2.4}$$

$$\tilde{H}^{\dagger}\tilde{\vec{\Psi}}^{\dagger} = -V^{-1}\frac{\partial}{\partial t}\tilde{\vec{\Psi}}^{\dagger} \tag{2.16}$$

Thus, any trial function used to approximate $\vec{\Psi}$ will make the value of $L(\vec{\Psi}^{\dagger},\vec{\Psi})$ an extremum if the weighting function $\vec{\Psi}^{\dagger}$ satisfies Eq. (2.16) and the same boundary conditions as $\vec{\Psi}$. This latter point raises an interesting question regarding the boundary conditions to be placed on the time variable. The first order time derivative in Eqs. (2.4) and (2.16) permits only one boundary condition with respect to the time variable for each component of the vectors $\vec{\Psi}$ and $\vec{\Psi}^{\dagger}$. However, the requirement that $\vec{\Psi}^{\dagger}V^{-1}\delta\vec{\Psi}$ vanish at both limits of the time domain seems to imply that $\vec{\Psi}$ is known at $t=0$ and also at $t=\infty$. It will be shown that this is not correct, but that the condition that $\vec{\Psi}^{\dagger}V^{-1}\delta\vec{\Psi}\big|_{t=0}^{\infty}$ vanish is not valid.

Multiplying Eqs. (2.4) by $\vec{\Psi}^{\dagger}$ and Eq. (2.16) by $\tilde{\vec{\Psi}}$, integrating over all values of $t,E,\vec{\Omega}$ and $\vec{r}$, and subtracting Eq. (2.16) from Eq. (2.4) yields:

$$(\vec{\Psi}^{\dagger},H\vec{\Psi}) - (\tilde{\vec{\Psi}},\tilde{H}^{\dagger}\tilde{\vec{\Psi}}^{\dagger}) = (\vec{\Psi}^{\dagger},V^{-1}\frac{\partial}{\partial t}\vec{\Psi}) + (\tilde{\vec{\Psi}},V^{-1}\frac{\partial}{\partial t}\tilde{\vec{\Psi}}^{\dagger}) - (\vec{\Psi}^{\dagger},\vec{S}) \tag{2.17}$$

The left-hand side of Eq. (2.17) is identically zero; rearranging the remainder of Eq. (2.17) yields:

$$\frac{\partial}{\partial t}\,(\vec{\Psi}^{\dagger} V^{-1} \vec{\Psi}) = (\vec{\Psi}^{\dagger}, \vec{S}) \tag{2.18}$$

Equation (2.18) indicates that, if there is no external source, the product $\vec{\Psi}^{\dagger}\vec{\Psi}$ is invariant with respect to time. In other words, the adjoint weighted flux is conserved. Therefore, it is not necessary to know the flux precisely at both time limits to insure that $\vec{\Psi}^{\dagger} V^{-1} \delta\vec{\Psi}\Big|_{t=0}^{\infty}$ vanishes. If a source is present during some specified period of time, then the change in the adjoint weighted flux is given by Eq. (2.18).

There are numerous methods for obtaining time-independent approximations of the solutions for the sourceless, steady-state form of Eqs. (2.4) and (2.16). Therefore, in the derivation which follows, a time-independent solution is assumed to be known. The trial function to be used in the functional given by Eq. (2.9) is:

$$\vec{\Psi} = \sum_{n=1}^{M} \vec{\Psi}_n(\vec{r},E,\vec{\Omega},t) = \sum_{n=1}^{M} \Psi_n(\vec{r},E,\vec{\Omega}) N_{k_\gamma}^{(n)}(t) \tag{2.19}$$

and

$$\vec{\Psi}^{\dagger} = \sum_{m=1}^{M} \tilde{\vec{\Psi}}_m^{\dagger}(\vec{r},E,\vec{\Omega},t) = \sum_{m=1}^{M} \Psi_m^{\dagger}(\vec{r},E,\vec{\Omega}) \tilde{\vec{N}}_{k_\gamma}^{(m)\dagger}(t) \tag{2.20}$$

where

$N^{(n)}_{\substack{k\\ \gamma}}(t)$ = the amplitude of $\vec{\Psi}_n(\vec{r},E,\vec{\Omega},t)$ in region R_k and energy range E_γ for any direction $\vec{\Omega}$; the configuration space has been divided into K regions $R_1, R_2, \cdots, R_k, \cdots, R_K$ and the energy space has been divided into Γ groups $E_1, E_2, \cdots, E_\gamma, \cdots, E_\Gamma$

The components of $\vec{N}^{(n)}_{\substack{k\\ \gamma}}(t)$ and $\vec{N}^{(m)^{\dagger}}_{\substack{k\\ \gamma}}(t)$ are given by:

$$\vec{N}^{(n)}_{\substack{k\\ \gamma}}(t) = [N^{(n)}_{\substack{k\\ \gamma}}(t)\;\; C^{(n)}_{1,\substack{k\\ \gamma}}(t)\;\; \cdots\;\; C^{(n)}_{D,\substack{k\\ \gamma}}(t)] \tag{2.21}$$

$$\vec{N}^{(m)^{\dagger}}_{\substack{k\\ \gamma}}(t) = [N^{(m)^{\dagger}}_{\substack{k\\ \gamma}}(t)\;\; C^{(m)^{\dagger}}_{1,\substack{k\\ \gamma}}(t)\;\; \cdots\;\; C^{(m)^{\dagger}}_{D,\substack{k\\ \gamma}}(t)] \tag{2.22}$$

and the initial conditions are:

$$\vec{N}^{(n)}_{\substack{k\\ \gamma}}(0) = [\,1\;1\;\cdots\;1\,]$$

$$\vec{N}^{(m)^{\dagger}}_{\substack{k\\ \gamma}}(0) = [\,1\;1\;\cdots\;1\,]$$

for all values of k and γ. The quantities $\Psi_n(\vec{r},E,\vec{\Omega})$ and $\Psi^{\dagger}_m(\vec{r},E,\vec{\Omega})$ are diagonal matrices given as follows:

$$\Psi_n(\vec{r},E,\vec{\Omega}) = \mathrm{diag}\,[\phi_n(\vec{r},E,\vec{\Omega})\ c_{1,m}(\vec{r})\ c_{2,n}(\vec{r})\ \cdots\ c_{D,n}(\vec{r})] \tag{2.23}$$

$$\Psi^{\dagger}_m(\vec{r},E,\vec{\Omega}) = \mathrm{diag}\,[\phi^{\dagger}_m(\vec{r},E,\vec{\Omega})\ c^{\dagger}_{1,m}(\vec{r},E)\ c^{\dagger}_{2,m}(\vec{r},E)\ \cdots\ c^{\dagger}_{D,m}(\vec{r},E)] \tag{2.24}$$

The quantities $\Psi_n(\vec{r},E,\vec{\Omega})$ and $\Psi^{\dagger}_m(\vec{r},E,\vec{\Omega})$ satisfy the following equations and the boundary conditions specified earlier:

$$H_n \Psi_n \vec{\xi} = 0 \tag{2.25}$$

$$\tilde{H}^{\dagger}_m \tilde{\Psi}^{\dagger}_m \vec{\xi} = 0 \tag{2.26}$$

where

$$\tilde{\vec{\xi}} = [\,1\ 1\ \cdots\ 1\,]$$

and H_n is given by Eq. (2.7) for $\lambda=\lambda^{(n)}$ and $H^{\dagger}_m$ is given by Eq. (2.12) for $\lambda=\lambda^{(m)}$. The quantity $\lambda^{(i)}$ is the eigenvalue corresponding to the i-th eigenfunction of Eqs. (2.25) and (2.26).

The symbols used in Eqs. (2.21)-(2.24) have the following definitions:

$\phi_n(\vec{r},E,\vec{\Omega})$ = the n-th eigenmode of the angular flux at steady state

$\phi^{\dagger}_n(\vec{r},E,\vec{\Omega})$ = the adjoint of $\phi_n(\vec{r},E,\vec{\Omega})$

$c_{i,n}(\vec{r})$ = the n-th eigenmode of the precursor concentration distribution for the i-th precursor group

$c^{\dagger}_{i,n}(\vec{r},E)$ = the adjoint of $c_{i,n}(\vec{r})$. (Referring back to Eqs. (2.7) and (2.12), it is observed that $c^{\dagger}_{i,n}$ is energy-dependent although $c_{i,n}$ is not)

$N^{(n)}_{k\,\gamma}(t)$ = the amplitude of the n-th eigenmode of the angular flux in region R_k and group E_γ at time t

$N^{(n)\dagger}_{k\,\gamma}(t)$ = the amplitude of the n-th eigenmode of the adjoint angular flux in region R_k and group E_γ at time t

$C^{(n)}_{ik\,\gamma}(t)$ = the amplitude of the n-th eigenmode of the i-th precursor group concentration in region R_k and group E_γ at time t

$C^{(n)\dagger}_{ik\,\gamma}(t)$ = the amplitude of the n-th eigenmode of the adjoint to the i-th precursor group concentration in region R_k and group E_γ at time t

Before substituting the trial function into Eq. (2.9), the functional is written in the form:

$$L(\vec{\Psi}^{\dagger},\vec{\Psi}) = \int_0^{\infty} dt \sum_{k=1}^{K} \sum_{\gamma=1}^{\Gamma} \int_{R_k} d\vec{r} \int_{E_\gamma} dE \int_{\vec{\Omega}} d\vec{\Omega}\; \vec{\Psi}^{\dagger}[V^{-1} \frac{\partial}{\partial t} \vec{\Psi} - H\vec{\Psi} - \vec{S}] \tag{2.27}$$

In order to simplify the mathematical expressions the following parenthesis notation will be used:

$$(Gg,Ff)_{\substack{k\\ \gamma}} \equiv \int_{R_k} d\vec{r} \int_{E_\gamma} dE \int_{\vec{\Omega}} d\vec{\Omega}\, [Gg]\, [Ff] \tag{2.28}$$

where G is operating on g and F is operating on f. If either F or G is not specified, then it is taken to be the identity operator.

Substituting the trial function and its adjoint given by Eqs. (2.19) and (2.20) into Eq. (2.27) yields:

$$L(\vec{\Psi}^\dagger,\vec{\Psi}) = \int_0^\infty dt \sum_{k=1}^{K} \sum_{\gamma=1}^{\Gamma} \sum_{m=1}^{M} \sum_{n=1}^{N} (\vec{\Psi}^\dagger_m, V^{-1} \frac{\partial}{\partial t} \vec{\Psi}_n)_{\substack{k\\ \gamma}} -$$

$$(\vec{\Psi}^\dagger_m, H\vec{\Psi}_n)_{\substack{k\\ \gamma}} - (\vec{\Psi}^\dagger_m, \vec{S})_{\substack{k\\ \gamma}} \tag{2.29}$$

Assuming separability, within region R_k and group E_γ, yields for the first term in the integrand:

$$(\vec{\Psi}^\dagger_m, V^{-1} \frac{\partial}{\partial t} \vec{\Psi}_n)_{\substack{k\\ \gamma}} = \vec{N}^{(m)^\dagger}_{\substack{k\\ \gamma}}(t)\, A^{(m,n)}_{\substack{k\\ \gamma}} \frac{d}{dt} \vec{N}^{(n)}_{\substack{k\\ \gamma}}(t) \tag{2.30}$$

where $\vec{N}_{\substack{k\\ \gamma}}^{(m)^\dagger}$ and $\vec{N}_{\substack{k\\ \gamma}}^{(n)}$ are given by Eqs. (2.21) and (2.22) and $A^{(m,n)}_{\substack{k\\ \gamma}}$ is a diagonal matrix given by

$$A^{(m,n)}_{\substack{k\\ \gamma}} = \text{diag}\, [(\phi^\dagger_m, \frac{1}{v} \phi_n)_{\substack{k\\ \gamma}} (c^\dagger_{1,m}, f_1 c_{1,n})_{\substack{k\\ \gamma}} \cdots$$

$$(c^\dagger_{D,m}, f_D c_{D,n})_{\substack{k\\ \gamma}}] \tag{2.31}$$

In a similar manner the third term in the integrand of Eq. (2.29) may be written in the form:

$$(\vec{\Psi}^{\dagger}, \vec{S})_{\underset{\gamma}{k}} = \vec{N}^{(m)^{\dagger}}_{\underset{\gamma}{k}}(t)\ \vec{S}^{(m)}_{\underset{\gamma}{k}}(t) \tag{2.32}$$

where $\vec{S}^{(m)}_{\underset{\gamma}{k}}$ is a vector with (D+1) components:

$$\tilde{\vec{S}}^{(m)}_{\underset{\gamma}{k}}(t) = [(\phi^{\dagger}_{m}, s)_{\underset{\gamma}{k}}\quad 0 \cdots 0 \cdots 0\ ] \tag{2.33}$$

The symbol "s" in Eq. (2.33) was defined earlier and represents an external source of neutrons.

The second term in the integrand of Eq. (2.29) is somewhat more complicated than the other two terms. It is advantageous to consider it term by term. The only non-zero elements in the matrix H are the following ones:

$$h_{1,1} = \chi \frac{P}{\lambda} - \sum_{i=1}^{D} \beta_i f_i \frac{P}{\lambda} + T - \Omega \cdot \nabla - \Sigma_T \tag{2.34}$$

$$h_{1,\ i+1} = \lambda_i f_i \tag{2.35}$$

$$h_{i+1,\ 1} = \beta_i f_i P/\lambda \tag{2.36}$$

$$h_{i+1,\ i+1} = -\lambda_i f_i \tag{2.37}$$

for $i = 1, 2, \cdots, D$.

The only non-zero elements of the matrix represented by $(\vec{\Psi}_m^\dagger, H\vec{\Psi}_n)_{\substack{k\\ \gamma}}$ are given by

$$\text{element } (1,1) = (\chi\bar{\Phi}_m^\dagger, \frac{P}{\lambda}\,\bar{\Phi}_n)_{\substack{k\\ \gamma}} - \sum_{i=1}^{D} \beta_i (f_i\bar{\Phi}^\dagger, \frac{P}{\lambda}\,\bar{\Phi}_n)_{\substack{k\\ \gamma}} +$$

$$(\bar{\Phi}_m^\dagger, T\bar{\Phi}_n)_{\substack{k\\ \gamma}} - (\bar{\Phi}_m^\dagger, \vec{\Omega}\cdot\nabla\bar{\Phi}_n)_{\substack{k\\ \gamma}} - (\bar{\Phi}_m^\dagger, \Sigma_T\bar{\Phi}_n)_{\substack{k\\ \gamma}} \qquad (2.38)$$

$$\text{element } (1,\ i+1) = \lambda_i (\bar{c}_{i,m}^\dagger, f_i\bar{c}_{i,n})_{\substack{k\\ \gamma}} \qquad (2.39)$$

$$\text{element } (i+1,\ 1) = \beta_i (\bar{\Phi}_m^\dagger, f_i\,\frac{P}{\lambda}\,\bar{\Phi})_{\substack{k\\ \gamma}} \qquad (2.40)$$

$$\text{element } (i+1,\ i+1) = -\lambda_i (\bar{c}_{i,m}^\dagger, f_i\bar{c}_{i,n})_{\substack{k\\ \gamma}} \qquad (2.41)$$

for $i=1,2,\cdots,D$.

A bar over a function in Eqs. (2.38)-(2.41) indicates that the function is still time-dependent; that is, separability has not yet been assumed. Consider now the first term of Eq. (2.38):

$$(\chi\bar{\Phi}_m^\dagger, \frac{P}{\lambda}\,\bar{\Phi}_n)_k = \int_{R_k} d\vec{r} \int_{E_\gamma} dE \int_{\vec{\Omega}} d\vec{\Omega}\ \chi(E)\bar{\Phi}_m^\dagger(\vec{r},E,\vec{\Omega},t) \int_{E'} dE' \cdot$$

$$\int_{\vec{\Omega}} d\vec{\Omega}\ \nu(E')\Sigma_f(\vec{r},E')\bar{\Phi}_n(\vec{r},E',\vec{\Omega}',t) =$$

$$\sum_{\alpha=1}^{G} N_{\substack{k\\ \gamma}}^{(m)^{\dagger}}(t)\ \left(\chi\Phi_m^{\dagger},\ \frac{P_\alpha}{\lambda}\,\Phi_n\right)_{\substack{k\\ \gamma}} N_{\substack{k\\ \alpha}}^{(n)}(t) \tag{2.42}$$

where

$$P_\alpha\Phi_n = \int_{E'_\alpha} dE' \int_{\vec{\Omega}'} d\vec{\Omega}'\ \nu(E')\Sigma_f(\vec{r},E')\Phi_n(\vec{r},E,\vec{\Omega}') \tag{2.43}$$

It will prove useful later to write Eq. (2.42) in the following form:

$$\left(\chi\Phi_m^{\dagger},\ \frac{P}{\lambda}\,\Phi_m\right)_{\substack{k\\ \gamma}} = \sum_{\alpha=1}^{G} N_{\substack{k\\ \gamma}}^{(m)^{\dagger}}(t)\ \frac{\left(\Phi_m^{\dagger},\ \frac{1}{v}\,\Phi_n\right)_{\substack{k\\ \gamma}}}{\Lambda_{\substack{k\\ \alpha\to\gamma}}^{(m,n)}}\ N_{\substack{k\\ \alpha}}^{(n)}(t) \tag{2.44}$$

where

$$\Lambda_{\substack{k\\ \alpha\to\gamma}}^{(m,n)} = \frac{\left(\Phi_m^{\dagger},\ \frac{1}{v}\,\Phi_n\right)_{\substack{k\\ \gamma}}}{\left(\chi\Phi_m^{\dagger},\ \frac{P_\alpha}{\lambda}\,\Phi_n\right)_{\substack{k\\ \gamma}}} \tag{2.45}$$

The parameter $\Lambda_{\substack{k\\ \alpha\to\gamma}}^{(m,n)}$ refers to neutrons existing in the n-th eigenstate in region R_k and group E_α. It gives the average time for transfer from group E_α to group E_γ per neutron in group E_γ by means of regeneration. The averaging process is weighted with respect to the importance of this transfer to the m-th eigenstate.

The second term in Eq. (2.38) is similar to the first and may be written in the form:

$$\beta_i \left(f_i \phi_m^{\dagger}, \frac{P}{\lambda} \phi_n\right)_{\substack{k \\ \gamma}} = \sum_{\alpha=1}^{G} N_{\substack{k \\ \gamma}}^{(n)\dagger}(t) \frac{\beta_{\substack{i,k \\ \alpha\to\gamma}}^{(m,n)}}{\Lambda_{\substack{k \\ \alpha\to\gamma}}^{(m,n)}} \left(\phi_m^{\dagger}, \frac{1}{v} \phi_n\right)_{\substack{k \\ \gamma}} \cdot$$

$$N_{\substack{k \\ \alpha}}^{(n)}(t) \tag{2.46}$$

where

$$\beta_{\substack{i,k \\ \alpha\to\gamma}}^{(m,n)} = \frac{(f_i \phi_m^{\dagger}, P_\alpha \phi_n)_{\substack{k \\ \gamma}} \beta_i}{(\chi \phi_m^{\dagger}, P_\alpha \phi_n)_{\substack{k \\ \gamma}}} \tag{2.47}$$

and

$$\beta_{\substack{k \\ \alpha\to\gamma}}^{(m,n)} = \sum_{i=1}^{D} \beta_{\substack{i,k \\ \alpha\to\gamma}}^{(m,n)} \tag{2.48}$$

The parameter $\beta_{\substack{k \\ \alpha\to\gamma}}^{(m,n)}$ gives the effective delayed neutron fraction averaged over the spectrum of the neutrons in the n-th eigenstate in region R_k that are transferred from group E_α to group E_γ by regeneration.

The third term in Eq. (2.38) follows in similar fashion:

$$(\bar{\phi}_m^{\dagger}, T\bar{\Phi}_n)_{\substack{k \\ \gamma}} = \sum_{\alpha=1}^{\Gamma} N_{\substack{k \\ \gamma}}^{(m)\dagger} (\phi_m^{\dagger}, T_\alpha \phi_n)_{\substack{k \\ \gamma}} N_{\substack{k \\ \alpha}}^{(m)} \tag{2.49}$$

$$= \sum_{\alpha=1}^{\Gamma} N_{k_\gamma}^{(m)\dagger} \frac{(\phi_m^\dagger, \frac{1}{v}\phi_n)_{k_\gamma}}{\tau_{k_{\alpha\to\gamma}}^{(m,n)}} N_{k_\alpha}^{(n)} \tag{2.50}$$

where

$$\tau_{k_{\alpha\to\gamma}}^{(m,n)} = \frac{(\phi_m^\dagger, \frac{1}{v}\phi_n)_{k_\gamma}}{(\phi_m^\dagger, T_\alpha\phi_n)_{k_\gamma}} \tag{2.51}$$

and

$$T_\alpha\phi_n = \int_{E'_\alpha} dE' \int_{\vec{\Omega}'} d\vec{\Omega}' \; \Sigma_s(\vec{r},E'\to E,\vec{\Omega}'\to\vec{\Omega})\,\phi_n(\vec{r},E',\vec{\Omega}') \tag{2.52}$$

The parameter $\tau_{k_{\alpha\to\gamma}}^{(m,n)}$ refers to neutrons existing in the n-th eigenstate in region R_k and group E_α. It gives the average time for transfer from group E_α to group E_γ per neutron in group E_γ by means of scattering collisions.

The fourth term in Eq. (2.38) represents the following expression:

$$(\bar{\Phi}_m^\dagger, \vec{\Omega}\cdot\nabla\bar{\Phi}_n)_{k_\gamma} = \int_{R_k} d\vec{r} \int_{E_\gamma} dE \int_{\vec{\Omega}} d\vec{\Omega} \; \bar{\Phi}_m^\dagger(\vec{r},E,\vec{\Omega},t)\,\vec{\Omega}\cdot\nabla\bar{\Phi}_n(\vec{r},E,\vec{\Omega},t) \tag{2.53}$$

Applying the divergence theorem (Spi 59) to the evaluation of the integral over the space variable yields

$$(\bar{\Phi}_m^\dagger, \vec{\Omega}\cdot\nabla\bar{\Phi}_n)_{k_\gamma} = \int_{E_\gamma} dE \int_{\vec{\Omega}} d\Omega \int_{S_k} d\vec{s}_k \vec{n}_k\cdot\vec{\Omega}\; \bar{\Phi}_m^\dagger(\vec{s}_k,E,\vec{\Omega},t)\; \bar{\Phi}_n(\vec{s}_k,E,\vec{\Omega},t) -$$

$$\int_{R_k} d\vec{r} \int_{E_\gamma} dE \int_{\vec{\Omega}} d\vec{\Omega}\; \bar{\Phi}_n^\dagger(\vec{r},E,\vec{\Omega},t)\vec{\Omega}\cdot\nabla\bar{\Phi}_m^\dagger(\vec{r},E,\vec{\Omega},t) \tag{2.54}$$

where S_k is the surface enclosing region R_k, $\vec{s}_k$, is the value of $\vec{r}$ on the surface S_k, and $\vec{n}_k$ is the outward drawn unit normal to region R_k. The vector $\vec{\Omega}\bar{\Phi}_n(\vec{s}_k,E,\vec{\Omega},t)$ gives the neutron current in the direction $\vec{\Omega}$. If $\vec{n}_{,}\cdot\vec{\Omega}$ is positive, the neutrons are leaving region R_k; if $\vec{n}_k\cdot\vec{\Omega}$ is negative, the neutrons are entering region R_k. With this consideration in mind, the first term of Eq. (2.54) may be expressed as the sum of a loss term and a source term as follows:

$$\int_{E_\gamma} dE \int_{\vec{\Omega}} d\vec{\Omega} \int_{S_k} d\vec{s}_k\; \vec{n}_k\cdot\vec{\Omega}\bar{\Phi}_m^\dagger(\vec{s}_k,E,\vec{\Omega},t)\bar{\Phi}_n(\vec{s}_k,E,\vec{\Omega},t) =$$

$$\int_{E_\gamma} dE \int_{\vec{\Omega}} d\vec{\Omega} \int_{S_k} d\vec{s}_k\; \vec{n}_k\cdot\vec{\Omega}\bar{\Phi}_m^\dagger(\vec{s}_k,E,\vec{\Omega},t)\bar{\Phi}_n(\vec{s}_k,E,\vec{\Omega},t) -$$

$$\sum_{\substack{j=1\\ j\neq k}}^{K} \int_{E_\gamma} dE \int_{\vec{\Omega}_j} d\vec{\Omega} \int_{S_{k,j}} d\vec{s}_k\; \vec{n}_k\cdot\vec{\Omega}\bar{\Phi}_m^\dagger(\vec{s}_k,E,\vec{\Omega},t)\bar{\Phi}_n(\vec{s}_k,E,\vec{\Omega},t) \tag{2.55}$$

where

$S_{k,j}$ = that part of the surface S_k that has a common interface with the surface S_j

$\vec{\Omega}_j$ = those values of $\vec{\Omega}$ for which the dot product $\vec{n}_j\cdot\vec{\Omega}$ is positive

Inserting Eq. (2.55) into Eq. (2.54) and rearranging terms yields the following expression for the last two terms of Eq. (2.38):

$$(\bar{\Phi}^{\dagger}_m, \Omega\cdot\nabla\bar{\Phi}_n)_{k_\gamma} + (\bar{\Phi}^{\dagger}_m, \Sigma_T\bar{\Phi}_n)_{k_\gamma} =$$

$$N_{k_\gamma}^{(m)^{\dagger}}(t)\left[(\phi^{\dagger}_m, \Sigma_T\phi_n)_{k_\gamma} - (\phi_n\cdot\vec{\Omega}\cdot\nabla\phi^{\dagger}_m)_{k_\gamma} + \right.$$

$$\left.\int_{E_\gamma} dE \int_{\vec{\Omega}_k} d\vec{\Omega} \int_{S_k} d\vec{s}_k\vec{n}_k\cdot\vec{\Omega}\phi^{\dagger}_m\phi_n\right] N_k^{(n)}(t) -$$

$$\sum_{\substack{j=1\\ j\neq k}}^{K} N_{k_\gamma}^{(m)^{\dagger}}(t)\ \left[\int_{E_\gamma} dE \int_{\vec{\Omega}_j} d\vec{\Omega} \int_{S_{k,j}} d\vec{s}_k\vec{n}_k\cdot\vec{\Omega}\phi^{\dagger}_m(\vec{s}_k\cdot E,\Omega)\ \cdot\right.$$

$$\left.\phi_n(\vec{s}_k,E,\vec{\Omega})\right]\ N_{j_\gamma}^{(n)}(t) = N_{k_\gamma}^{(m)^{\dagger}}(t)\ \cdot$$

$$\frac{(\phi^{\dagger}_m, \frac{1}{v}\ \phi_n)_{k_\gamma}}{\theta_{k_\gamma}^{(m,n)}}\ N_{k_\gamma}^{(n)}(t)\ -$$

$$\sum_{\substack{j=1\\ j\neq k}}^{K} N_k^{(m)\dagger}(t) \, \frac{(\phi_m^\dagger, \frac{1}{v}\,\phi_n)_{\substack{k\\ \gamma}}}{\sigma^{(m,n)}_{\substack{j\to k\\ \gamma}}} \, N^{(n)}_{\substack{j\\ \gamma}}(t) \tag{2.56}$$

where

$$\theta_k^{(m,n)} = \frac{(\phi_m, \frac{1}{v}\,\phi_n)_{\substack{k\\ \gamma}}}{(\phi_m^\dagger, \Sigma_T\phi_n)_k - (\phi_n, \Omega\cdot\nabla\phi_m^\dagger)_k + \int_{E_\gamma} dE \int_{\vec{\Omega}_k} d\Omega \int_{S_k} d\vec{s}_k \vec{n}_k\cdot\vec{\Omega}\phi_m^\dagger\phi_n} \tag{2.57}$$

and

$$\sigma^{(m,n)}_{\substack{j\to k\\ \gamma}} = \frac{(\phi_m^\dagger, \frac{1}{v}\,\phi_n)_{\substack{k\\ \gamma}}}{\int_{E_\gamma} dE \int_{\vec{\Omega}} d\vec{\Omega} \int_{S_{k,j}} d\vec{s}_k \vec{n}_k\cdot\vec{\Omega}\phi_m^\dagger\phi_n} \tag{2.58}$$

The quantity $\theta^{(m,n)}_{\substack{k\\ \gamma}}$ gives the average inverse loss rate of neutrons belonging to the n-th mode in region R_k and group E_γ. The quantity $\sigma^{(m,n)}_{\substack{j\to k\\ \gamma}}$ gives the average inverse transfer rate from region R_j to region R_k for neutrons belonging to the n-th mode in group E_γ.

Collecting the terms expressed by Eqs. (2.44), (2.46), (2.50) and (2.56) and substituting them into Eq. (2.38) yields the following expression for element (1,1) of the $(\bar{\Phi}_m^\dagger, H\bar{\Psi}_n)_{\substack{k\\ \gamma}}$ matrix:

$$\text{element }(1,1) = N^{(m)\dagger}_{\substack{k\\ \gamma}} \left[\sum_{\alpha=1}^{\Gamma} \left\{ \frac{(1-\beta^{(m,n)}_{\substack{k\\ \alpha\to\gamma}})}{\Lambda^{(m,n)}_{\substack{k\\ \alpha\to\gamma}}} + \frac{1}{\tau^{(m,n)}_{\substack{k\\ \alpha\to\gamma}}} \right\} \cdot \right.$$

$$(\phi^{\dagger}_{m}, \frac{1}{v}\phi_n)\, N^{(n)}_{\substack{k\\ \alpha}} + \sum_{\substack{j=1\\ j\neq k}}^{K} \frac{(\phi^{\dagger}_{m}, \frac{1}{v}\phi_n)_{\substack{k\\ \gamma}}}{\sigma^{(m,n)}_{\substack{j\to k\\ \gamma}}}\, N^{(n)}_{\substack{k\\ \gamma}} -$$

$$\left. \frac{(\phi_{m}, \frac{1}{v}\phi_n)_{\substack{k\\ \gamma}}}{\theta^{(m,n)}_{\substack{k\\ \gamma}}}\, N^{(n)}_{\substack{k\\ \gamma}} \right] \tag{2.59}$$

Element (1, i+1) expressed by Eq. (2.39) may be written in separated form directly:

$$\text{element }(1, i+1) = C^{(m)\dagger}_{\substack{i,k\\ \gamma}} (c_{i,m}, f_i c_{i,n})_{\substack{k\\ \gamma}}\, \lambda_i C^{(m)}_{\substack{i,k\\ \gamma}} \tag{2.60}$$

for i = 1,2,⋯,D.

Element (i+1, 1) expressed by Eq. (2.40) must be manipulated as follows:

$$\beta_i(\bar{\phi}^{\dagger}_{m}, f_i\, \frac{P}{\lambda}\, \phi_n)_{\substack{k\\ \gamma}} = N^{(m)\dagger}_{\substack{k\\ \gamma}} \sum_{\alpha=1}^{\Gamma} \beta_i(\phi^{\dagger}_{m}, f_i\, \frac{P_\alpha}{\lambda}\, \phi_n)_{\substack{k\\ \gamma}}\, N^{(n)}_{\substack{k\\ \alpha}}$$

$$= N^{(m)\dagger}_{\substack{k\\ \gamma}} \sum_{\alpha=1}^{\Gamma} \beta_i(\phi^{\dagger}_{m}, f_i\, \frac{P_\alpha}{\lambda}\, \phi_n)_{\substack{k\\ \gamma}}\, N^{(n)}_{\substack{k\\ \gamma}}$$

$$\text{element } (1,\ i+1) = N_{k_\gamma}^{(m)^\dagger} \sum_{\alpha=1}^{\Gamma} \frac{\beta_{i,k_{\alpha\to\gamma}}^{(m,n)}}{\Lambda_{k_{\alpha\to\gamma}}^{(m,n)}} \left(\phi_m^\dagger,\ \frac{1}{v}\,\phi_n\right)_{k_\gamma} N_{k_\alpha}^{(n)} \tag{2.61}$$

for $i = 1,2,\cdots,D$.

The diagonal terms, element (i+1, i+1), expressed by Eq. (2.41) are given by:

$$\text{element } (i+1,\ i+1) = \lambda_i C_{i,k_\gamma}^{(m)^\dagger} \left(c_{i,m}^\dagger, f_i c_{i,n}\right)_{k_\gamma} C_{i,k_\gamma}^{(n)} \tag{2.62}$$

for $i = 1,2,\cdots,D$.

Collecting the terms given by Eqs. (2.30), (2.32), (2.59), (2.60), (2.61) and (2.62), rearranging and inserting them into the expression for the Lagrangian given by Eq. (2.29) yields:

$$L(\vec{N}^\dagger, \vec{N}, \dot{\vec{N}}) = \int_0^\infty dt \sum_{k=1}^{K} \sum_{\gamma=1}^{\Gamma} \sum_{m=1}^{M} \sum_{n=1}^{N} N_k^{(m)^\dagger}(t) \cdot$$

$$\Big\{ A_{k_\gamma}^{(m,n)} \frac{d}{dt} \vec{N}_{k_\gamma}^{(n)}(t) - \vec{S}_{k_\gamma}^{(m)}(t) -$$

$$\sum_{\alpha=1}^{G} B_{k_{\alpha\to\gamma}}^{(m,n)} A_{k_\gamma}^{(m,n)} N_{k_\alpha}^{(n)}(t) -$$

$$\sum_{j=1}^{K} D^{(m,n)}_{\substack{j\,k\\ \gamma}} \; A^{(m,n)}_{\substack{k\\ \gamma}} \; \vec{N}^{(n)}_{\substack{j\\ \gamma}}(t) + L^{(m,n)}_{\substack{k\\ \gamma}} \; A^{(m,n)}_{\substack{k\\ \gamma}} \; \vec{N}^{(n)}_{\substack{k\\ \gamma}}(t) \Big\}$$

(2.63)

where

$\vec{N}^{\dagger}$ represents the vectors $\vec{N}^{(m)\,\dagger}_{\substack{k\\ \gamma}}(t)$

$\vec{N}$ represents the vectors $\vec{N}^{(n)}_{\substack{k\\ \gamma}}(t)$ and

$\dot{\vec{N}} = \frac{d}{dt}\vec{N}$

The matrix $A^{(m,n)}_{\substack{k\\ \gamma}}$ is given by Eq. (2.29). The other matrices are defined as follows:

$$B^{(m,n)}_{\substack{k\\ \alpha\to\gamma}} = \begin{bmatrix} \left\{ \dfrac{\left(1-\beta^{(m,n)}_{\substack{k\\ \alpha\to\gamma}}\right)}{\Lambda^{(m,n)}_{\substack{k\\ \alpha\to\gamma}}} + \dfrac{1}{\tau^{(m,n)}_{\substack{k\\ \alpha\to\gamma}}} \right\} & 0 & \cdots & 0 \\ \beta^{(m,n)}_{\substack{1,k\\ \alpha\to\gamma}} \Big/ \Lambda^{(m,n)}_{\substack{k\\ \alpha\to\gamma}} & 0 & \cdots & 0 \\ \vdots & \vdots & & \vdots \\ \beta^{(m,n)}_{\substack{D,k\\ \alpha\to\gamma}} \Big/ \Lambda^{(m,n)}_{\substack{k\\ \alpha\to\gamma}} & 0 & \cdots & 0 \end{bmatrix}$$

(2.64)

$$D^{(m,n)}_{\substack{j\to k\\ \gamma}} = \begin{bmatrix} \dfrac{(1-\delta_{jk})}{\sigma^{(m,n)}_{\substack{j\to k\\ \gamma}}} & 0 & \cdots & 0 \\ 0 & 0 & \cdots & 0 \\ \vdots & \vdots & & \vdots \\ 0 & 0 & \cdots & 0 \end{bmatrix} \tag{2.65}$$

$$L^{(m,n)}_{\substack{k\\ \gamma}} = \begin{bmatrix} 1/\theta^{(m,n)}_{\substack{k\\ \gamma}} & & -\lambda_1 & \cdots & -\lambda_i & \cdots & -\lambda_D \\ 0 & & \lambda_1 & \cdots & 0 & \cdots & 0 \\ \vdots & & & & & & \\ 0 & \cdots & 0 & \cdots & \lambda_i & \cdots & 0 \\ \vdots & & \vdots & & \vdots & & \vdots \\ 0 & \cdots & 0 & \cdots & 0 & \cdots & \lambda_D \end{bmatrix} \tag{2.66}$$

The necessary condition that the $\vec{N}^{\dagger}$ and $\vec{N}$ make the Lagrangian an extremum is that the Euler-Lagrange equations (Mor 53) be satisfied, i.e.,

$$\frac{\partial}{\partial \vec{N}^{\dagger}} F(\vec{N}^{\dagger},\vec{N},\dot{\vec{N}}) - \frac{d}{dt}\left[\frac{\partial}{\partial \dot{\vec{N}}^{\dagger}} F(\vec{N}^{\dagger},\vec{N},\dot{\vec{N}})\right] = 0 \tag{2.67}$$

and

$$\frac{\partial}{\partial \vec{N}} F(\vec{N}^{\dagger},\vec{N},\dot{\vec{N}}) - \frac{d}{dt}\left[\frac{\partial}{\partial \dot{\vec{N}}} F(\vec{N}^{\dagger},\vec{N},\dot{\vec{N}})\right] = 0 \tag{2.68}$$

where $F(\vec{N}^{\dagger},\vec{N},\dot{\vec{N}})$ represents the integrand of the functional expressed by Eq. (2.63).

Application of Eq. (2.67) yields the equations of motion for the components of $\vec{N}$:

$$\sum_{n=1}^{M} A_{k\gamma}^{(m,n)} \Big[\frac{d}{dt} \vec{N}_{k\gamma}^{(n)}(t) - \sum_{\alpha=1}^{\Gamma} B_{k\gamma}^{(m,n)} \vec{N}_{k\alpha}^{(n)}(t) - \sum_{j=1}^{K} D_{j\to k\,\gamma}^{(m,n)} \vec{N}_{j\gamma}^{(n)}(t) + L_{k\gamma}^{(m,n)} \vec{N}_{k\gamma}^{(n)}(t) \Big] = \vec{S}_{k\gamma}^{(m)}(t) \tag{2.69}$$

for $m = 1,2,\cdots,M$ modes

$\gamma = 1,2,\cdots,\Gamma$ energy groups

$k = 1,2,\cdots,K$ regions

The equations of motion for the components of $\vec{N}^\dagger$ may be found with Eq. (2.68); however, since these equations are not of much practical use, they will not be given here. Let us proceed with an examination of Eq. (2.69).

Equation (2.69) will be clarified somewhat if the set of equations represented by the matrix notation is written out in full as follows:

$$\begin{aligned}
&\sum_{n=1}^{M} (\phi_m^\dagger, \tfrac{1}{v}\,\phi_n) \Big[\frac{d}{dt} N^{(n)}_{\substack{k\\ \gamma}}(t) - \sum_{\alpha=1}^{\Gamma} \Big\{ \frac{(1-\beta^{(m,n)}_{\substack{k\\ \alpha\to\gamma}})}{\Lambda^{(m,n)}_{\substack{k\\ \alpha\to\gamma}}} + \\
&\qquad \frac{1}{\tau^{(m,n)}_{\substack{k\\ \alpha\to\gamma}}} \Big\} N^{(n)}_{\substack{k\\ \alpha}}(t) - \sum_{j=1}^{K} \frac{(1-\delta_{jk})}{\sigma^{(m,n)}_{\substack{j\to k\\ \gamma}}} N^{(n)}_{\substack{j\\ \gamma}}(t) + \\
&\qquad \frac{1}{\theta^{(m,n)}_{\substack{k\\ \gamma}}} N^{(n)}_{\substack{k\\ \gamma}}(t) - \sum_{i=1}^{D} \frac{(c_{i,m}^\dagger, f_i c_{i,n})_{\substack{k\\ \gamma}}}{(\phi_m^\dagger, \tfrac{1}{v}\,\phi_n)_{\substack{k\\ \gamma}}} \;\cdot \\
&\qquad \lambda_i\, C^{(n)}_{\substack{i,k\\ \gamma}}(t) \Big] = S^{(m)}_{\substack{k\\ \gamma}}(t)
\end{aligned} \qquad (2.70)$$

$$\sum_{n=1}^{M} (\phi_m^{\dagger}, \frac{1}{v}\phi_n)_{k_\gamma} \left[\frac{(c_{i,m}^{\dagger}, f_i c_{i,n})_{k_\gamma}}{(\phi_m, \frac{1}{v}\phi_n)_{k_\gamma}} \left\{ \frac{d}{dt} + \lambda \right\} C_{i,k_\gamma}^{(n)} - \right.$$

$$\left. \sum_{\alpha=1}^{\Gamma} \frac{\beta_{ik_{\alpha\to\gamma}}^{(m,n)}}{\Lambda_{k_{\alpha\to\gamma}}^{(m,n)}} N_{k_\alpha}^{(n)}(t) \right] = 0 \tag{2.71}$$

where

$m = 1,2,\cdots,M$ modes

$k = 1,2,\cdots,K$ regions

$\gamma = 1,2,\cdots,\Gamma$ energy groups

$i = 1,2,\cdots,D$ precursor groups

δ_{jk} = the Kronecker delta

When the kinetics of the neutron field is represented by one mode, one region, and one energy group, Eqs. (2.70) and (2.71) reduce to

$$\frac{d}{dt} N(t) = \frac{(1-\beta)}{\Lambda} N(t) - \frac{N(t)}{\ell} + S(t) + \sum_{i=1}^{D} \frac{(c_i^{\dagger}, f_i c_i)}{(\phi^{\dagger}, \frac{1}{v}\phi)} \lambda_i C_i(t) \tag{2.72}$$

and

$$\frac{(c_i^{\dagger}, f_i c_i)}{(\phi^{\dagger}, \frac{1}{v}\phi)} \frac{d}{dt} C_i(t) = \frac{\beta_i}{\Lambda} N(t) - \frac{(c_i^{\dagger}, f_i c_i)}{(\phi^{\dagger}, \frac{1}{v}\phi)} \lambda_i C_i(t) \tag{2.73}$$

where

$\Lambda =$ generation time

$\ell = (1/\theta - 1/\tau)^{-1} =$ lifetime

and if the normalization factor $(c_i^{\dagger}, f_i c_i)/(\phi^{\dagger}, \frac{1}{v}\phi)$ is absorbed into $C_i(t)$, then it is seen that Eqs. (2.72) and (2.73) are the familiar point-model reactor kinetics equations. This result is, of course, as it should be; however, in connection with this, an important observation should be made. Note that the method used to derive the very complicated coupled kinetics equations also yields the point-model kinetics equation. Now, the simplicity of the point-model kinetics equations are appealing in comparison with the appallingly complicated coupled kinetics equations expressed by Eqs. (2.70) and (2.71). However, the idea is not to complicate a simple problem but rather to simplify a complicated kinetics problem that is not well represented by Eqs. (2.72) and (2.73). Equations (2.70) and (2.71) should find their greatest applicability in the study of reactor cores with weakly coupled fuel regions.

The derivation of the coupled kinetics equations would not be complete without showing how to reconstruct the flux in terms of the coupled parameters. The components of the vector $\vec{\Psi}$ were written in separable form according to Eq. (2.19):

$$\vec{\Psi} = \sum_{n=1}^{M} \Psi_n(\vec{r},E,\vec{\Omega})\, \vec{N}^{(n)}_{k_\gamma}(t) \qquad (2.19)$$

where $\vec{\Psi}$ is defined by Eq. (2.5); $\Psi_n(\vec{r},E,\vec{\Omega})$ is a matrix of the steady state values of the angular flux and the precursor concentrations and is defined by Eq. (2.23); and $\vec{N}^{(n)}_{k_\gamma}(t)$ is the vector defined by Eq. (2.21). Multiplying $\vec{\Psi}$ by $\Psi_m^{\dagger}(\vec{r},E,\vec{\Omega})V^{-1}$, integrating over region R_k, all $\vec{\Omega}$, and energy group E_γ, and summing over all values of m yields:

$$\sum_{m=1}^{M} (\Psi_m^{\dagger}, V^{-1}\Psi)_{k_\gamma}\, \vec{N}_{k_\gamma}(t) = \sum_{m=1}^{M} \sum_{n=1}^{M} (\Psi_m^{\dagger}, V^{-1}\Psi_n)_{k_\gamma}\, \vec{N}^{(n)}_{k_\gamma}(t) \qquad (2.74)$$

Assuming the eigenfunctions are members of a complete set and that M such modes are adequate to describe the functions represented by $\Psi_m^{\dagger}$, the left hand side of Eq. (2.74) is given by:

$$\sum_{m=1}^{M} (\Psi_m^{\dagger}, V^{-1}\Psi)_{k_\gamma} = (\Psi^{\dagger}, V^{-1}\Psi)_{k_\gamma} = A_{k_\gamma} \qquad (2.75)$$

where A_{k_γ} is the matrix defined by Eq. (2.31) summed over all values of m and n.

On the left hand side of Eq. (2.74)

$$(\psi^{\dagger}_{m}, V^{-1}\psi_{n})_{\substack{k\\ \gamma}} = A^{(m,n)}_{\substack{k\\ \gamma}} \tag{2.76}$$

Substituting Eq. (2.75) and (2.76) into Eq. (2.74) and operating from the left with $A^{-1}_{\substack{k\\ \gamma}}$ yields:

$$\vec{N}_{\substack{k\\ \gamma}}(t) = \sum_{n=1}^{M} \left\{ \sum_{m=1}^{M} A^{-1}_{\substack{k\\ \gamma}} A^{(m,n)}_{\substack{k\\ \gamma}} \right\} \vec{N}^{(n)}_{\substack{k\\ \gamma}}(t) \tag{2.77}$$

Equation (2.77) shows that the amplitude of the neutron population in region R_k and group E_γ is given by a weighted sum of the amplitudes of the neutron population in each mode. The term in {} of Eq. (2.77) gives the fractional contribution of the n-th mode to the total population in region R_k and energy group E_γ.

Similarly, it can be shown that the time-dependence of the flux average over the entire reactor is given by

$$\vec{N}(t) = \sum_{k=1}^{K} \sum_{\gamma=1}^{\Gamma} \sum_{n=1}^{M} \sum_{m=1}^{M} A^{-1} A^{(m,n)}_{\substack{k\\ \gamma}} \vec{N}^{(n)}_{\substack{k\\ \gamma}}(t) \tag{2.78}$$

where

$$A = \sum_{m=1}^{M} \sum_{n=1}^{N} (\psi^{\dagger}_{m}, V^{-1}\psi_{n})$$

To aid in the exposition of the theory a method for determining a space- and energy-dependent transfer function is discussed in the next section. To be specific the pile oscillator experiment is discussed; however, the resulting expressions are also applicable to other studies involving a localized time-dependent perturbation in the absorption cross-section.

Application to the Pile Oscillator Experiment

One method of determining the zero-power transfer function for a reactor is by means of a pile oscillator experiment. In such an experiment, a time-dependent perturbation is created at some point in the reactor while fluctuations in the neutron population are measured with a detector at some other point. The ratio of the detector output to the input perturbation yields the transfer function. In a reactor with a compact, or "tightly coupled" core, such an experiment yields meaningful results; however, in composite or "weakly coupled" cores, it has been found that the transfer function is space-dependent, e.g., see reference (Kyl 65). Therefore, in analyzing the kinetics of a weakly coupled system one is not able to determine a meaningful transfer function on the basis of space-independent reactor kinetics. It will now be shown how the coupled kinetics equations may be used to determine a meaningful space- and energy-dependent transfer function.

Consider the problem in which a perturbation is caused by oscillating, in region R_k, some material that only absorbs neutrons in energy group $E_{\gamma'}$. On the basis of first order perturbation theory the only parameters directly affected by the perturbation are the $\theta_{\substack{k'\\ \gamma'}}^{(m,n)}$. The fractional change in $1/\theta_{\substack{k'\\ \gamma'}}^{(m,n)}$ is given by

$$\frac{\delta[1/\theta_{\substack{k'\\ \gamma'}}^{(m,n)}(t)]}{1/\theta_{\substack{k'\\ \gamma'}}^{(m,n)}} = \frac{(\phi_m^\dagger, \delta\Sigma_T\phi_n)_{\substack{k'\\ \gamma'}}}{(\phi_m^\dagger, \Sigma_T\phi_n)_{\substack{k'\\ \gamma'}} - (\phi_n, \vec{\Omega}\cdot\nabla\phi_m^\dagger)_{\substack{k'\\ \gamma'}}} + \frac{(\phi_m^\dagger, \delta\Sigma_T\phi_n)_{\substack{k'\\ \gamma'}}}{\int_{E_{\gamma'}} dE \int_{\vec{\Omega}_{k'}} d\vec{\Omega} \int_{S_{k'}} d\vec{s}_{k'}, \vec{n}_{k'}\cdot\vec{\Omega}\ \phi_m^\dagger\phi_n} \tag{2.79}$$

Equation (2.79) follows directly from the definition of $\theta_{\substack{k\\ \gamma}}^{(m,n)}$ given by Eq. (2.57). To simplify the notation the perturbed parameter will be written in the following way:

$$1/\theta_{\substack{k'\\ \gamma'}}^{(m,n)}(t) = 1/\theta_{\substack{k'\\ \gamma'}}^{(m,n)}(0)\ \{1 + \epsilon_{\substack{k'\\ \gamma'}}^{(m,n)}(t)\} \tag{2.80}$$

where

$$\epsilon_{\substack{k'\\ \gamma'}}^{(m,n)}(t) = \frac{\delta[1/\theta_{\substack{k'\\ \gamma'}}^{(m,n)}(t)]}{1/\theta_{\substack{k'\\ \gamma'}}^{(m,n)}(0)} \tag{2.81}$$

Assuming that small variations in $1/\theta_{\substack{k\\ \gamma}}^{(m,n)}$ produce correspondingly small variations in the neutron population, we may expand $N_{\substack{j\\ \alpha}}^{(n)}$ in a Taylor series about its steady state value and truncate the series after the second term to obtain:

$$N_{\substack{j\\ \alpha}}^{(n)}(t) = 1 + \delta N_{\substack{j\\ \alpha}}^{(n)}(t) \tag{2.82}$$

Substituting Eqs. (2.80) and (2.82) into the coupled kinetics equations given by Eqs. (2.70) and (2.71), neglecting terms of the order δ^2, Fourier transforming the resulting expression, and rearranging yields:

$$\mathcal{H}\, n_{\substack{j\\ \alpha}}^{(n)}(\omega) = \mathcal{S}(\omega) \tag{2.83}$$

where the elements of $\mathcal{H}$ are given by

$$h_{pq} = (\phi_m^{\dagger}, \frac{1}{v}\,\phi_n)_{\substack{k\\ \gamma}} \Big[\delta_{\ell k}\delta_{\alpha\gamma}\Big\{ j\omega + \frac{1}{\theta_{\substack{k\\ \gamma}}^{(m,n)}} \Big\} - \delta_{\ell k}\Big\{ \frac{1}{\Lambda_{\substack{k\\ \alpha\to\gamma}}^{(m,n)}} + \frac{j\omega}{\Lambda_{\substack{k\\ \alpha\to\gamma}}^{(m,n)}} \sum_{i=1}^{D} \frac{\beta_{\substack{ik\\ \alpha\to\gamma}}^{(m,n)}}{(j\omega + \lambda_i)} + \frac{1}{\tau_{\substack{k\\ \alpha\to\gamma}}^{(m,n)}} \Big\} - \delta_{\alpha\gamma}(1-\delta_{\ell k})\, \frac{1}{\sigma_{\substack{\ell\to k\\ \gamma}}^{(m,n)}} \Big] \tag{2.84}$$

and the elements of the column vector $\mathcal{S}(\omega)$ are given by

$$I_p = \delta_{kk'}\delta_{\gamma\gamma'} \sum_{n'=1}^{M} \frac{(\phi^{\dagger}_{m}, \frac{1}{v}\phi_{n'})_k}{\theta^{(m,n')}_{\substack{k\\ \gamma}}} \mathcal{E}^{(m,n')}_{\substack{k\\ \gamma}}(\omega) \tag{2.85}$$

for $p = (m-1)\Gamma K + (\gamma-1)K + k$

$q = (n-1)\Gamma K + (\alpha-1)k + \ell$

m and $n = 1,2,\cdots,M$ modes

α and $\gamma = 1,2,\cdots,\Gamma$ energy groups

k and $\ell = 1,2,\cdots,K$ regions

$$n^{(n)}_{\substack{j\\ \alpha}}(\omega) = \int_{-\infty}^{\infty} e^{-j\omega t}\, \delta N^{(n)}_{\substack{j\\ \alpha}}(t)\, dt \tag{2.86}$$

$$\mathcal{E}^{(m,n)}_{\substack{k\\ \gamma}} = \int_{-\infty}^{\infty} e^{-j\omega t}\, \varepsilon^{(m,n)}_{\substack{k\\ \gamma}}(t)\, dt \tag{2.87}$$

The solution of Eq. (2.83) is found by applying Cramer's rule (Wyl 60) which gives

$$n^{(n)}_{\substack{j\\ \alpha}}(\omega) = \frac{|\mathcal{H}_q|}{|\mathcal{H}|} \tag{2.88}$$

where $|\mathcal{H}_q| = |\mathcal{H}|$ with the q-th column replaced by the vector $\mathcal{S}$.

Summing over all modes yields the following expression for the Fourier transform of $\delta N_{\substack{j\\ \alpha}}(t)$:

$$\eta_{\substack{j\\ \alpha}}(\omega) = \sum_{\ell=1}^{M} \frac{(\phi^{\dagger}, \frac{1}{v}\phi_{\ell})_{\substack{j\\ \alpha}}}{(\phi^{\dagger}, \frac{1}{v}\phi)_{\substack{j\\ \alpha}}} \frac{|H_q|}{|H|} \qquad (2.89)$$

where $q = (n-1)\Gamma K + (\alpha-1)K + \ell$. The quantity $\eta_{\substack{j\\ \alpha}}(\omega)$ represents the output that would be measured in some region R_j and group E_α due to a pile oscillator in region $R_{k'}$ that absorbs neutrons in group $E_{\gamma'}$. Summing over all modes yields the total input to region $R_{k'}$ and group $E_{\gamma'}$:

$$\mathcal{E}_{\substack{k'\\ \gamma'}}(\omega) = \sum_{m=1}^{M} \sum_{n=1}^{M} \frac{\theta_{\substack{k'\\ \gamma'}}}{\theta^{(m,n)}_{\substack{k'\\ \gamma'}}} \frac{(\phi^{\dagger}_{m}; \frac{1}{v}\phi_{n})}{(\phi^{\dagger}, \frac{1}{v}\phi)_{\substack{k'\\ \gamma'}}} \mathcal{E}^{(m,n)}_{\substack{k'\\ \gamma'}}(\omega) \qquad (2.90)$$

The transfer function is computed as the ratio of the output to the input. In this case the transfer function $\mathcal{J}_{k'\gamma'/j,\gamma}$ for an output in region R_j and group E_α that is caused by an input to region $R_{k'}$ and group $E_{\gamma'}$ is given by:

$$\mathcal{J}_{k'\gamma'/j,\alpha} = \frac{\eta_{\substack{j\\ \alpha}}(\omega)}{\mathcal{E}_{\substack{k'\\ \gamma'}}(\omega)}$$

$$= \frac{\displaystyle\sum_{\ell=1}^{M} \left\{ \frac{(\phi^{\dagger},\, \frac{1}{v}\, \phi_{\ell})_{\substack{j\\ \alpha}}}{(\phi^{\dagger},\, \frac{1}{v}\, \phi)_{\substack{j\\ \alpha}}} \right\} |\mathcal{H}_{q}|}{|\mathcal{H}| \displaystyle\sum_{m=1}^{M} \sum_{n=1}^{M} \left\{ \frac{\theta_{\substack{k'\\ \gamma'}}}{\theta^{(m,n)}_{\substack{k'\\ \gamma'}}} \; \frac{(\phi^{\dagger},\, \frac{1}{v}\, \phi_{n})}{(\phi^{\dagger},\, \frac{1}{v}\, \phi)_{\substack{k'\\ \gamma'}}} \right\} \mathcal{E}^{(m,n)}(\omega)}$$

$$= \frac{\displaystyle\sum_{\ell=1}^{M} \text{Я}^{(\ell)}_{\substack{j\\ \alpha}} |\mathcal{H}_{q}|}{|\mathcal{H}| \displaystyle\sum_{m=1}^{M} \sum_{n=1}^{M} \text{Ю}^{(m,n)}_{\substack{k'\\ \gamma'}} \; \mathcal{E}^{(m,n)}_{\substack{k'\\ \gamma'}}(\omega)} \tag{2.91}$$

where $\text{Я}^{(\ell)}_{\substack{j\\ \alpha}}$ and $\text{Ю}^{(m,n)}_{\substack{k'\\ \gamma'}}$ are constants and are equal to the corresponding terms in {} in the numerator and denominator. (Note: Я is pronounced "ya", and Ю is pronounced "yu".)

In Eq. (2.92) the determinant $|\mathcal{H}|$ that appears in the denominator is the function of interest. This function describes the behavior of the system irrespective of the measuring device. In fact, $1/|\mathcal{H}|$ is analogous to the space-independent transfer function derived from the point-model kinetics equation. The other parameters appearing in Eq. (2.91) account for the localized nature of the experimental arrangement that is being used to measure a quantity that varies from one point to the next. The behavior of the numerator depends on the location of the detector as well as the perturbation, and the behavior of the denominator depends on the location of the perturbation.

Diffusion Theory Form of the Kinetics Coefficients

In order to keep the derivation of the coupled kinetics equations as general as possible, the neutron transport equation was used. However, in a practical problem the transport equation is too difficult to solve and approximations must be made. The most common approximate representation of the transport problem is that given by diffusion theory (Wei 58).

Except for $\theta_{\substack{k\\ \gamma}}^{(m,n)}$ and $\sigma_{\substack{j\to k\\ \gamma}}^{(m,n)}$ the mathematical definitions of the kinetics parameters also apply to the diffusion approximation if we replace the leakage operator $\vec{\Omega}\cdot\nabla$ by $-\nabla\cdot D\nabla$ where $D(\vec{r},E)$ is the diffusion coefficient. It is this change in leakage operator that brings about the changes in the form of $\theta_{\substack{k\\ \gamma}}^{(m,n)}$ and $\sigma_{\substack{j\to k\\ \gamma}}^{(m,n)}$. The diffusion theory expression for these parameters is:

$$\theta_{k_\gamma}^{(m,n)} = \frac{(\phi_m^\dagger, \frac{1}{v}\phi_n)_{k_\gamma}}{\left\{(D, \nabla\phi_m^\dagger \cdot \nabla\phi_n)_{k_\gamma} + (\phi_m^\dagger, \Sigma_T\phi_n)_k + \frac{1}{4}\int_{E_\gamma} dE \int_{S_k} d\vec{s}_k\, \phi_m^\dagger(\vec{s}_k,E)\,\phi_n(\vec{s}_k,E) - \frac{1}{2}\int_{E_\gamma} dE \int_{S_k} d\vec{s}_k\, \phi_m^\dagger(\vec{s}_k,E)\, D\nabla\phi_n(\vec{s}_k,E)\cdot\vec{n}_k\right\}} \quad .$$

(2.92)

$$\sigma_{j\to k_\gamma}^{(m,n)} = \frac{(\phi^\dagger, \frac{1}{v}\phi_n)_{k_\gamma}}{\frac{1}{4}\int_{E_\gamma} dE \int_{S_{k,j}} d\vec{s}_k\, \phi_m^\dagger(\vec{s}_k,E)\,\phi_n(s_k,E) + \frac{1}{2}\int_{E_\gamma} dE \int_{S_{k,j}} d\vec{s}_k\, \phi_m^\dagger(\vec{s}_k,E)\, D\nabla\phi_n(\vec{s}_k,E)\cdot\vec{n}_k}$$

(2.93)

where

S_k = surface of region R_k

$S_{j,k}$ = common interface between regions R_k and R_j

$\vec{n}_k$ = outward drawn normal from surface S_k

The diffusion coefficient $D(\vec{r},E)$ is assumed to be independent of $\vec{r}$ at all points within a region but may vary from region to region. For diffusion theory the parenthesis notation does not include integration over $\vec{\Omega}$.

Conclusion

The theory of coupled reactor kinetics has been established on a firm basis by deriving the pertinent set of equations from the general Boltzmann equation. The formulation of the equations from first principles on the basis of a semidirect variational method allows the computation of coupling parameters in a consistent way. Since no restrictions have been placed on the reactor configuration, on the division of the total system into regions, on the division of the spectrum into groups, nor on the mathematical representation of the steady state flux, the set of kinetics equations presented here is in a very suitable form to study the dynamic behavior of a variety of composite systems.

To facilitate the utilization of the coupled formulation, the next chapter is devoted to the presentation of the coupled kinetics parameters in terms of multigroup diffusion theory.

CHAPTER III

MULTIGROUP DIFFUSION THEORY FORMULATION OF COUPLED KINETICS PARAMETERS

Introduction

Before undertaking a study of the dynamic behavior of a nuclear reactor core, it is necessary to study the static problem, which may be approached analytically, numerically, or some combination of the two. There are numerous analytical methods of studying static reactor physics problems but these methods are generally very difficult to apply to composite cores. The usual approach is to approximate the general transport equation with diffusion theory and then to solve the diffusion equation numerically. This method involves the use of multigroup diffusion theory. Because of the widespread use of multigroup diffusion theory, a presentation of the coupled kinetics parameters in terms of this formulation should be most beneficial.

Since the primary purpose of this thesis is to develop a method for studying the kinetic behavior of a reactor consisting of coupled cores, a method is discussed regarding the numerical determination of eigenmodes for representing the flux in a coupled system.

Multigroup Diffusion Equation

The notation in this section is similar to that used by D. C. Baller in his description of the FAIM code (Bal 62). In order to simplify the presentation the discussion in this section, and in the remainder of the chapter as well, is limited to a 1-dimensional configuration such as a slab, sphere or cylinder. The extension to 2- and 3-dimensional configurations is straightforward.

The multigroup diffusion equation is given by

$$-D^i\nabla^2\phi^i(r) + \Sigma_T^i\phi^i(r) = \chi^i S(r) + \sum_{\substack{j=1\\ j\neq i}}^{i-1} \Sigma_{s,j\to i}\,\phi^j(r) \qquad (3.1)$$

for $1 \leq i \leq G$. G = number of groups.

The symbols are defined as

$\phi^i(r)$ = neutron flux in i-th group at position r

D^i = diffusion constant for the i-th group

Σ_T^i = total removal from the i-th group

$\Sigma_T^i = D^i(B^2)^i + \Sigma_a^i + \sum_{j=i+1}^{G} \Sigma_{s,i\to j}$ for $i<G$

$\Sigma_T^i = D^i(B^2)^i + \Sigma_a^i$ for $i=G$

$(B^2)^i$ = transverse buckling for the i-th group

Σ_a^i = absorption cross-section for the i-th group

$\Sigma_{s,i\to j}$ = scattering or transfer from group i to group j (includes both elastic and inelastic scattering)

χ^{i} = the integral of the fission spectrum over the energy range represented by group i

r = distance measured from the origin

$S(r)$ = fission source distribution given by

$$S(r) = \sum_{i=1}^{G} \frac{(\nu\Sigma_f)^i}{\lambda} \phi^i(r)$$

λ = the eigenvalue

$(\nu\Sigma_f)^i$ = the average number of neutrons produced by a fission in the i-th group times the fission cross-section in the i-th group

Coupled Kinetics Parameters in Terms of Multigroup Diffusion Theory

Before proceeding with the formulation of the coupled kinetics parameters a few remarks should be made concerning the nomenclature to be used. The terms "broad region" and "broad group" will refer to regions of the type R_j and groups of the type E_α discussed in Chapter II. The terms "region" and "group" refer to the partitioning of the reactor according to the nuclear properties of each section and to the groups in the multigroup structure. Each broad group E_α consists of one or more groups and each broad region R_j may consist of one or more regions.

In order to simplify the notation the subscripts and superscripts specifying the particular eigenmode of the flux or adjoint flux are not shown. The addition of this notation to the following formulas is straightforward from the definitions given in Chapter II.

$$(\phi^{\dagger}, \frac{1}{v}\,\phi)_{k_{\gamma}} = \sum_{i\epsilon E_{\gamma}} \int_{R_k} dV\ \phi^{\dagger i}\left(\frac{1}{v}\right)_i \phi^i \tag{3.2}$$

where

$\phi^{\dagger i}$ = the adjoint of ϕ^i

dV = dr (plane geometry)

= $2\pi r\ dr$ (cylindrical geometry)

= $4\pi r^2\ dr$ (spherical geometry)

Let the weighted production rate be represented by $\mathcal{P}_{k_{\alpha\to\gamma}}$ where

$$\mathcal{P}_{k_{\alpha\to\gamma}} = \sum_{i\epsilon E_{\alpha}} \sum_{j\epsilon E_{\gamma}} \int_{R_k} \chi^i \phi^{\dagger i} (\nu\Sigma_f)^j \phi^j\ dV \tag{3.3}$$

then the transfer time by regeneration is given by

$$\Lambda^{k}_{\alpha\to\gamma} = \frac{(\phi^{\dagger}, \frac{1}{v}\,\phi)_{k_{\gamma}}}{\mathcal{P}_{k_{\alpha\to\gamma}}} \tag{3.4}$$

The coupled effective delayed neutron fraction for the ℓ-th precursor group is given by

$$\beta_{\ell,k_{\alpha\to\gamma}} = \frac{\beta_\ell}{\mathscr{P}_{k_{\alpha\to\gamma}}} \sum_{i\varepsilon E_\alpha} \sum_{i\varepsilon E_\gamma} \int_{R_k} f_\ell^i \phi^{\dagger i} (\nu\Sigma_f)^j \phi^j \, dV \quad . \tag{3.5}$$

where

f_ℓ^i = the integral of the delayed neutron spectrum for the ℓ-th precursor group over the energy range represented by group i

If all of the neutrons emitted by the ℓ-th precursor group belong to some I-th energy group, then

$$f_\ell^i = \delta_{iI} \qquad (\delta_{iI} = \text{Kronecker delta})$$

and Eq. (3.5) becomes

$$\beta_{\ell,k_{\alpha\to\gamma}} = \frac{\beta_\ell}{\mathscr{P}_{k_{\alpha\to\gamma}}} \sum_{i\varepsilon E_\alpha} \delta_{iI} \sum_{j\varepsilon E_\gamma} \phi^{\dagger I} (\nu\Sigma_f)^j \phi^j \, dV \tag{3.6}$$

The average transfer time by scattering from group E E_α to group E_γ is given by

$$\tau_{k_{\alpha\to\gamma}} = \frac{\left(\phi^\dagger, \frac{1}{v}\phi\right)_{k_\gamma}}{\sum_{i\varepsilon E_\gamma} \sum_{j\varepsilon E_\alpha} \int_{R_k} \phi^{\dagger i} \, \Sigma_{S,j\to i} \, \phi^j \, dV} \tag{3.7}$$

The inverse average total loss rate from broad region R_k and broad group E_γ is given by

$$\theta_{k\gamma} = \frac{(\phi^\dagger, \frac{1}{v}\phi)_{k\gamma}}{\sum\limits_{i\epsilon E_\gamma}\int\limits_{R_k} \{D^i \nabla\phi^{\dagger i}\nabla\phi^i + \phi^{\dagger i}\Sigma_T^i\phi^i\} dV + \{\phi^{\dagger i}J_+^i\}_{r=R_k^R} + \{\phi^{\dagger i}J_-^i\}_{r=R_k^L}}$$

where (3.8)

$\nabla = \frac{d}{dr}$

R_k^R = the outer boundary of broad region R_k

R_k^L = the inner boundary of broad region R_k

$$J_\pm^i = C_p \cdot (r)^P \left\{ \frac{\phi^i(r)}{4} \mp \frac{D^i}{2} \frac{d}{dr}\phi^i(r) \right\} \tag{3.9}$$

$C_p = 1$; $P=0$ (plane geometry)
$= 2\pi$; $=1$ (cylindrical geometry)
$= 4\pi$; $=2$ (spherical geometry)

The inverse average transfer rate into region R_k is given by

$$\sigma_{(k+1)\to k\,\gamma} = \frac{(\phi^\dagger, \frac{1}{v}\phi)_{k\gamma}}{\sum\limits_{i\epsilon E_\gamma} \{\phi^{\dagger i}J_-^i\}_{r=R_k^R}} \tag{3.10}$$

and

$$\sigma_{\substack{(k-1)\to k\\ \gamma}} = \frac{(\phi^{\dagger}, \frac{1}{v}\phi)_{\substack{k\\ \gamma}}}{\sum\limits_{i\varepsilon E_{\gamma}} \{\phi^{\dagger i} J_{+}^{i}\}_{r=R_{k}^{L}}} \tag{3.11}$$

In conclusion the adjoint weighted precursor concentration at steady state is given by

$$(c_{\ell}^{+}, f_{\ell} c_{\ell})_{\substack{k\\ \gamma}} = (\phi^{\dagger}, \frac{1}{v}\phi)_{\substack{k\\ \gamma}} \sum_{\alpha=1}^{\Gamma} \frac{\beta_{\ell,k_{\alpha\to\gamma}}}{\Lambda_{k_{\alpha\to\gamma}}} \tag{3.12}$$

The theory as developed in Chapter II permits the description of the neutron field in terms of eigenmodes. In the next section this feature is discussed in more detail.

Modal Representation of the Flux in a Coupled System

Within the framework of multigroup diffusion theory one may obtain an "exact" solution to the equations represented by Eq. (3.1) by solving this set of equations numerically. The accuracy of the "exact" solution depends on the numerical technique that is used. The term "exact" is used as opposed to an approximate analytical solution in which one expands the flux in some finite series of eigenfunctions belonging to an infinite set.

In the study of a reactor consisting of weakly coupled cores there may be some advantage to be gained by expanding the flux representing the total system in a series of partial fluxes, each representing some region of the system. One method of classification is to label the partial fluxes according to the region in which they originated, i.e.,

$$\phi^i(r) = \sum_{n=1}^{M} \phi_n^i(r) \tag{3.13}$$

where

$\phi_n^i \equiv$ the flux in the i-th energy group due to neutrons born in some n-th region of the reactor

The summation over n includes all fuel regions of the reactor. By definition the ϕ_n^i are solutions of the following set of equations:

$$-D^i\nabla^2\phi_n^i(r) + \Sigma_T^i\phi_n^i(r) - \sum_{\substack{j=1 \\ j\neq i}}^{i-1} \Sigma_{s,j\to i}\,\phi_n^j(r) = \chi^i S_n(r) \tag{3.14}$$

where

$$S_n(r) = \sum_{i=1}^{G} \frac{(\nu\Sigma_f)^i\phi^i(r)}{\lambda} \quad \text{if r is the n-th fuel region}$$

$$= 0 \text{ otherwise}$$

A set of partial adjoint fluxes is defined similarly.

The method presented above was used by Avery in his "Theory of Coupled Reactors" (Ave 58a) and later by Dougherty in the development of his space-time neutron kinetics equations (Dou 61). Also, Stewart has presented a method (Ste 58) similar to this one.

The procedure for determining the $\phi_n^i(r)$ is as follows. One first solves the set of homogeneous equations expressed by Eq. (3.1) to determine the group fluxes $\phi^i(r)$ and the eigenvalue. He then uses this set of fluxes in the source term on the right hand side of Eq. (3.14) and solves the set of equations expressed by Eq. (3.14) to determine $\phi_n^i(r)$ for $n = 1,2,\cdots,M$, where M is the number of weakly coupled fuel regions in the core. The partial flux $\phi_n^i(r)$ then represents the contribution of neutrons originating in the n-th fuel region to the total flux in energy group i at point r. To say that a reactor is weakly coupled implies that the reactor not only consists of regions that are nearly critical by themselves but also that these regions are capable of behaving almost independently during a transient. It is for the latter reason that it may be advantageous to study weakly coupled reactors in terms of these partial fluxes, or spatial eigenmodes.

One very useful property of these eigenmodes is that they form a complete set with only a finite number of components in the sense that a system $\{\phi_n(r)\}$ is termed complete (Kap 52) if a function $\phi(r)$ can be approximated as closely as desired by a finite number of components $\phi_n(r)$.

Another advantage in using eigenmodes that are representative of a particular region of the reactor is that the number of coupled kinetics equations for a given problem may be greatly reduced. This results from the restriction that the precursors do not diffuse which requires that

$$(c^{\dagger}_{\ell,m}, f_{\ell} c_{\ell,n})_{k_{\gamma}} = \delta_{m,n}(c^{\dagger}_{\ell,n}, f_{\ell} c_{\ell,n})_{k_{\gamma}}$$

$$= \delta_{m,n}(\phi^{\dagger}_{m} \frac{1}{v} \phi_{n})_{k_{\gamma}} \sum_{\alpha=1}^{\Gamma} \frac{\beta^{(m,n)}_{\ell,k_{\alpha\to\gamma}}}{\Lambda^{(m,n)}_{k_{\alpha\to\gamma}}} \tag{3.15}$$

The quantity $c_{\ell,n}$ gives the number of neutrons emitted into the n-th spatial mode by the ℓ-th precursor group. The quantity $c^{\dagger}_{\ell,n}$ is the adjoint to $c_{\ell,n}$ and both quantities are non-zero only within the fuel region specified by the subscript n. Furthermore, $\beta^{(m,n)}_{\ell,k_{\alpha\to\gamma}}$ is non-zero only if the n-th fuel region is within broad region R_k. In the general case discussed in Chapter II it was necessary to solve up to MΓK(1+D) coupled first order differential equations. In this case it is only necessary to solve up to ΓK(M+D) coupled first order differential equations.

One disadvantage of the method discussed above is that most multigroup diffusion theory codes are not programmed to perform the calculations necessary for determining the partial fluxes and their adjoints. However, this problem is not a real hindrance since with a few modifications some existing code can be made up to perform the additional operations. Such modifications have been made in the FAIM code (Bal 62) and the modified code has been given the name SAIM (Coc 65a).

The SAIM code computes values for the partial fluxes and partial adjoints and punches them on cards along with the corresponding cross-sections. This punched card output is then read directly into a numerical integration code called C0UPKIN which computes the coupled kinetics parameters according to Eq. (3.2) - (3.11).

The C0UPKIN code is dimensioned to compute the coupling parameters for a system having up to twenty broad regions with the energy-dependence expressed by up to eighteen broad groups. A complete description of the code is given in reference (Coc 65b).

Conclusions

Formulas have been given for computing the coupled kinetics parameters in terms of multigroup diffusion theory, and a method has been suggested for studying weakly coupled systems by expanding the flux in spatial eigenmodes.

In the next chapter the coupled kinetics formulas are applied to a kinetics study of a simplified model of an Argonaut-type reactor with a two-slab loading.

CHAPTER IV

SPACE-TIME ANALYSIS OF THE PULSED NEUTRON-BEAM EXPERIMENT IN A REACTOR WITH WEAKLY COUPLED FUEL REGIONS

Introduction

One type of experiment that is well suited to the purpose of determining certain fundamental reactor parameters is based on the pulsed neutron-beam technique (Sjö 56). This experiment consists essentially of emitting a very short burst of neutrons into the reactor and measuring the decay constant of the most slowly decaying mode. Then on the basis of a 1-point reactor kinetics model this measured decay constant is related to certain of the reactor parameters. Typically, one uses this technique to determine the ratio of the effective delayed neutron fraction, β, to the mean generation time, Λ, at delayed critical, and then by assuming that β/Λ is independent of the reactivity, it is possible to make reactivity measurements. In the study of reactors with a single fuel region analysis of the experimental data on the basis of 1-point-model kinetic theory has been shown to give excellent agreement with theoretical computations, for example see reference (Per 60). However, when theoretical computations were compared with experimental measurements made on an Argonaut-type reactor with a 2-slab loading, the comparison was so poor that questions arose regarding both the experimental measurements and the theoretical computations. Among these questions were the following: (a) Will 1-point-model reactor kinetics correctly predict the prompt neutron decay constant for a reactor with weakly coupled fuel regions? (b) Will the coupled kinetics formulation give a better prediction? (c) How well do these point-model approximations agree with the true value? (d) What effect does the graphite in the region between the fuel slabs have on the value of the decay constant? (e) Is the experimenter actually measuring the prompt neutron decay constant, or is he measuring the die-away of the pulsed neutron beam in the graphite?

An answer to these questions was sought through the study of a very simplified model of a reactor with two weakly coupled fuel regions. This model is shown schematically in Figure 1. One important feature that has been retained in this model is the separation of the two fuel regions, 1 and 3, by a reflector region, 2. Three methods of analysis will be presented. The first method will be considered an exact representation of this model which is based on the time- and space-dependent monoenergetic diffusion theory model. The second method will utilize the coupled kinetics formulation and the third method will present the 1-point-model representation. Numerical computations of the prompt neutron decay constant as predicted by the

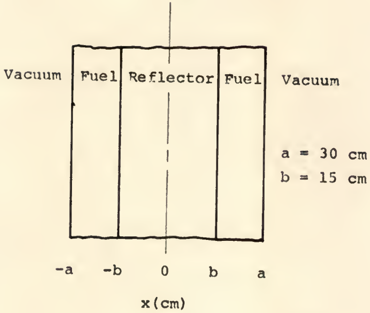

Figure 1. One-Dimensional Representation of a Reactor With Two Coupled Fuel Regions

three methods will be compared in order to answer questions (a), (b), and (c). Also, in the process of obtaining these numerical values the answers to questions (d) and (e) will be revealed.

Space- and Time-Dependent Reactor Kinetics Representation

Consider the following problem. A reactor is delayed critical and operating at steady state. At time t=0 a high intensity neutron beam of short duration is introduced. The neutrons from this external source cause fissions which produce more neutrons, both prompt and delayed. The net result, after the delayed neutrons begin to appear, is an increase in the steady-state flux. However, during the short time interval between the introduction of the neutron beam and the appearance of the additional delayed neutrons, there is a measurable decrease in the neutron population as a function of time which exponentially approaches a steady-state distribution. At first, this decrease in the neutron population is due primarily to the loss of the injected neutrons by absorption and leakage, but it will be shown that the duration of this effect is brief compared to the duration of the phenomena in which we are interested. The phenomenon of interest is the rate at which the prompt neutron population, or flux, that resulted from fissions caused by the injected neutrons, dies away. The die-away occurs because the prompt neutrons are unable to sustain a chain reaction in a delayed critical reactor. These prompt neutrons will be referred to as "excess prompt neutrons" in the discussion that follows:

Following the injection of the neutron beam at time $t=0$, the flux in the reactor consists of a steady-state portion $\phi(x)$ which also existed at $t<0$ and a time varying portion made up of the excess prompt neutron flux $\psi(x,t)$ and the source flux $S(x,t|0,0)$. The function $S(x,t|0,0)$ gives the flux of source neutrons at x and t due to injection of a neutron beam at $x=0$ and $t=0$.

For the delayed critical reactor shown in Figure 1 the steady-state flux must satisfy the following set of equations:

$$\nabla^2\phi(x) + B_m^2\,\phi(x) = 0 \qquad b \le |x| \le a \tag{4.1}$$

$$\nabla^2\phi(x) - \kappa^2\phi(x) = 0 \qquad 0 \le |x| \le b \tag{4.2}$$

where

$$B_m^2 = \frac{\nu\Sigma_f - \Sigma_{RF}}{D_F} \tag{4.3}$$

$$\kappa^2 = \frac{\Sigma_{RG}}{D_G} \tag{4.4}$$

The subscripts F and G refer to the fuel regions and the graphite reflector between the fuel regions, respectively.

The removal cross-section includes losses due to absorption and transverse leakage.

The following boundary conditions must be satisfied at all times:

$$\phi(\pm a) = 0 \tag{4.5}$$

$$\lim_{\varepsilon \to 0} \phi(\pm\{b+\varepsilon\}) = \lim_{\varepsilon \to 0} \phi(\pm\{b-\varepsilon\}) \tag{4.6}$$

$$\lim_{\varepsilon \to 0} D_F \nabla\phi(x)\Big|_{x=\pm(b+\varepsilon)} = \lim_{\varepsilon \to 0} D_G \nabla\phi(x)\Big|_{x=\pm(b-\varepsilon)} \tag{4.7}$$

The solution of Eqs. (4.1) and (4.2) is straightforward and is given by:

$$\phi(x) = A_1 \sin B_m(a-|x|) \qquad b \leq |x| \leq a \tag{4.8}$$

$$\phi(x) = A_2 \cosh \kappa|x| \qquad 0 \leq |x| \leq b \tag{4.9}$$

where the coefficients A_1 and A_2 satisfy the following set of homogeneous equations:

$$Q\vec{A} = 0 \tag{4.10}$$

$$\tilde{\vec{A}} = [\, A_1 \quad A_2 \,] \tag{4.11}$$

$$Q = \begin{bmatrix} \sin B_m(a-b) & -\cosh \kappa b \\ D_F B_m \cos B_m(a-b) & D_G \kappa \sinh \kappa b \end{bmatrix} \qquad (4.12)$$

A non-trivial solution exists for Eq. (4.9) only if the determinant of Q is identically zero. This is accomplished by adjusting the macroscopic cross-sections. Let us proceed to the solution of excess prompt neutron flux.

The flux represented by $\psi(x,t)$ is given by the solution to the following set of equations:

$$\nabla^2\psi(x,t) + B^2\psi(x,t) = \frac{1}{D_F v}\frac{\partial}{\partial t}\psi(x,t) - \frac{(1-\beta)\nu\Sigma_f}{D_F} S(x,t|0,0)$$

$$b \leq |x| \leq a \qquad (4.13)$$

$$\nabla^2\psi(x,t) - \kappa^2\psi(x,t) = \frac{1}{D_G v}\frac{\partial}{\partial t}\psi(x,t)$$

$$0 \leq |x| \leq b \qquad (4.14)$$

where

$$B^2 = \frac{(1-\beta)\nu\Sigma_f - \Sigma_{RF}}{D_F} \qquad (4.15)$$

Laplace transforming Eqs. (4.13) and (4.14) yields:

$$\nabla^2\bar{\psi}(x,s) + \bar{B}^2\bar{\psi}(x,s) = \frac{(1-\beta)\nu\Sigma_f}{D_F}\ \bar{S}(x,s|0,0) \qquad b\le|x|\le a \qquad (4.16)$$

$$\nabla^2\bar{\psi}(x,s) - \bar{\kappa}^2\bar{\psi}(x,s) = 0 \qquad 0\le|x|\le b \qquad (4.17)$$

where

$$\bar{B}^2 = B^2 - \frac{s}{D_F v} = \frac{(1-\beta)\nu\Sigma_f - \Sigma_{RF} - s/v}{D_F} \qquad (4.18)$$

$$\bar{\kappa}^2 = \kappa^2 + \frac{s}{D_G v} = \frac{\Sigma_{RG} + s/v}{D_G} \qquad (4.19)$$

$$\bar{\psi}(x,s) = \int_0^\infty \psi(x,t)\, e^{-st}\, dt$$

$$\bar{S}(x,s|0,0) = \int_0^\infty S(x,t|0,0)\, e^{-st}\, dt$$

Equations (4.16) and (4.17) must satisfy the boundary conditions given by Eqs. (4.5)- (4.7). Application of these boundary conditions yields the following solution for the Laplace transform of the excess prompt neutron flux:

$$\bar{\psi}(x,s) = C_1(s)\ \sin \bar{B}(a-|x|) + \bar{\psi}_p(x,s)$$

$$b \le |x| \le a \qquad (4.20)$$

$$\bar{\psi}(x,s) = C_2(s)\ \cosh\ \bar{\kappa}|x| \qquad 0 \le |x| \le b \qquad (4.21)$$

where $\bar{\psi}_p(x,s)$ is the particular solution that results from the source term on the right hand side of Eq. (4.16). The solution $\bar{\psi}_p(x,s)$ represents the flux due to those neutrons that are produced directly by fissions caused by the injected source neutrons. The coefficients of the complementary solution are given by the solution to the following set of equations:

$$Z(s)\ \vec{C}(s) = \vec{W}(s) \qquad (4.22)$$

where

$$\tilde{\vec{C}}(s) = [C_1(s) \quad C_2(s)] \qquad (4.23)$$

$$\tilde{\vec{Z}}(s) = \begin{bmatrix} \sin \bar{B}(a-b) & -\cosh \bar{\kappa}\ b \\ D_F\bar{B} \cos \bar{B}(a-b) & D_G\bar{\kappa}\ \sinh \bar{\kappa}\ b \end{bmatrix} \qquad (4.24)$$

$$\vec{W}(s) \quad \begin{bmatrix} -\ {}_p(b^{\dagger},s) \\ D_F\nabla\Psi_p(b^{\dagger},s) \end{bmatrix} \qquad (4.25)$$

Using Cramer's rule (Kap 52) to solve Eq. (4.25) yields:

$$C_i(s) = \frac{|Z_i(s)|}{|Z(s)|} \qquad i=1,2 \tag{4.26}$$

where $|Z_i(s)|$ is the determinant of the matrix $Z(s)$ with the i-th column replaced by $W(s)$.

The time- and space-dependent solution of Eqs. (4.13) and (4.14) is given by the inverse Laplace transform of $\bar{\psi}(x,s)$:

$$\psi(x,t) = \frac{1}{2\pi i} \int_{\sigma-i_\infty}^{\sigma+i_\infty} \bar{\psi}(x,s)\, e^{st}\, ds \tag{4.27}$$

Substituting Eqs. (4.20) and (4.21) into Eq. (4.27) and using the expression for $C_1(s)$ and $C_2(s)$ given by Eq. (4.26) yields:

$$\psi(x,t) = \frac{1}{2\pi i} \int_{\sigma-i_\infty}^{\sigma+i_\infty} \frac{|Z_1(s)|}{|Z(s)|} \sin \bar{B}(a-|x|)\, e^{st}\, ds \quad +$$

$$\frac{1}{2\pi i} \int_{\sigma-i_\infty}^{\sigma+i_\infty} \bar{\psi}_p(x,s)\, e^{st}\, ds \qquad b\leq|x|\leq a \tag{4.28}$$

$$\psi(x,t) = \frac{1}{2\pi i} \int_{\sigma-i_\infty}^{\sigma+i_\infty} \frac{|Z_2(s)|}{|Z(s)|} \cosh \bar{\kappa}|x| \; e^{st} \, ds$$

$$0 \leq |x| \leq b \qquad (4.29)$$

The integral over $\bar{\psi}_p(x,s)$ gives the contribution from fissions caused directly by the source neutrons which die away rapidly compared to the asymptotic mode of the excess prompt neutron flux which is given by the residue at the smallest zero of $|Z(s)|$. It is the decay constant of the asymptotic mode that is measured in the pulsed neutron-beam experiment. The asymptotic solutions of Eqs. (4.28) and (4.29) are given by:

$$\psi_{asym}(x,t) \approx \frac{|Z_1(s_o)|}{\left.\frac{d}{ds}|Z(s)|\right|_{s=s_0}} \sin \bar{B}_0(a-|x|) \; e^{-s_0 t}.$$

$$b \leq |x| \leq a \qquad (4.30)$$

$$\psi_{asym}(x,t) \approx \frac{|Z_2(s_o)|}{\left.\frac{d}{ds}|Z(s)|\right|_{s=s_0}} \cosh \bar{\kappa}_0|x| \; e^{-s_0 t}$$

$$0 \leq |x| \leq b \qquad (4.31)$$

where

$$\bar{B}_0 = \sqrt{B^2 - \frac{s_o}{D_F v}}$$

$$\bar{\kappa}_o = \sqrt{\kappa^2 + \frac{s_o}{D_G v}}$$

The value of s_o is given by the smallest root of the following transcendental equation:

$$\frac{\tan \bar{B}(a-b)}{D_F \bar{B}} = - \frac{\coth \bar{\kappa}\, b}{D_G \bar{\kappa}} \tag{4.32}$$

Equation (4.32) was obtained by setting $|Z(s)| = 0$.

In order to continue this study let us assume some realistic values for the system parameters. The University of Florida Training Reactor (Dun 58) will be used as a guide. In this case the following values are assumed:

$$\begin{aligned} a &= 30 \text{ cm} & \Sigma_{RF} &= 0.10 \text{ cm}^{-1} \\ b &= 15 \text{ cm} & D_F &= 0.25 \text{ cm} \\ \kappa &= 0.04 \text{ cm}^{-1} & \beta &= 0.0064 \\ D_G &= 1.00 \text{ cm} & v &= 2.2 \times 10^5 \text{cm/sec} \end{aligned} \tag{4.33}$$

The reflector region between the fuel slabs in the UFTR is graphite which has a value of 0.02 cm^{-1} for the quantity represented by κ. However, to make the values used in this model more realistic the value of κ has been increased to account for transverse leakage. Likewise, the value of Σ_{RF} is greater than the value for the thermal absorption cross-section in the fuel region of the UFTR in order to account for absorption while slowing down and for transverse leakage.

When these values are inserted into the determinant of Q given by Eq. (4.12), the smallest value of B_m which satisfies the critical condition that $|Q| = 0$ is

$$B_m = 0.1412 \text{ cm}^{-1} \tag{4.34}$$

which requires that

$$\nu\Sigma_f = 0.10498 \text{ cm}^{-1} \tag{4.35}$$

and

$$\frac{A_2}{A_1} = 0.7205$$

Inserting the values given by Eqs. (4.33) and (4.35) into Eqs. (4.18) and (4.19) yields the following expressions for $\bar{B}$ and $\bar{\kappa}$:

$$\begin{aligned} \bar{B} &= 0.00426 \sqrt{948-s} \\ \bar{\kappa} &= 0.00213 \sqrt{352+s} \end{aligned} \tag{4.36}$$

The root of $|Z(s)|$ with the smallest magnitude is at

$$s_o = -73.5 \text{ sec}^{-1} \tag{4.37}$$

Thus, the decay constant of the most slowly decaying mode of the excess prompt neutron flux is equal to -73.5 sec^{-1}.

In the next section the coupled kinetics formulation presented in Chapter II is used to analyze this problem in terms of a 3-point model.

Coupled Point-Model Representation

In terms of the coupled point-model representation the equations describing the kinetics of the flux in the reactor shown in Figure 1 are as follows:

$$\frac{d}{dt} N_1(t) = \left[\frac{1-\beta}{\Lambda_F} + \frac{1}{\tau_F} - \frac{1}{\theta_F}\right] N_1(t) + \frac{1}{\sigma_{G\to F}} N_2(t) \tag{4.38}$$

$$\frac{d}{dt} N_2(t) = -\left[\frac{1}{\theta_G} - \frac{1}{\tau_G}\right] N_2(t) + \frac{1}{\sigma_{F\to G}} N_1(t) + \frac{1}{\sigma_{F\to G}} N_3(t) \tag{4.39}$$

$$\frac{d}{dt} N_3(t) = \left[\frac{1-\beta}{\Lambda_F} - \frac{1}{\theta_F} + \frac{1}{\tau_F}\right] N_3(t) + \frac{1}{\sigma_{G\to F}} N_2(t) \tag{4.40}$$

where

Λ_F = the generation time of the neutrons in region 1 or 3

$[\frac{1}{\theta} - \frac{1}{\tau}]$ = the loss rate of neutrons due to leakage and absorption. Subscript F refers to the fuel regions and subscript G refers to the reflector region

$\frac{1}{\sigma_{G \to F}}$ = the transfer rate of neutrons from the reflector to the fuel

$\frac{1}{\sigma_{G \to F}}$ = the transfer rate of neutrons from the fuel to the reflector

For simplicity only one space mode is considered.

The formulas for evaluating the parameters follow directly from the general theory presented in Chapter II. For clarity they are presented here in terms of this simple example.

$$(\phi^{\dagger}, \frac{1}{v}\,\phi)_F = \frac{A_1^2}{v} \int_b^a \sin^2 B_m(a-x)\,dx \tag{4.41}$$

$$(\phi^{\dagger}, \frac{1}{v}\,\phi)_G = \frac{2A_2^2}{v} \int_o^b \cosh^2 \kappa\, x\, dx \tag{4.42}$$

$$\frac{1}{\Lambda_F} = \frac{(\phi^{\dagger}, \nu\Sigma_f\phi)_F}{(\phi^{\dagger}, \frac{1}{v}\,\phi)_F} = v\nu\Sigma_f \tag{4.43}$$

$$\frac{1}{\sigma_{F \to G}} = \frac{\phi^{\dagger}(b)\, j_-(b)}{(\phi^{\dagger}, \frac{1}{v}\,\phi)_G} \tag{4.44}$$

$$\frac{1}{\sigma_{G \to F}} = \frac{\phi^{\dagger}(b)\, j_+(b)}{(\phi^{\dagger}, \frac{1}{v}\,\phi)_F} \tag{4.45}$$

$$\left[\frac{1}{\theta_F} - \frac{1}{\tau_F}\right] = v\Sigma_{RF} + \frac{(\nabla\phi^{\dagger}, D_F\nabla\phi)_F}{(\phi^{\dagger}, \frac{1}{v}\,\phi)_F} + \frac{\phi^{\dagger}(b)\,j_-(b)}{(\phi^{\dagger}, \frac{1}{v}\,\phi)_F} \tag{4.46}$$

$$\left[\frac{1}{\theta_G} - \frac{1}{\tau_G}\right] = v\Sigma_{RM} + \frac{(\nabla\phi^{\dagger}, D_G\phi)_G}{(\phi^{\dagger}, \frac{1}{v}\,\phi)_G} + \frac{2\phi^{\dagger}(b)\,j_+(b)}{(\phi^{\dagger}, \frac{1}{v}\,\phi)_G} \tag{4.47}$$

$$\phi^{\dagger}(x) = \phi(x) \tag{4.48}$$

$$\begin{aligned} j_{\mp}(b) &= \frac{A_2\cosh\kappa b}{4} \pm \frac{A_2 D_G\,\kappa\sinh\kappa b}{2} \\ &= \frac{A_1\sin B_m(a-b)}{4} \mp \frac{A_1 D_F B_m\cos B_m(a-b)}{2} \end{aligned} \tag{4.49}$$

Expressions for $\phi(x)$ are given by Eqs. (4.11) and (4.12). The parenthesis notation indicates integration over the region specified by the subscript.

Inserting the values given by Eqs. (4.36)-(4.38) into Eqs. (4.41)-(4.49) yields the following values for the kinetics parameters:

$$(\phi^{\dagger}, \frac{1}{v}\phi)_F = 4.125 \times 10^{-5} A_1^2 \tag{4.50}$$

$$(\phi^{\dagger}, \frac{1}{v}\phi)_G = 1.540 \times 10^{-4} A_2^2$$

$$\frac{1-\beta}{\Lambda_F} = 2.2948 \times 10^{4} \text{ sec}^{-1}$$

$$\frac{1}{\sigma_{F\to G}} = 2.378 \times 10^{3} \text{ sec}^{-1}$$

$$\frac{1}{\sigma_{G\to F}} = 4.224 \times 10^{3} \text{ sec}^{-1}$$

$$[\frac{1}{\theta_F} - \frac{1}{\tau_F}] = 2.770 \times 10^{4} \text{ sec}^{-1}$$

$$[\frac{1}{\theta_G} - \frac{1}{\tau_G}] = 4.752 \times 10^{4} \text{ sec}^{-1}$$

Laplace transforming Eqs. (4.38)-(4.40) yields

$$\mathcal{H}(s)\, \vec{\eta}(s) = \vec{\xi} \tag{4.51}$$

$$\tilde{\vec{\eta}} = [\eta_1(s) \quad \eta_2(s) \quad \eta_3(s)] \tag{4.52}$$

$$\tilde{\vec{\xi}} = [1 \quad 1 \quad 1] \tag{4.53}$$

$$\mathcal{H}(s) = \begin{bmatrix} \left\{s - \frac{(1-\beta)}{\Lambda_F} - \frac{1}{\tau_F} + \frac{1}{\theta_F}\right\} & -\frac{1}{\sigma_{G\to F}} & 0 \\ -\frac{1}{\sigma_{F\to G}} & \left\{s - \frac{1}{\tau_G} + \frac{1}{\theta_G}\right\} & -\frac{1}{\sigma_{F\to G}} \\ 0 & -\frac{1}{\sigma_{G\to F}} & \left\{s - \frac{(1-\beta)}{\Lambda_F} - \frac{1}{\tau_F} + \frac{1}{\theta_F}\right\} \end{bmatrix} \tag{4,54}$$

$$\eta_j(s) = \int_0^\infty N_j(t)\, e^{st}\, dt \qquad j = 1,2,3 \tag{4.55}$$

Application of Cramer's rule yields an expression for the $\eta_j(s)$:

$$\eta_j(s) = \frac{|\mathcal{H}_j(s)|}{|\mathcal{H}(s)|} \tag{4.56}$$

where $|\mathcal{H}_j(s)|$ is the determinant of $\mathcal{H}(s)$ with the j-th column replaced by $\vec{\xi}$. The solution of Eqs. (4.38)-(4.40) is given by the inverse Laplace transform of the $\eta_j(s)$:

$$N_j(t) = \frac{1}{2\pi i} \int_{\sigma-i\infty}^{\sigma+i\infty} \frac{|\mathcal{H}_j(s)|}{|\mathcal{H}(s)|}\, e^{st}\, ds \tag{4.57}$$

The solutions of the $N_j(t)$ are given by the sum of three exponential terms determined by the residue at the three zeros of $|\mathcal{H}(s)|$. The smallest root of $|\mathcal{H}(s)|$ is

$$s_o = -74.8\ \text{sec}^{-1}$$

Thus, the value for the prompt neutron decay constant predicted by the coupled kinetics formulation is 1.77 per cent higher than the value predicted by the exact method.

Let us now proceed to an analysis of the problem in terms of the 1-point-model kinetics equation.

1-Point-Model Representation

The 1-point-model kinetics equation for a delayed critical reactor is given by

$$\frac{d}{dt} N(t) = -\frac{\beta}{\Lambda} N(t) \tag{4.58}$$

where λ is the mean generation time averaged over the entire reactor. Note that delayed neutrons have been neglected as in the first two analyses.

The solution of Eq. (4.63) is

$$N(t) = N(0)\, e^{-\frac{\beta}{\Lambda} t} \tag{4.59}$$

The formula for computing $-\frac{\beta}{\Lambda}$ is as follows:

$$-\frac{\beta}{\Lambda} = -\frac{\beta(\phi^{\dagger}, \nu\Sigma_f\phi)_{\text{REACTOR}}}{(\phi^{\dagger}, \frac{1}{v}\phi)_{\text{REACTOR}}}$$

$$= -\frac{2\beta(\phi^{\dagger}, \nu\Sigma_f\phi)_F}{2(\phi^{\dagger}, \frac{1}{v}\phi)_F + (\phi^{\dagger}, \frac{1}{v}\phi)_G}$$

$$= \frac{-\frac{\beta}{\Lambda_F}}{1 + \frac{(\phi^{\dagger}, \frac{1}{v}\phi)_G}{2(\phi^{\dagger}, \frac{1}{v}\phi)_F}}$$

$$= -\frac{147.8}{1 + \frac{0.492}{0.508}}$$

$$= -75.1 \text{ sec}^{-1} \tag{4.60}$$

We see from Eq. (4.60) that the region between the fuel slabs has the effect of decreasing the magnitude of the prompt neutron decay constant and increasing the mean generation time of the reactor. Note that approximately half the weighted neutron population is in region 2. This doubles the mean generation time and as a result slows down the system response.

Comparing the value of the prompt neutron decay constant predicted by the 1-point-model kinetics equation with the exact value indicates an error of 2.2 per cent.

Discussion of the Results

The prompt neutron decay constant as predicted by the three models considered in this study is summarized in the following table:

TABLE 1

SUMMARY OF RESULTS

Model	Decay Constant	Error
Exact	$-73.5\ \text{sec}^{-1}$	-
3-point	$-74.8\ \text{sec}^{-1}$	1.77%
1-point	$-75.1\ \text{sec}^{-1}$	2.20%

The agreement between the three methods of computation is remarkable and speaks well for the variational principle upon which the point-model representations are based. Recall from Chapter II that both the 1-point-model and the 3-point-model are based on the general theory of coupled point-model reactor kinetics developed in Chapter II. This study indicates that, at least for this 1-group approximation, spatial effects are not an important consideration in predicting the asymptotic behavior of the prompt neutrons. Since the 1-point-model does very accurately predict the prompt neutron decay constant, then Rossi-α measurements are meaningful even for this coupled system and one may deduce from measurements of the Rossi-α the quantities ρ and β/Λ for the system. It must be emphasized, however, that broad generalizations should not be made on so simple a model. This model is indeed an over-simplification of the true system. However, in the next chapter the results of an 18-group computation performed on the University of Florida Training Reactor are presented, and it is shown there, also, that an "exact" numerical computation and the 1-point model are in close agreement.

This study has indicated the importance of the graphite reflector in increasing the mean generation time. As shown in Eq. (4.60) approximately one-half of the weighted neutron population was in the reflector between the fuel regions. This doubled the mean generation time. This effect requires that a certain precaution be taken when an equivalent 1-dimensional model is used to represent a core of this type. In a 1-dimensional representation the transverse leakage is assumed to be proportional to the flux. The constant of proportionality is taken to be the product of the diffusion coefficient times the transverse geometric buckling (Gla 52). Now, the transverse buckling is not easily determined for a reactor of this type and this creates a problem when one attempts a 1-dimensional computation. If a single value is assumed for the transverse buckling for all groups in a multigroup calculation, this single value will over-estimate the removal cross-section for the thermal group because the transverse buckling for the thermal group is smaller than this "average" value that is assumed for all groups. Recall from Chapter III that the total removal cross-section Σ_T for the thermal group is given by

$$\Sigma_T = \Sigma_a + DB^2$$

In the fuel the transverse leakage term DB^2 is small compared to the large thermal absorption cross-section Σ_a. As a result, the total removal cross-section in the fuel is not strongly affected by an error in the transverse buckling. However, in the graphite the thermal absorption cross-section is very small and the value of the total removal cross-section is strongly dependent on the transverse leakage term. The significance of this source of error is demonstrated in the next chapter.

One additional problem that must be considered is whether or not the asymptotic decay constant is really due to the prompt neutron die-away. It is conceivable that one might actually be measuring the die-away of the pulsed neutron-beam because of the low thermal absorption cross-section of graphite. The values in Table 2 taken from reference (Per 65) will be used to investigate this possibility.

TABLE 2

THERMAL NEUTRON PARAMETERS AS DETERMINED FROM VARIOUS DIE-AWAY EXPERIMENTS IN GRAPHITE

Investigator	$\alpha_o (\mathrm{sec}^{-1})$	$D_o \times 10^{-5}$ $(\mathrm{cm}^2\ \mathrm{sec}^{-1})$
Lalande (Lal 61)	79.5 ± 3	2.07 ± .04
Starr & Price (Sta 62)		
Type GBF	74.6 ± .06	2.14 ± .01
Type AA	68.1 ± .08	2.19 ± .03
Klose, et al. (Klo 62)	88.3 ± 1.2	2.13 ± .02
Sagot, et al. (Sag 64)	74.1 ± 3	2.19 ± .03

The decay constant of the source is given by

$$\alpha_{\mathrm{SOURCE}} = -\alpha_o - D_o B^2 + O(B^4) \qquad (4.61)$$

where α_o and D_o are given in Table 2 and B^2 is the geometric buckling. Consider the graphite region between the fuel slabs. The geometric buckling of this region can be very well approximated by

$$B^2 \approx \left(\frac{\pi}{2b}\right)^2$$

where 2b is the distance between the fuel slabs. The value of 2b for the model used in this chapter is 30 cm (for the UFTR 2b = 30.48 cm) which gives a value of

$$B^2 \approx \left(\frac{\pi}{30}\right)^2 = 0.011\ \text{cm}^{-2} \tag{4.62}$$

From Table 2 it is seen that

$$\alpha_o \approx 75\ \text{sec}^{-1} \tag{4.63}$$

Substituting the values given by Eqs. (4.62)-(4.64) into Eq. (4.61) yields

$$\alpha_{SOURCE} \approx -2385\ \text{sec}^{-1}$$

Therefore, the pulsed neutron-beam dies away quickly and should not contaminate the asymptotic die-away of the prompt neutrons even if the measurements are made with a detector located in the graphite at the center of the reactor.

Conclusions

A 1-group, 1-dimensional model of a reactor with two weakly coupled fuel regions has been studied. The results show that the 1-point-model kinetics equation gives a reasonably accurate estimate of the asymptotic decay constant in a prompt neutron die-away experiment. This result tends to indicate that spatial effects are not so great as to prohibit the use of a 1-point-model reactor kinetics for analyzing the data from a pulsed neutron-beam experiment. Therefore, one may deduce meaningful system-averaged values for β/Λ and the reactivity from measurements of the asymptotic decay constant.

The fact that the decay constant predicted by the 3-point model was closer to the exact value than was the value predicted by the 1-point model indicates that the coupled formulation converges toward the exact representation as the number of nodes is increased. This result gives confidence in the formulas used to compute the coupling parameters. Actually, using the coupled kinetics equations to determine the asymptotic decay constant introduces unnecessary complexity to the computation. The coupled kinetics equations are better suited for studying space- and energy-dependent effects. In fact the virtue of using this method is that it provides a means of extending static space- and energy-dependent flux computations into the time domain by solving a set of first order differential equations.

CHAPTER V

A DISCUSSION OF COMPUTER CALCULATIONS AND A SUMMARY OF THE RESULTS

Introduction

In this chapter the results of a numerical study of the neutron flux in the University of Florida Training Reactor are presented. Both a 4-group, 2-dimensional and an 18-group, 1-dimensional computation of the flux have been performed. The results of the computations are used to determine the effective delayed neutron fraction, the mean generation time and the kinetics parameters for several coupled point models. A method is also presented for computing the asymptotic decay constant that is measured in a prompt neutron die-away experiment. This method is considered "exact" in the sense that it does not require the assumption of separability that is required in point-model kinetics calculations. The decay constant predicted by the exact method is compared with the decay constant predicted by the 1-point model, as well as by several coupled multiple-point models. This comparison is made in order to check the accuracy of the theory presented in Chapter II. To check the accuracy of the 18-group, 1-dimensional numerical computations, the calculated value of the decay constant is compared with the values measured by a pulsed neutron-beam experiment and by a random noise experiment.

In addition to numerical results a brief discussion of the computer codes that were used is also presented. In the concluding section a procedure is suggested for determining a region-dependent transfer function.

Exact Determination of the Prompt Decay Constant

Since it is the smallest decay constant that is of interest in a prompt neutron die-away experiment, it is possible to use a variational method to determine this parameter. The term "exact" is used in the sense that separability of time and space is not assumed. As far as the "accuracy" of the method is concerned, it is only as good as the model used to represent the UFTR, namely multigroup diffusion theory.

Following the injection of a burst of neutrons into the reactor, the excess prompt neutron flux is described by:

$$\frac{1}{v}\frac{\partial}{\partial t}\psi(\vec{r},E,t) = H\psi(\vec{r},E,t) \tag{5.1}$$

The "excess" prompt neutrons are those neutrons that resulted from fissions caused by the pulsed neutron-beam source. The operator H is given by

$$H\psi(\vec{r},E,t) = (1-\beta)\chi_p(E)\int_{E'} dE'\nu\Sigma_f(\vec{r},E')\psi(\vec{r},E',t) \quad +$$

$$\nabla\cdot D(\vec{r},E)\nabla\psi(\vec{r},E,t) - \Sigma_T(\vec{r},E)\psi(\vec{r},E,t) \quad +$$

$$\int_{E'} dE'\Sigma_s(\vec{r},E'\rightarrow E)\psi(\vec{r},E't) \tag{5.2}$$

where

$$(1-\beta)\chi_p(E) = \chi(E) - \sum_{i=1}^{D} f_i(E)\beta_i$$

$\chi_p(E)$ = prompt neutron fission spectrum

$\chi(E)$ = fission spectrum for all neutrons resulting from a fission

The other symbols have the usual meanings and have been defined in preceding chapters.

Laplace transforming Eq. (5.1) yields:

$$H\bar{\psi}(\vec{r},E,s) = \frac{s}{v}\bar{\psi}(\vec{r},E,s) \tag{5.3}$$

In order to minimize the error in determining s from Eq. (5.3) a variational method will be used. Multiplying Eq. (5.3) by a weighting function $\bar{\psi}^{\dagger}(\vec{r},E,s)$ and integrating over all values of E and $\vec{r}$ yields:

$$\int dE \int d\vec{r}\ \bar{\psi}^{\dagger}(\vec{r},E,s)H\bar{\psi}(\vec{r},E,s) = s\int dE \int d\vec{r}\ \bar{\psi}^{\dagger}(\vec{r},E,s)\ \frac{1}{v}\ \bar{\psi}(\vec{r},E,s) \tag{5.4}$$

Taking variations with respect to s, $\bar{\psi}^{\dagger}$ and $\bar{\psi}$ and requiring δs to vanish yields:

$$\int dE \int d\vec{r}\ [\delta\bar{\psi}^{\dagger}\{H\bar{\psi} - \frac{s}{v}\,\bar{\psi}\} + \delta\bar{\psi}\{H^{\dagger}\bar{\psi}^{\dagger} - \frac{s}{v}\,\bar{\psi}^{\dagger}\}] = 0 \tag{5.5}$$

where the operator $H^{\dagger}$ is the adjoint of H and is defined by (Sel 58):

$$\int_{\text{all } \vec{x}} gH^{\dagger}f\ d\vec{x} \ \equiv\ \int_{\text{all } \vec{x}} fHg\ d\vec{x}$$

Applying the usual argument that $\delta\bar{\psi}^{\dagger}$ and $\delta\bar{\psi}$ in general are non-zero everywhere except at the end points and therefore the terms in curly brackets must be identically zero yields an equation for the weighting function $\bar{\psi}^{\dagger}(\vec{r},E,s)$:

$$H^{\dagger}\bar{\psi}^{\dagger}(\vec{r},E,s) \ = \ \frac{s}{v}\ \psi^{\dagger}(\vec{r},E,s) \tag{5.6}$$

and requires that $\bar{\psi}(\vec{r},E,s)$ satisfy Eq. (5.3). The stationary value of s is given by the following expression obtained from Eq. (5.4):

$$s_o \ = \ \frac{\int dE \int d\vec{r}\ \bar{\psi}^{\dagger}(\vec{r},E,s_o)\ H\ \bar{\psi}(\vec{r},E,s_o)}{\int dE \int d\vec{r}\ \bar{\psi}^{\dagger}(\vec{r},E,s_o)\ \frac{1}{v}\ \bar{\psi}(\vec{r},E,s_o)} \tag{5.7}$$

Equation (5.7) may be written in terms of reactivity, mean generation time, and effective delayed neutron fraction as follows:

$$s_o = \frac{\rho(s_o) - \beta_{eff}(s_o)}{\Lambda(s_o)} \tag{5.8}$$

where $\rho(s_o)$, $\beta_{eff}(s_o)$ and $\Lambda(s_o)$ are given by

$$\rho(s_o) = 1 - \frac{\int dE \int d\vec{r}\ \bar{\psi}^{\dagger}(\vec{r},E,s_o)\ L\bar{\psi}(\vec{r},E,s_o)}{\int dE \int d\vec{r}\ \bar{\psi}^{\dagger}(\vec{r},E,s_o)\chi(E)P\bar{\psi}(\vec{r},E',s_o)} \tag{5.9}$$

$$\beta_{eff}(s_o) = \frac{\sum_{i=1}^{D} \beta_i \int dE \int d\vec{r}\ \bar{\psi}^{\dagger}(\vec{r},E,s_o)f_i(E)P\bar{\psi}(\vec{r},E',s_o)}{\int dE \int d\vec{r}\ \bar{\psi}^{\dagger}(\vec{r},E,s_o)\chi(E)P\bar{\psi}(\vec{r},E',s_o)} \tag{5.10}$$

$$\Lambda(s_o) = \frac{\int dE \int d\vec{r}\ \bar{\psi}^{\dagger}(\vec{r},E,s_o)\ \frac{1}{v}\ \bar{\psi}(\vec{r},E,s_o)}{\int dE \int d\vec{r}\ \bar{\psi}^{\dagger}(\vec{r},E,s_o)\chi(E)P\bar{\psi}(\vec{r},E',s_o)} \tag{5.11}$$

$$P\bar{\psi}(\vec{r},E',s_o) = \int_{E'} dE'\ \nu\Sigma_f(\vec{r},E')\bar{\psi}(\vec{r},E',s_o) \tag{5.12}$$

$$L\bar{\psi}(\vec{r},E,s_o) = -\nabla\cdot D(\vec{r},E)\nabla\bar{\psi}(\vec{r},E,s_o) + \Sigma_T(\vec{r},E)\bar{\psi}(\vec{r},E,s_o) - \int_{E'} dE'\ \Sigma_s(\vec{r},E'\to E)\bar{\psi}(\vec{r},E',s_o) \tag{5.13}$$

Equation (5.8) follows directly from Eq. (5.7) by rearranging Eq. (5.2) in terms of the quantities defined by Eqs. (5.9)-(5.13).

In the usual 1-point-model formulation of Eq. (5.9) separability is assumed and the resulting expressions for ρ, β_{eff}, and Λ are independent of s. In the expressions for ρ, β_{eff}, and Λ the functions $\bar{\psi}^{\dagger}(\vec{r},E,s_o)$ and $\bar{\psi}(\vec{r},E,s_o)$ are replaced by $\psi(\vec{r},E,0)$ which satisfy the following equations

$$H_o\psi(\vec{r},E,0) = 0 \tag{5.14}$$

$$H_o^{\dagger}\psi^{\dagger}(\vec{r},E,0) = 0 \tag{5.15}$$

where

$$\begin{aligned} H_o\psi(\vec{r},E,0) = {} & \chi(E) \int_{E'} dE'\nu\Sigma_f(\vec{r},E)\psi(\vec{r},E,0) + \\ & \nabla\cdot D(\vec{r},E)\nabla\psi(\vec{r},E,0) - \Sigma_T(\vec{r},E)\psi(\vec{r},E,0) + \\ & \int_{E'} dE'\ \Sigma_s(\vec{r},E'\to E)\psi(\vec{r},E',0) \ . \end{aligned} \tag{5.16}$$

The difference between H as given by Eq. (5.2) and H_o is in the fission spectrum. The spectrum of all fission neutrons is contained in H_o whereas only the prompt neutron spectrum reduced by a factor of $(1-\beta)$ is contained in H.

In the numerical computations to be presented later it is the value of s_o given by Eq. (5.8) that is referred to as the "exact" value of the prompt neutron decay constant.

Computer Codes

The objectives for performing computations on the UFTR were the following:

(a) to obtain a set of group constants that well represent the neutronic properties of the UFTR

(b) to perform a detailed computation of the space- and energy-dependent flux and adjoint flux

(c) to compute the mean generation time and the effective delayed neutron fraction

(d) to compute the decay constant of the prompt neutron die-away using the exact method presented in the preceding section, the 1-point approximation and several coupled approximations and to compare the results of these computations with each other and with experimental measurements

To accomplish these objectives it was necessary to utilize a series of computer codes. Figure 2 shows a block diagram of the codes required to go from the initial basic data to the final result, namely the decay constant for the prompt neutron die-away. One additional code that was used in some preliminary investigations is the TWENTY GRAND. The computations performed by these codes are discussed in this section.

Group Constants -- Two codes, TEMPEST (Shu 60) and GAM-I (Joa 61), were used to compute group constants for the UFTR.

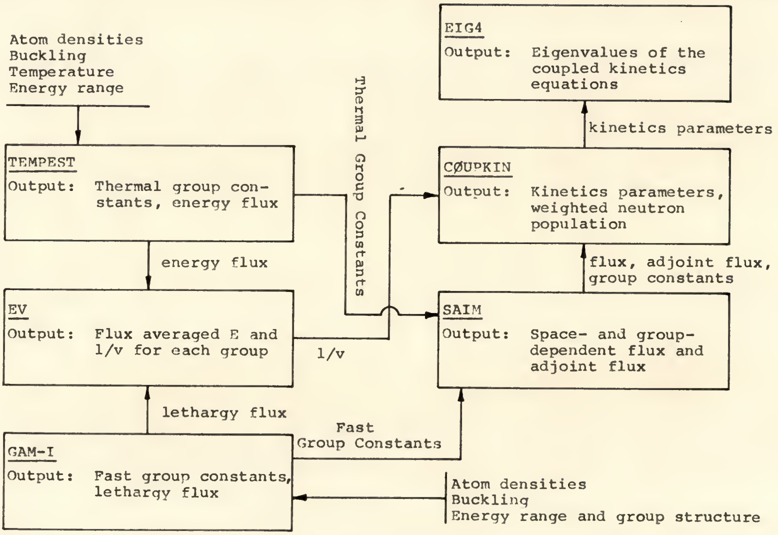
Atom densities
Buckling
Temperature
Energy range
TEMPEST
Output: Thermal group constants, energy flux
Thermal Group Constants
energy flux
EV
Output: Flux averaged E and 1/v for each group
1/v
lethargy flux
GAM-I
Output: Fast group constants, lethargy flux
Fast Group Constants
Atom densities
Buckling
Energy range and group structure
SAIM
Output: Space- and group-dependent flux and adjoint flux
flux, adjoint flux, group constants
CØUPKIN
Output: Kinetics parameters, weighted neutron population
kinetics parameters
EIG4
Output: Eigenvalues of the coupled kinetics equations

Figure 2. Flow Diagram of Several of the Computer Codes Used in the Theoretical Computations

TEMPEST is a neutron thermalization code based upon the Wigner-Wilkins approximation for light moderators and the Wilkins approximation for heavy moderators. For the UFTR computations, the Wigner-Wilkins approximation was used in the fuel regions, and the Wilkins approximation was used in the graphite regions.

GAM-I is a consistent P_1 multigroup code for the calculation of fast neutron spectra and multigroup constants. A very complete description of this code is given in reference (Joa 61).

Flux Computations -- The principle code used in the flux computations was the SAIM code. SAIM is a modification of the FAIM code (Bal 62), a multigroup, 1-dimensional diffusion equation code. This code will handle as many as 18 energy groups, 101 space points, and 20 regions. Neutrons are permitted to scatter from a given group to as many as 8 lower energy groups. Basically, the code solves the equation given by Eq. (3.1). In order to perform the computations required in this study and to expedite the data processing the following modifications were made in the FAIM code:

(1) The nuclear data library was removed because it was not necessary and only increased the running time.

(2) The FAIM code is a chain job and therefore cannot be run under monitor control on the University of Florida computer. After removing the nuclear data library and the subroutines that used this data,

it was possible to reduce the size of the program so that it could be run under monitor control.

(3) The FAIM code has an option in which it will search for the transverse buckling in a region, or in several regions, required to make the reactor have a specified multiplication constant. Thus, the FAIM code will search for a region-dependent transverse buckling, but not a group-dependent transverse buckling. It became necessary to modify the code so that a group-dependent transverse buckling could be determined.

(4) Another modification was the option to perform the partial flux and partial adjoint flux computations discussed in Chapter III.

(5) To expedite data processing an option was added for punched output of the flux, adjoint flux, and input data. This punched output may be read directly into the CØUPKIN code.

Another code that was used for a preliminary calculation of the flux is the TWENTY GRAND, a few-group, 2-dimensional diffusion equation code (Tob 62). This code is capable of solving neutron diffusion problems in cylindrical or slab geometry for 1 to 6 groups. Up to 3000 mesh points may be used. Execution of the code requires an enormous amount of computer time. For example, a 4-group computation with a 50 by 50 mesh point layout requires several hours of running time on the IBM-709 computer. Unfortunately, in its original form this code had no restart option and only wrote the output tape at the completion of the computations. As a result the program might run for several hours without any indication of the convergence of the calculation. To make matters worse, if the desired convergence criteria were not met before the maximum number of iterations were performed, it was necessary to repeat all of these iterations if it were later decided to attain better convergence by performing more interations. Several modifications were made in the code to remove these undesirable limitations. The modifications are summarized as follows:

(1) On-line print-out of convergence information occurs every time the program goes through LØØP iterations, where LØØP is a value set by the user.

(2) The flux is stored on tape at the completion of each LØØP-th iteration.

(3) The user has the option to obtain punched output of the flux and adjoint flux.

(4) A problem may be restarted either with the punched output or with the storage tape.

In addition to group constants, flux, and ajoint flux it is also necessary to compute the average inverse speed of the neutrons in each group. This computation required another computer code which is discussed in the next section.

Computation of the Average Inverse Speed -- In order to compute kinetics parameters it is necessary to determine the average inverse speed of each group. A simple example will serve to illustrate why the average inverse speed is needed instead of the average speed. The mean generation time is given by

$$\Lambda = \frac{\int dE \int d\vec{r}\ \phi^{\dagger}(\vec{r},E)\ \frac{1}{v(E)}\ \phi(\vec{r},E)}{\int dE \int d\vec{r}\ \chi(E)\phi^{\dagger}(\vec{r},E) \int dE'\ \nu\Sigma_f(\vec{r},E')\phi(\vec{r},E')} \tag{5.17}$$

Note that it is the reciprocal of v(E) that appears under the integral in the numerator of Eq. (5.17). In terms of multigroup diffusion theory the mean generation time is given by

$$\Lambda = \frac{\sum_{i=1}^{N} \int d\vec{r}\ \phi^{\dagger i}(\vec{r}) \left\langle\frac{1}{v}\right\rangle^{i} \phi^{i}(\vec{r})}{\sum_{j=1}^{N} \sum_{i=1}^{N} \int d\vec{r}\ \chi^{i}\phi^{\dagger i}(\vec{r})\ \nu\Sigma_f^{j}(\vec{r})\ \phi^{j}(\vec{r})} \tag{5.18}$$

where

$\phi^{i}(\vec{r})$ = the flux in group i at point $\vec{r}$

$\phi^{\dagger i}(\vec{r})$ = the adjoint of the flux in group i at point $\vec{r}$

$\left\langle\frac{1}{v}\right\rangle^{i}$ = the average inverse speed of the neutrons in group i. This average is also space-dependent if the neutron spectrum is space-dependent

Equation (5.18) indicates that the generation time is directly proportional to the inverse speed of the neutrons. Therefore, one should be careful in his selection of a method of averaging, as well as in the arithmetic computations. Consider the difference between $\left\langle \frac{1}{v} \right\rangle$ and $\frac{1}{\langle v \rangle}$ for neutrons with a Maxwell-Boltzmann distribution. $\left\langle \frac{1}{v} \right\rangle$ is given by

$$\left\langle \frac{1}{v} \right\rangle = \frac{\int_0^\infty \frac{1}{v(E)} n(E)\, dE}{\int_0^\infty n(E)\, dE} \tag{5.19}$$

and $\langle v \rangle$ is given by

$$\langle v \rangle = \frac{\int_0^\infty v(E)\, n(E)\, dE}{\int_0^\infty n(E)\, dE} \tag{5.20}$$

where

$$n(E) = M(E) = \left(\frac{4}{\pi}\right)^{\frac{1}{2}} \frac{1}{(kT)^{3/2}} E^{\frac{1}{2}} e^{-E/kT}$$

neutrons per unit energy (Ros 61)

(5.21)

$$v(E) = 1.38 \times 10^9 \sqrt{E} \quad \text{cm/sec (Gla 52)}$$

(5.22)

T = temperature, °K

k = the Boltzmann constant

$= 8.6275 \times 10^{-5}$ ev/°K

E = energy, MeV

Substituting Eqs. (5.21) and (5.22) into Eqs. (5.19) and (5.20) and performing the integration yields:

$$\left\langle \frac{1}{v} \right\rangle = \frac{4}{\pi} \frac{1}{\langle v \rangle}$$

$$= \frac{1.273}{\langle v \rangle} \tag{5.23}$$

It is seen from this computation that a significant error may be introduced by using $\frac{1}{\langle v \rangle}$ instead of $\left\langle \frac{1}{v} \right\rangle$. The result of this example justifies the somewhat elaborate averaging procedure which follows.

Let us first consider the average inverse speed for the thermal group. In addition to the thermal group constants the TEMPEST code also prints out values for the energy flux F^i, where:

F^i = the flux of neutrons per unit energy in the energy interval ΔE_i

$\Delta E_i = E_i - E_{i-1} \qquad i \geq 1$

Making the substitutions:

$n(E) = \phi(E)/v(E)$

and

$$v(E) = 1.38 \times 10^9 \sqrt{E}$$

into Eq. (5.19) yields:

$$\left\langle \frac{1}{v} \right\rangle = \frac{1}{1.38 \times 10^9} \frac{\int_0^{E_{MAX}} E^{-1} \phi(E)\, dE}{\int_0^{E_{MAX}} E^{-\frac{1}{2}} \phi(E)\, dE}$$

$$\approx \frac{1}{1.38 \times 10^9} \frac{\sum_{i=1}^{N} \left\langle E^{-1} \right\rangle^i F^i \Delta E_i}{\sum_{i=1}^{N} \left\langle E^{-\frac{1}{2}} \right\rangle^i F^i \Delta E_i} \qquad (5.24)$$

E_{MAX} = the upper bound of the thermal group

N = the number of energy increments into which the range from zero to E_{MAX} is divided

Maxwellian averaged values are used for $\left\langle E^{-1} \right\rangle^i$ and $\left\langle E^{-\frac{1}{2}} \right\rangle^i$. These values are given by the following expressions:

$$\left\langle E^{-1} \right\rangle^i = \frac{\int_{E_{i-1}}^{E_i} E^{-1} M(E)\, dE}{\int_{E_{i-1}}^{E_i} M(E)\, dE} \qquad (5.25)$$

$$\left\langle E^{-\frac{1}{2}} \right\rangle^i = \frac{\int_{E_{i-1}}^{E_i} E^{-\frac{1}{2}} M(E)\, dE}{\int_{E_{i-1}}^{E_i} M(E)\, dE} \tag{5.26}$$

Substituting Eq. (5.21) into Eqs. (5.25) and (5.26) and integrating, yields

$$\left\langle E^{-1} \right\rangle^i = 2 \left\{ \frac{E_i\, e^{-E_i/kT} - E_{i-1}\, e^{-E_{i-1}/kT}}{\Delta_i} + \frac{1}{kT} \right\} \tag{5.27}$$

$$\left\langle E^{-\frac{1}{2}} \right\rangle^i = \frac{kT}{\Delta_i} \left\{ e^{-E_{i-1}/kT} - e^{-E_i/kT} \right\} \tag{5.28}$$

$$\Delta_i \approx \left\{ \frac{E_i\, e^{-E_i/kT} + E_{i-1}\, e^{-E_{\lambda-1}/kT}}{2} \right\} \Delta E_i \tag{5.29}$$

The expressions for averaging the inverse speed of the neutrons above thermal are in terms of lethargy rather than energy. In addition to the fast group constants the GAM-I code also prints out values for the lethargy flux, G^i, where

G^i = the flux of neutrons per unit lethargy in the lethargy interval ΔU_i

$\Delta U_i = U_i - U_{i-1} \qquad i \geq 1$

The relationship between lethargy and energy is given by

$$E = 10\, e^{-U}$$

and the speed of a neutron with lethargy U is expressed by

$$V(U) = \sqrt{10} \times 1.38 \times 10^{9}\ e^{-U/2}$$

In terms of lethargy the average inverse speed for some I-th fast group is given by

$$\left\langle \frac{1}{v} \right\rangle^{I} = \frac{\int_{U_{i-1}}^{U_i} \frac{1}{v(U)}\, n(U)\, dU}{\int_{U_{i-1}}^{U_i} n(U)\, dU}$$

$$= \frac{1}{\sqrt{10} \times 1.38 \times 10^{9}} \; \frac{\int_{U_{i-1}}^{U_i} e^{U}\, \phi(U)\, dU}{\int_{U_{i-1}}^{U_i} e^{U/2}\, \phi(U)\, dU}$$

$$\simeq \frac{1}{\sqrt{10} \times 1.38 \times 10^{9}} \; \frac{\sum_{i \epsilon I} \left\langle e^{U} \right\rangle^{i} G^{i}\, \Delta U_i}{\sum_{i \epsilon I} \left\langle e^{U/2} \right\rangle^{i} G^{i}\, \Delta U_i} \tag{5.30}$$

Lethargy averaged values are used for $\left\langle e^{U}\right\rangle^{i}$ and $\left\langle e^{U/2}\right\rangle^{i}$. These values are given by the following expressions

$$\left\langle e^{U}\right\rangle^{i} = \frac{\int_{U_{i-1}}^{U_i} e^{U}\, dU}{\Delta U_i}$$

$$= \frac{e^{U_i} - e^{U_{i-1}}}{\Delta U_i} \qquad (5.31)$$

and similarly,

$$\left\langle e^{U/2}\right\rangle^{i} = \frac{2(e^{U_i/2} - e^{U_{i-1}/2})}{\Delta U_i} \qquad (5.32)$$

A code, called EV, has been written to compute values for the average inverse speed using the method discussed in this section. In addition to the inverse speed the program also computes the average energy of each group.

Computation of the Kinetics Parameters -- A code has been written to perform the computation of kinetics parameters according to the multigroup formulation presented in Chapter III. The name of the code is CØUPKIN. It is designed to take the punched output from the SAIM code without additional processing. The code is dimensioned to compute the coupling parameters for a reactor described by up to 20 broad regions and up to 18 broad groups. It will perform computations for 1-dimensional slab, spherical or cylindrical geometries. Numerical integrations are performed with the use of a modified trapezoidal rule given on page 118 of reference (Mil 49), and numerical derivatives are computed with a 5-point scheme given on page 97 of reference (Mil 49).

Eigenvalue Computations -- The eigenvalues in this study were computed with a subroutine, EIG4, obtained from Ray Booth. The subroutine was originally obtained through SHARE and has the identification name NU EIG4 (Par 63). This subroutine computes the eigenvalues of a given complex N x N matrix for $2 \leq N \leq 70$. It was only necessary for the author to write a calling program in order to use this subroutine.

Results of UFTR Computations

Figure 3 shows a schematic drawing of the core of the UFTR. A more detailed description of the core is given in Thompson's thesis (Tho 61). All of the computations presented in this study are based on a 3500 g U-235 loading of 20 per cent enriched uranium. The atom densities for this arrangement are given in Table A-1 of the Appendix. For this loading the value of k_{eff} as determined by positive period measurements is in the range of 1.0030 to 1.0057 depending on the fuel arrangement, water temperature, and

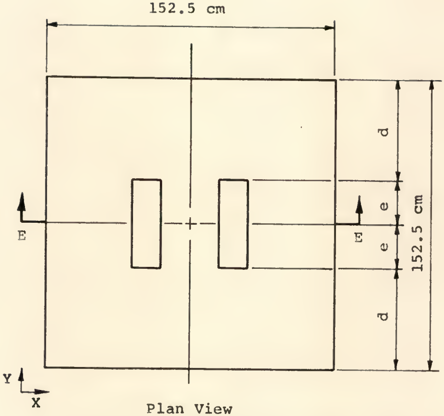

Plan View
Two-Dimensional Representation

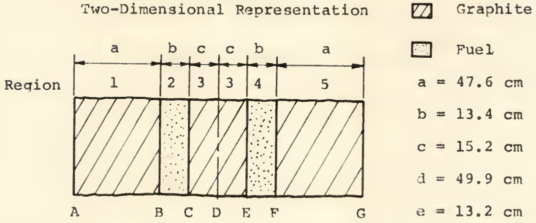

Section E-E

One-Dimensional Representation
of UFTR

Figure 3. Schematic Drawing of the University of Florida Training Reactor

any extraneous poison that might be present in the core (But 64). In this study a value of 1.0057 was assumed for k_{eff} with all control blades removed and with a core temperature of 300°K.

Before undertaking an 18-group calculation, 4-group calculations were made with the SAIM and TWENTY GRAND codes. The 4-group SAIM results were checked against the output of the old version of the FAIM code for verification that the SAIM code was performing properly. The 4-group TWENTY GRAND output was used to obtain an estimate of the buckling. The original group constant calculations were based on experimentally measured values of the buckling reported in Thompson's thesis. Then, after the 4-group computations were made, the estimated values of the buckling were revised. On the basis of hand calculation using the output from TWENTY GRAND, the values given in Table 3 were used in the final computation of the constants for 18 groups. In computing values for the total buckling of a given region it was assumed that the buckling in the vertical direction equals that in the Y direction. The X and Y directions are shown in Figure 3. The vertical direction is normal to the X-Y plane. The group constants used in the 4-group computations are listed in Butterfield's thesis (But 65). For the 18-group computations the constants are listed in Tables A-2 through A-6 in the Appendix. The values of χ^i given in Table A-5

TABLE 3

BUCKLING VALUES USED IN GROUP CONSTANT CALCULATIONS

Group	B^2 (cm^{-2})		
	Regions 1 & 5	Regions 2 & 4	Region 3
1,2,3,4	-0.0101	0.0112	-0.00304
5,6,7,8,9,10,11	-0.00516	0.00421	0.00239
12,13,14,15,16,17	-0.00145	0.00312	0.00250
18	0.00282	0.00222	0.00282

were obtained from values taken from ANL-5800 (Arg 63) manipulated in the following manner.

Table 1-11 of ANL-5800 gives the U-235 prompt fission spectrum as a function of lethargy and Table 1-17 gives the mean energies of the delayed groups. In terms of the prompt fission spectrum and the delayed fission spectrum the total fission spectrum is given by

$$\chi(U) = (1-\beta)F(U) + \sum_{j=1}^{6} \delta(U-\bar{U}_j)\beta_j$$

where

$F(U)$ = the prompt fission spectrum

$\bar{U}_j$ = the average lethargy of the j-th delayed group

The value of χ^i in Table A-5 is given by

$$\chi^i = \int_{U_{i-1}}^{U_i} \chi(U)\, dU$$

$$\chi^i = (1-\beta)\int_{U_{i-1}}^{U_i} F(U)\, dU + \sum_{j=1}^{6} \beta_j \int_{U_{i-1}}^{U_i} \delta(U-\bar{U}_j)\, dU \tag{5.33}$$

The integral over F(U) is given in Table 1-11 and mean energies corresponding to $\bar{U}_j$ are given in Table 1-17.

The EV code was used to compute the average inverse speed and average energy of the neutrons in each group and these values are given in Tables A-7 and A-8 of the Appendix. Since the neutrons in the thermal group have a Maxwell-Boltzmann distribution, we may use the following formula (Ros 61) based on the kinetic theory of gases to compute an effective neutron temperature T_n (Meg 60):

$$\langle E \rangle = \frac{3}{2} k T_n$$

where $\langle E \rangle$ is given in Table A-8 and k is the Boltzmann constant. The effective neutron temperature for the thermal neutrons in the fuel region is 153°C and in the graphite it is 93°C. On the basis of differential measurements of the spectrum at the center of the UFTR Salah determined a value of 115 ± 6°C for T_n and using an integral method he found a value of 76 ± 2.9°C (Sal 64). The theoretical value of 93°C is bracketed by the two measured values.

In performing a 1-dimensional calculation of a 3-dimensional core it is necessary to account for neutron diffusion in the transverse direction by a buckling term. If the flux in the transverse direction in known, the buckling can be computed according to the formula

$$B^2 = \frac{\int dE \int d\vec{r}\, \phi^\dagger(\vec{r},E) \nabla^2{}_{y,z} \phi(\vec{r},E)}{\int dE \int d\vec{r}\, \phi^\dagger(\vec{r},E)\, \phi(\vec{r},E)}$$

where $\nabla^2{}_{y,z}$ is the Laplacian in the Y-Z plane. However, in these calculations since the value of B^2 was not known very accurately as compared to the value of k_{eff}, a search was made by the SAIM code for the value of the transverse buckling that would yield a value of 1.0057 for k_{eff}. A constant value was assumed for all groups and all regions. The search yielded a value of 0.00254 cm^{-2} for the transverse buckling. A search was then made to determine the amount of thermal group poison that must be added to region 2 in order to reduce k_{eff} from 1.0057 to 1.0000. This search yielded a value of 0.00109 cm^{-1} for the macroscopic cross-section of the poison. The CØUPKIN code was then used for computing β_{eff} and Λ averaged over all groups and all space points. The resulting values were $\beta_{eff} = 0.00696$ and $\Lambda = 188$ μsec which gives a value of 37.0 sec^{-1} for β_{eff}/Λ.

According to the 1-point-model approximation, the decay constant of the prompt neutron die-away for a reactor pulsed at delayed critical is given by the ratio of β_{eff}/Λ. However, according to Butterfield's measurements (But 65) the decay constant at delayed critical is 22.2 ± 0.5 sec^{-1}, and according to random noise measurements made by Kavipurapu (Kav 64), the value is 29 ± 5 sec^{-1} (the error of ±5 was suggested by Ohanian (Oha 65) because of poor statistics in the data). It was at first thought that the wide discrepancy between the theoretical value and the experimental value was due to the inability of 1-point-model kinetics to accurately predict the decay constant for a reactor with weakly coupled fuel regions. However, when an exact computation of the decay constant was found to be within a few per cent of the 1-point-model value, it became apparent that the discrepancy must be due to some computational error.

The simple problem that was analyzed in Chapter IV gave a clue as to where a major portion of the apparent error might result. Consider the thermal group. The mean generation time averaged over all groups and all regions is strongly dependent on the weighted neutron population in the thermal group. Since most of the thermal neutrons are in the graphite, then the mean generation time is strongly dependent on the removal cross-section in the thermal group. The thermal removal cross-section is given by

$$\Sigma_T^{th} = \Sigma_a^{th} + D^{th}B^2$$

For the graphite $\Sigma_a^{th} = 0.000241 \text{ cm}^{-1}$, $D^{th} = 0.9156$ cm and if $B^2 = 0.00254 \text{ cm}^{-2}$, then

$$\Sigma_T^{th} = 0.000241 + 0.00233 = 0.00257 \text{ cm}^{-1}$$

In this case approximately 90 per cent of the thermal removal in the graphite is attributed to transverse leakage.

Let us examine Figures 4 through 7. These figures indicate that the distribution of the flux is not strongly region-dependent; however, observe the change in curvature from one group to the next. To emphasize the difference in curvature and to obtain an approximate value for the transverse buckling, each curve has been fitted with a

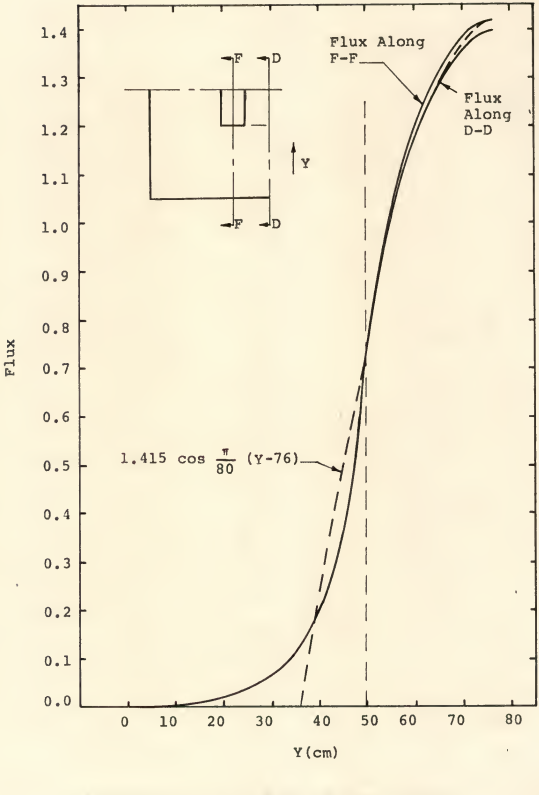

Figure 4. Group 1 Flux as Computed by the TWENTY GRAND Code

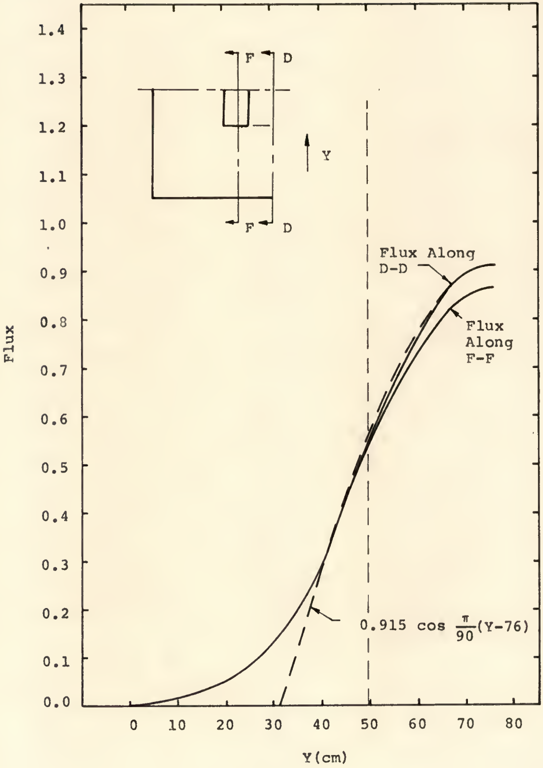

Figure 5. Group 2 Flux as Computed by the TWENTY GRAND Code

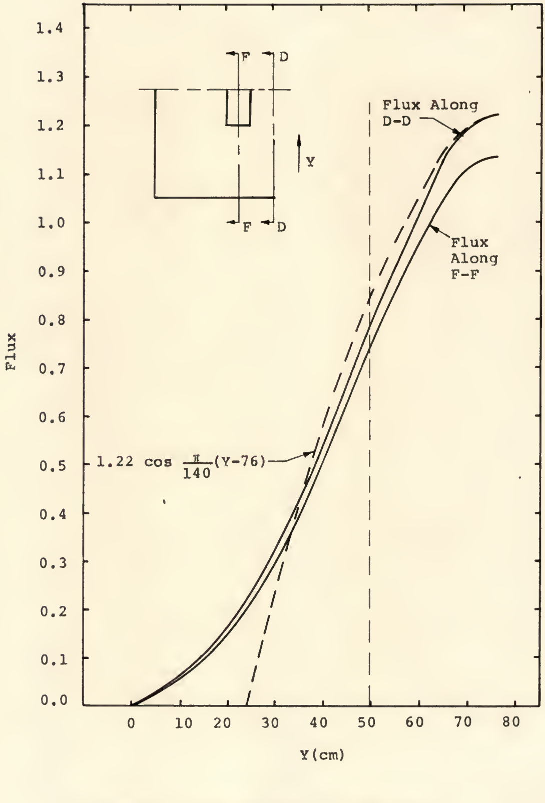

Figure 6. Group 3 Flux as Computed by the TWENTY GRAND Code

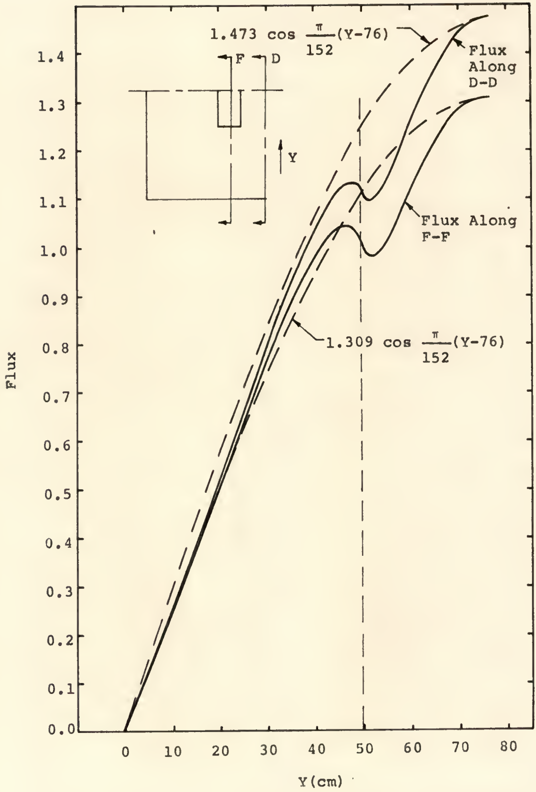

Figure 7. Group 4 (Thermal) Flux as Computed by the TWENTY GRAND Code

cosine shape. Values were obtained for the transverse buckling for the top three groups by assuming that the flux has the same shape in the vertical direction as in the Y direction. For the thermal group the actual height of the graphite, 142 cm, was used to compute the vertical buckling which was added to the buckling in the Y direction to obtain the transverse buckling. These values are listed in Table 4.

Another flux computation was performed with the SAIM code. In this computation the transverse buckling for the thermal group was held constant at $0.000921\ \mathrm{cm}^{-2}$ and a search was made in groups 1 through 17 that would yield a value of 1.0057 for k_{eff}. A value of $0.00304\ \mathrm{cm}^{-2}$ was determined for the transverse buckling. A search was then made to determine the amount of thermal group poison that must be added to region 2 in order to reduce k_{eff} from 1.0057 to 1.0000. This search yielded a value of $0.000909\ \mathrm{cm}^{-1}$ for the macroscopic cross-section of the poison. When the COUPKIN code was used to compute β_{eff} and Λ, their values were determined to be $\beta_{eff} = 0.00703$ and $\Lambda = 247.5\ \mu\mathrm{sec}$ which gives a value of $28.4\ \mathrm{sec}^{-1}$ for β_{eff}/Λ. This value agrees reasonably well with the experimentally measured values given earlier. Also, Chastain (Cha 61) deduced from transfer function measurements a value of 240 μsec for the prompt neutron generation time which is in good agreement with the calculated value of Λ.

TABLE 4

GROUP-DEPENDENT VALUES OF THE TRANSVERSE BUCKLING OBTAINED FROM THE TWENTY GRAND COMPUTATIONS

Group (Based on a 4-group Calculation)	Transverse Buckling (cm^{-2})
1	0.00309
2	0.00245
3	0.00182
4	0.000921

On the basis of the preceding comparison of calculated values with measured values, it appears that the computed group constants give a fairly accurate description of the neutronic properties of the UFTR in terms of multigroup diffusion theory. Certainly, the breach between theory and experiment has been closed, e.g., the prompt neutron generation time given in the hazards report for the UFTR (Dun 58) is 140 μsec which is far below any values deduced from experimental measurements. Of course, refinements can be made in these flux calculations and several are suggested later in this section.

To check the accuracy of the 1-point model an exact computation of the decay constant was performed. Also, several coupled representations were included in the study. The results of these computations are listed in Table 5. Values for the coupled kinetics parameters are given in Tables 6, 7 and 8. The nomenclature for the coupled representation is as follows: for the 2-broad-region representation, broad-region 1 extends from A to D shown in Section E-E of Figure 3 and broad-region 2 extends from D to G; for the 3-broad-region representation, broad-region 1 extends from A to C, broad-region 2 extends from C to E and broad-region 3 extends from E to G; and for the 2-broad-group representation, broad-group 1 includes the first seventeen groups and broad-group 2 is the thermal group. The use of these parameters for studying space-dependent kinetics is discussed in a later section.

TABLE 5

VALUES OF THE DECAY CONSTANT FOR THE PROMPT NEUTRON DIE-AWAY

Model	Number of Points in Phase Space	Decay Constant (sec^{-1})
Exact	-	-27.6
1-broad-region, 1-broad-group	1	-28.4
2-broad-regions, 1-broad-group	2	-27.6
3-broad-regions, 1-broad-group	3	-28.4
2-broad-regions, 2-broad-groups	4	-28.0
3-broad-regions, 2-broad-groups	6	-27.9

TABLE 6

KINETICS PARAMETERS FOR A 2-REGION AND A 3-REGION REPRESENTATION OF THE UFTR

j	k	$(\phi^{\dagger}, \frac{1}{v}\phi)_{j_l}$	$\frac{1-\beta_{j_{l+1}}}{\Lambda_{j_{l+1}}}$ (sec^{-1})	$\frac{1}{\tau_{j_{l+1}}}$ (sec^{-1})	$\frac{1}{\theta_{j_{l+1}}}$ (sec^{-1})	$\frac{1}{\sigma_{k \to j_l}}$ (sec^{-1})	$\frac{\beta_{j_{l+1}}}{\Lambda_{j_{l+1}}}$ (sec^{-1})	$\frac{\beta_{j_{l+1}}}{\beta}$
2-broad-regions and 1-broad-group								
1	2	0.464266	3.93062(+3)	3.52884(+4)	4.20248(+4)	2.77994(+3)	2.77780(+1)	1.09648
2	1	0.535733	4.08307(+3)	3.65257(+4)	4.30206(+4)	2.38279(+3)	2.89308(+1)	1.09932
		3-broad-regions and 1-broad-group						
1	2	0.264687	6.89437(+3)	5.28898(+4)	6.50199(+4)	5.19023(+3)	4.87232(+1)	1.09648
2	1	0.412325	0.0	1.20996(+4)	1.99212(+4)	3.61161(+3)	0.0	0.0
2	3	--	--	--	--	4.21084(+3)	--	--
3	2	0.322986	6.77248(+3)	5.25182(+4)	6.42084(+4)	4.86904(+3)	4.79867(+1)	1.09932

Note: Number in parentheses indicates the power of 10 by which the given value is to be multiplied.

TABLE 7

KINETICS PARAMETERS FOR A 2-REGION, 2-GROUP REPRESENTATION OF THE UFTR

j	k	α	γ	$(\phi^{\dagger}, \frac{1}{v}\phi)_{\substack{j\\ \alpha}}$	$\frac{1-\beta_{\substack{j\\ \gamma\to\alpha}}}{\Lambda_{\substack{j\\ \gamma\to\alpha}}}$ (sec^{-1})	$\frac{1}{\tau_{\substack{j\\ \gamma\to\alpha}}}$ (sec^{-1})	$\frac{1}{\theta_{\substack{j\\ \alpha}}}$ (sec^{-1})	$\frac{1}{\sigma_{\substack{k\to j\\ \alpha}}}$ (sec^{-1})	$\frac{\beta_{\substack{j\\ \gamma\to\alpha}}}{\Lambda_{\substack{j\\ \gamma\to\alpha}}}$ (sec^{-1})	$\frac{\beta_{\substack{j\\ \alpha\to\gamma}}}{\beta}$
1	2	1	1	0.011985	8.84166(+3)	1.22230(+6)	1.42677(+6)	5.11171(+4)	6.24840(+1)	1.09647
1	2	1	2	--	1.43419(+5)	0.0	--	--	1.01356(+3)	1.09648
1	2	2	1	0.452281	0.0	3.83361(+3)	5.33008(+3)	1.49905(+3)	0.0	0.0
2	1	1	1	0.013908	9.08769(+3)	1.25764(+6)	1.45947(+6)	4.33438(+4)	6.43885(+1)	1.09928
2	1	1	2	--	1.48183(+5)	0.07790(+3)	--	--	1.04996(+3)	1.09933
2	1	2	1	0.521825	0.0	3.97790(+3)	5.26641(+3)	1.29101(+3)	0.0	0.0

Note: Number in parentheses indicates the power of 10 by which the given value is to be multiplied.

TABLE 8

KINETICS PARAMETERS FOR A 3-REGION,
2-GROUP REPRESENTATION OF THE UFTR

j	k	α	γ	$(\phi^{\dagger}, \frac{1}{v}\phi)_{j_{\alpha}}$	$\frac{1-\beta_{j_{\gamma\to\alpha}}}{\Lambda_{j_{\gamma\to\alpha}}}$ (sec^{-1})	$\frac{1}{\tau_{j_{\gamma\to\alpha}}}$ (sec^{-1})	$\frac{1}{\theta_{j_{\alpha}}}$ (sec^{-1})	$\frac{1}{\sigma_{k\to j_{\alpha}}}$ (sec^{-1})	$\frac{\beta_{j_{\gamma\to\alpha}}}{\Lambda_{j_{\gamma\to\alpha}}}$ (sec^{-1})	$\frac{\beta_{j_{\gamma\to\alpha}}}{\beta}$
1	2	1	1	0.007339	1.44380(+4)	1.68707(+6)	2.04241(+6)	1.05104(+5)	1.02033(+2)	1.09647
1	2	1	2	--	2.34197(+5)	--	--	--	1.65509(+3)	1.09648
1	2	2	1	0.257348	0.0	6.28324(+3)	8.62513(+3)	2.34070(+3)	0.0	0.0
2	1	1	1	0.009680	0.0	4.90227(+5)	7.08344(+5)	1.00318(+5)	0.0	0.0
2	1	2	1	0.402642	0.0	6.03887(+2)	3.36924(+3)	1.28646(+3)	0.0	0.0
2	3	1	1	--	0.0	--	--	1.17807(+5)	0.0	0.0
2	3	2	1	--	0.0	--	--	1.47960(+3)	0.0	0.0
3	2	1	1	0.008873	1.42449(+4)	1.69197(+6)	2.04083(+6)	1.00585(+5)	1.00928(+2)	1.09928
3	2	1	2	--	2.32276(+5)	--	--	--	1.64580(+3)	1.09933
3	2	2	1	0.314116	0.0	6.20634(+3)	8.37223(+3)	2.16521(+3)	0.0	0.0

Note: Number in parentheses indicates the power of 10 by which the given number is to be multiplied.

In Table 5 the values given by the coupled point-model representation are only good to two significant figures. The determinants from which these eigenvalues are computed have elements of the order of 10^3 to 10^6 and although each element is accurate to four significant figures, accuracy is lost in taking small differences between large numbers. The next to the smallest eigenvalues in each of the coupled representations is approximately -5000 $\sec^{-1}$. In all cases all of the eigenvalues are pure real. The numerical accuracy in determining the decay constant from the exact computation and the 1-point-model computation is much better because both of these methods only require taking the ratio of two values which are accurate to four significant figures. In comparing the value given by the exact computation with that given by the 1-point model, it is observed that they differ by only 2.9 per cent.

The agreement between the exact computation and the 1-point approximation as well as the coupled approximations is very good. Much of the difference between the theoretical computation and the experimental measurements can be attributed to the difficulty in representing the UFTR by a 1-dimensional model. There are some definite improvements that can be made in the theoretical computations. The following suggestions are offered to anyone who might find it necessary to refine the computations.

(1) The TWENTY GRAND calculations should be repeated using a refined set of cross-sections and group-dependent values for the vertical buckling. Table 9 gives the recommended energy boundaries for a 4-group calculation, the total buckling to be used in the group constant calculations, and the group-dependent vertical buckling for the TWENTY GRAND calculation. For these computations symmetry may be assumed and only one quadrant of the core need be considered. This TWENTY GRAND calculation would require about two hours of time on the University of Florida IBM-709 computer or about one hour on the CDC-1604 computer at the Oak Ridge National Laboratory. If the problem is run on the CDC-1604 computer, punched output should be requested.

(2) The revised TWENTY GRAND calculations may be used to obtain better values of the transverse buckling and the total buckling. These revised values for the buckling based on the 4-group calculation, may then be used to compute a new set of group constants for an 18-group calculation.

(3) The values given in Table 7 show that 97.3 per cent of the weighted neutron population. i.e., $\phi^{\dagger} 1/v\ \phi$, is in the thermal group. Because of the significance of the thermal neutrons in the UFTR, one should give some consideration to performing a multigroup calculation with several thermal groups.

In the course of this study several volumes of numerical data have accumulated. The computer output has been bound and labeled and is available to anyone who requests it. Also, the group constants, the output from the TWENTY GRAND calculations, and the output from the SAIM runs are on punched cards. Given the format, a user may process this information to suit his needs. The output from

TABLE 9

RECOMMENDED BUCKLING VALUES FOR FUTURE CALCULATIONS

Group	Lethargy* Upper Boundary	Vertical Buckling All Regions (cm^{-2})	Total Buckling (cm^{-2})		
			Regions 1 & 5	Regions 2 & 4	Region 3
1	3.0	0.00154	-0.00861	0.0134	-0.00882
2	7.0	0.00122	0.00432	0.00216	0.00376
3	16.5	0.000910	0.00147	0.00290	0.00209
4	∞	0.000490	0.00305	-0.0130	0.00306

* A lethargy of zero corresponds to an energy of 10 MeV.

the final SAIM run is summarized in Figures 8 through 11. The values in these graphs were obtained using a transverse buckling of 0.000921 cm^{-2} for the thermal group and 0.00304 cm^{-2} for the other groups with a thermal poison cross-section of 0.000909 cm^{-1} in region 2. The values in these four figures all have the same normalization.

The results of the numerical computations presented in this section have shown that the 1-point model is adequate to predict the asymptotic decay constant measured in a pulsed neutron-beam experiment. Therefore, it is not necessary to use a more elaborate kinetics model to analyze this experiment. However, if it is the transfer function that is being measured, then it is necessary to use a set of coupled point models whose behavior is described by the set of coupled kinetics equations derived in Chapter II. In the next section it is shown how the numerical values given in Tables 6, 7 and 8 may be used to predict the response of one region of the reactor due to a time-dependent perturbation in another region.

Parameters for a Space-Dependent Kinetics Study

In the section entitled Application to the Pile Oscillator Experiment in Chapter II a region- and group-dependent transfer function was derived. Values for all of the parameters appearing in this transfer function are given in Tables 6, 7 and 8 for a 1-mode representation of the flux. If the input perturbation is a time varying

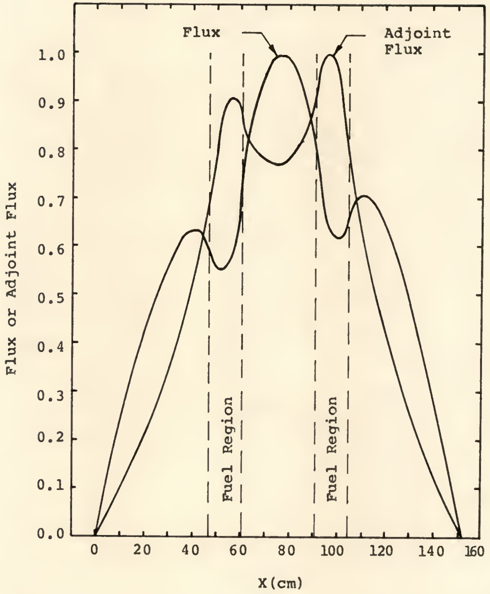

Figure 8. Flux and Adjoint Flux for the Thermal Group as Computed by SAIM

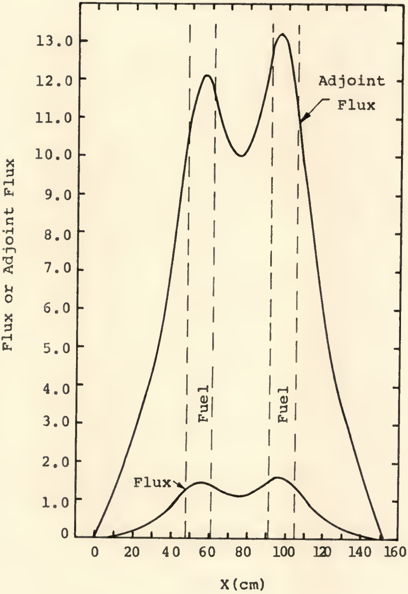

Figure 9. Flux and Adjoint Flux Summed Over the Groups Above Thermal as Computed by SAIM

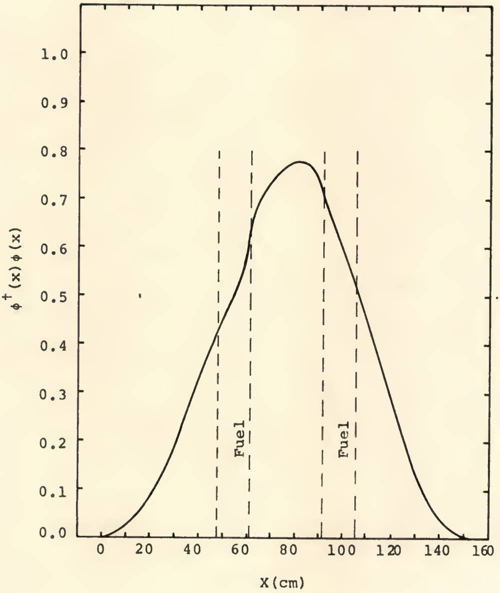

Figure 10. Adjoint Weighted Flux for the Thermal Group

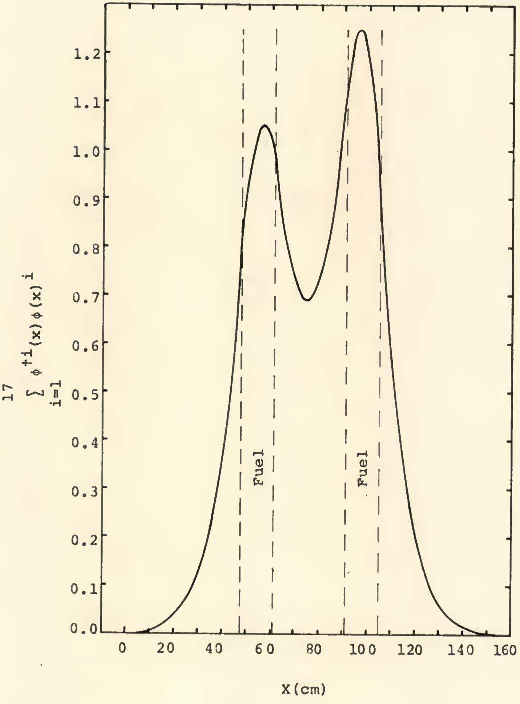

Figure 11. Adjoint Weighted Flux for the Neutrons Above Thermal

thermal group poison, the parameter $\varepsilon_{\substack{k'\\ \gamma'}}(t)$ representing the input perturbation is given by:

$$\varepsilon_{\substack{k'\\ \gamma'}}(t) = \frac{\left\{\int_{E_{\gamma'}} dE \int_{\text{Vol. of poison}} d\vec{r}\; \Phi^{\dagger}\Phi\Sigma_p\right\} f(t)}{\left\{(D\nabla\Phi^{\dagger}\cdot\nabla\Phi)_{k'} + (\Phi^{\dagger}\Sigma_T\Phi)_{k'} + \frac{1}{4}\int_{E_{\gamma'}} dE \int_{S_{k'}} ds_{k'}\, \Phi^{\dagger}\Phi - \frac{1}{2}\int_{E_{\gamma'}} dE \int_{S_{k'}} ds_{k'}\, \Phi^{\dagger} D\nabla\Phi\cdot n_k \right\}} \tag{5.34}$$

In Eq. (5.34) γ' represents the thermal group if a 2-broad-group representation is used. The subscript k' represents the broad region in which the perturbation is located. The function f(t) gives the time-dependence of the poison with a magnitude of Σ_p. Values for the denominator of the expression on the right-hand side of Eq. (5.34) are given in Table 10 and values of $\Phi^{\dagger}\Phi$ for the thermal group are given in Figure 10. In this 1-dimensional representation of the UFTR it is not possible to calculate Σ_p directly but it can be determined indirectly by a combination of reactivity measurements and eigenvalue calculations. With the poison in a given position bring the reactor to critical

TABLE 10

DENOMINATOR OF THE EXPRESSION ON THE RIGHT-HAND SIDE OF EQUATION (5.34)

Model	Region	Denominator
2-broad-regions, 1-broad-group	1	5.5560737
	2	6.5642879
2-broad regions, 2-broad-groups	1	0.6864955
	2	0.7825920
3-broad-regions, 1-broad-group	1	4.8908975
	2	2.3391127
	3	5.9057559
3-broad-regions, 2-broad-groups	1	0.6320942
	2	0.3863222
	3	0.7489065

and determine the worth of the poison in that position by referring to a control rod calibration curve. Then, perform a SAIM calculation and have the program search for the value of the thermal group poison in the given position that will produce the measured reactivity. By repeating this procedure for several positions of the poison, it will be possible to determine Σ_p as a function of position. The function f(t) gives the position as a function of time, so the product of f(t) and Σ_p gives the variation of the poison as a function of time.

Coupled kinetics parameters for a 2-mode representation of the flux will not be given. Early in the study when it was thought that the discrepancy between the theoretical computations and the experimental measurements of the asymptotic decay constant was due to the weak coupling between the fuel regions, a 2-mode calculation of the flux was performed. Figure 12 shows a plot of the total flux and the partial fluxes resulting from an 18-group computation by the SAIM code. When the asumptotic decay constant was determined for several 2-mode, multi-broad-region,multi-broad-group representations, the values that resulted were in good agreement with the 1-point value. After the transverse buckling values were revised, the 2-mode calculations were not repeated. These computations are expensive and it was felt that the simpler 1-mode representation, multi-broad-region, multi-broad-group representation should be studied

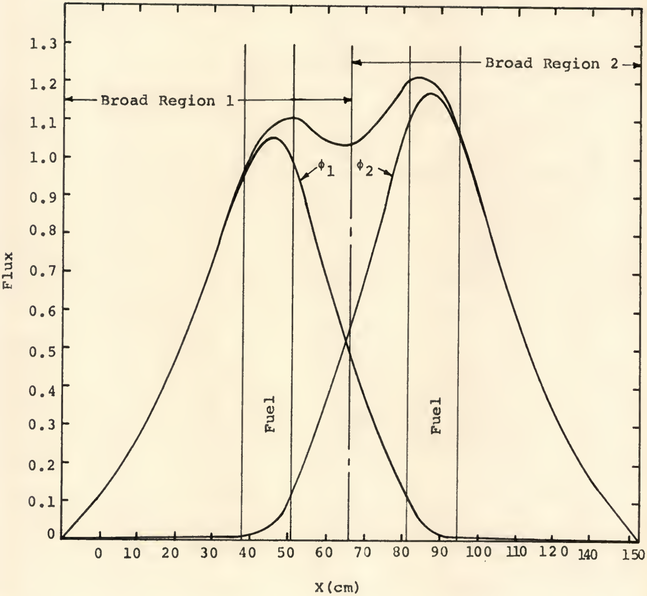

Figure 12. Flux in the UFTR as Computed by the SAIM Code; ϕ_i is the Flux Due to Neutrons Born in the i-th Region

more thoroughly before going to a more elaborate model. However, it should be noted that the codes for performing the modal calculations, namely SAIM and CØUPKIN, are already written.

Conclusions

The results of computer calculations of the flux in the University of Florida Training Reactor have been presented along with a brief discussion of the codes used to make these computations. Theoretical computations of the asymptotic decay constant of the prompt neutron die-away at delayed critical agreed favorably with the values determined by a pulsed neutron-beam experiment and a random noise experiment. Furthermore, it was shown that the 1-point-model kinetics equation very accurately predicts the value of this decay constant. For the UFTR the values $\beta_{eff} = 0.00703$ and $\Lambda = 247.5$ μsec were computed. A procedure for improving these values was suggested.

In addition to the results of the flux calculations, kinetics parameters have been presented for several different coupled point-model representations of the UFTR and a procedure for using these parameters to determine a space-dependent transfer function has been suggested.

CHAPTER VI

SUMMARY AND CONCLUSIONS

A general method of studying energy- and space-dependent reactor kinetics problems in terms of a nodal, or point-model, representation has been presented and established on a firm basis by deriving the pertinent set of equations from the general integro-differential form of the Boltzmann neutron transport equation. The formulation of the equations from first principles on the basis of a semidirect variational method guided the defining of coupling parameters in a consistent way. The derivation was so general as to permit the reduction of the space- , energy-, angle- and time-dependent reactor neutron field to any number of nodes that depend only on time. These nodes may represent the integrated neutron field divided into energy groups, configuration regions, or a combination of the two. Furthermore, the steady-state flux and adjoint flux from which the coupling parameters are computed may be represented by any number of eigenmodes.

For the sake of generality the coupled kinetics equation was derived in terms of the neutron transport equation; however, in order to facilitate the computation of the coupling parameters and to clarify the general treatment, formulas were given for computing the coupling parameters in terms of diffusion theory.

In connection with this work a number of computer codes were developed for use on the University of Florida IBM-709 computer. These codes have a wide range of applicability for studying both static and dynamic reactor physics problems and are valuable additions to the research facilities of the Nuclear Engineering Department.

Both a 4-group, 2-dimensional and an 18-group, 1-dimensional flux calculation for the University of Florida Training Reactor have been performed. A summary of these computations was presented in Chapter V. A complete listing of the printed output has been bound under separate cover. Also, punched output from these computer runs is filed in the IBM card storage room of the Nuclear Engineering Department. The cross-sections for the 18-group calculations are listed in the Appendix and those for the 4-group calculations are listed in Butterfield's thesis (But 65). This information will be valuable for future theoretical studies of the UFTR.

An exact computation of the asymptotic prompt neutron decay constant was used to check the accuracy of the theory presented in Chapter II. The decay constant predicted by several point-models ranging from a 1-point model to a 6-point model (3 regions and 2 groups) was computed. The value predicted by all of the point models was within

3 per cent of the value predicted by the exact computation. The results of this comparison give credence to the validity of the coupled kinetics formulation. Another important result of this comparison was the close agreement of the values predicted by the 1-point-model computation and the exact computation. This result indicates that the 1-point-model kinetics equation is sufficiently accurate to analyze neutron die-away measurements even in a reactor with weakly coupled fuel regions.

The following values were computed with the 18-group, 1-dimensional flux and adjoint flux:

$\beta_{eff} = 0.00703$

$\Lambda = 247.5\ \mu sec$

The exact computation of the asymptotic prompt neutron decay constant yielded a value of $-27.6\ sec^{-1}$ which is in fair agreement with measured values of -22.2 ± 0.5 (But 65) and $-29 \pm 5\ sec^{-1}$ (Kav 64). Suggestions were made for refining the theoretical computations. Of the two parameters, β_{eff} and Λ, the value for β_{eff} is by far the more accurate. It was shown in Chapters IV and V that the value for Λ is a sensitive function of the transverse buckling which is not very accurately known for the UFTR.

Multiple point-model representations of the reactor neutron field should find their greatest applicability in the study of transients and of the propagation of perturbations in a reactor with weakly coupled fuel regions. A general formula was derived in Chapter II for a region- and group-dependent transfer function and values for the parameters appearing in this transfer function were reported in Chapter V with the UFTR data.

APPENDIX

APPENDIX

Presented on the following pages are tables describing the neutronic properties of the UFTR for an 18-group diffusion theory model. These values are based on a 20 per cent enriched uranium fuel loading with a 3500 g U-235 critical mass.

TABLE A-1
ATOM DENSITIES
FOR THE UFTR (THO 61)
WITH 20 PERCENT U-235 FUEL

REGION	ELEMENT	DENSITY (ATOMS/CC)
2 AND 4	HYDROGEN	3.914(+22)
2 AND 4	U-235	1.069(+20)
2 AND 4	U-238	4.222(+20)
2 AND 4	ALUMINUM	1.997(+22)
1, 3 AND 5	GRAPHITE	8.025(+22)

NOTE NUMBER IN PARENTHESES INDICATES THE POWER OF 10 BY WHICH THE GIVEN VALUE IS TO BE MULTIPLIED.

TABLE A-2
GROUP BOUNDARIES
BY ENERGY AND BY LETHARGY

GROUP NUMBER	ENERGY (MEV) LOWER BOUNDARY	LETHARGY UPPER BOUNDARY
	10.0000000	0.0
1	6.0653066	0.5
2	3.6787944	1.0
3	2.2313016	1.5
4	4.9787068(-1)	3.0
5	1.8315639(-1)	4.0
6	1.1108996(-1)	4.5
7	6.7379470(-2)	5.0
8	4.0867715(-2)	5.5
9	2.4787522(-2)	6.0
10	1.5034392(-2)	6.5
11	9.1188197(-4)	7.0
12	5.5308437(-4)	7.5
13	3.3546263(-4)	8.0
14	1.2340980(-4)	9.0
15	4.5399930(-5)	10.0
16	6.1442123(-6)	12.0
17	6.8256035(-7)	16.5
18	0.0	INFINITY

NOTE NUMBER IN PARENTHESES INDICATES THE POWER OF 10 BY WHICH THE GIVEN VALUE IS TO BE MULTIPLIED.

TABLE A-3
VALUES OF THE DIFFUSION CONSTANT FOR 18 GROUPS

GROUP NUMBER	D (CM) GRAPHITE REGIONS 1 AND 5	D (CM) FUEL REGIONS 2 AND 4	D (CM) GRAPHITE REGION 3
1	5.17803	4.89794	5.02004
2	4.25305	3.92550	3.92556
3	2.51475	3.21046	2.51475
4	1.88733	2.66530	1.88733
5	1.84187	3.59117	1.14187
6	1.04608	2.52128	1.04045
7	0.97892	2.08773	0.97358
8	0.94844	2.03009	0.94303
9	0.96784	1.56574	0.96213
10	0.95491	1.67446	0.94917
11	0.94745	1.54715	0.94185
12	0.94705	1.76832	0.94207
13	0.94772	1.61025	0.93559
14	0.93653	1.45434	0.93372
15	0.93525	1.31442	0.93242
16	0.93480	1.19188	0.93196
17	0.93481	1.10335	0.93197
18	0.9155	0.3339	0.9155

TABLE A-4
VALUES OF THE ABSORPTION CROSS-SECTION FOR 18 GROUPS*

GROUP NUMBER	SIGMA ABS. (1/CM) FUEL REGIONS 2 AND 4
1	1.96230(-3)
2	7.17739(-4)
3	3.90592(-4)
4	2.52664(-4)
5	2.12427(-4)
6	4.88448(-4)
7	3.71221(-4)
8	1.05610(-3)
9	7.49251(-4)
10	6.78011(-4)
11	6.82464(-4)
12	1.13067(-3)
13	1.50298(-3)
14	1.20770(-3)
15	3.41225(-3)
16	5.57001(-3)
17	9.15107(-3)
18	6.798 (-2)

* THE ABSORPTION CROSS-SECTION FOR GRAPHITE IS NEGLIGIBLY SMALL FOR ALL GROUPS EXCEPT THE 18-TH. FOR GROUP NUMBER 18 THE ABSORPTION CROSS-SECTION IS 0.0002414 (1/CM) IN REGIONS 1, 3 AND 5.

NOTE NUMBER IN PARENTHESES INDICATES THE POWER OF 10 BY WHICH THE GIVEN VALUE IS TO BE MULTIPLIED.

TABLE A-5
VALUES OF NU*SIGMA FISSION AND CHI FOR 18 GROUPS

GROUP NUMBER	NU*SIGMA F (1/CM) FUEL REGIONS 2 AND 4	CHI
1	1.97505(-3)	0.02307
2	1.14457(-3)	0.10749
3	1.07598(-3)	0.20896
4	5.49440(-4)	0.52700
5	3.59160(-4)	0.10037
6	4.27290(-4)	0.01702
7	4.93640(-4)	0.00836
8	5.52730(-4)	0.00405
9	6.59660(-4)	0.00193
10	7.72190(-4)	0.00092
11	9.20170(-4)	0.00044
12	1.03196(-3)	0.00021
13	1.21542(-3)	0.00010
14	1.57819(-3)	0.00007
15	2.93795(-3)	0.00002
16	5.82172(-3)	0.00000
17	1.14071(-2)	0.00000
18	1.108 (-1)	0.00000

NOTE NUMBER IN PARENTHESES INDICATES THE POWER OF 10 BY WHICH THE GIVEN VALUE IS TO BE MULTIPLIED.

TABLE A-6
VALUES OF THE TOTAL SCATTERING CROSS-SECTION FOR 18 GROUPS

GROUP	SIGMA S (1/CM) GRAPHITE REG. 1 AND 5	SIGMA S (1/CM) FUEL REG. 2 AND 4	SIGMA S (1/CM) GRAPHITE REGION 3
FROM 1 TO 1	3.90153(-2)	2.74899(-2)	4.38674(-2)
FROM 1 TO 2	3.15875(-2)	1.88118(-2)	2.96291(-2)
FROM 2 TO 2	8.06147(-2)	4.20850(-2)	7.91725(-2)
FROM 1 TO 3	7.68348(-3)	1.26735(-2)	7.68348(-3)
FROM 2 TO 3	3.68585(-2)	3.04768(-2)	3.68585(-2)
FROM 3 TO 3	8.72161(-2)	6.53425(-2)	6.58929(-2)
FROM 1 TO 4	1.18153(-2)	2.28862(-2)	1.18153(-2)
FROM 2 TO 4	1.78686(-3)	3.53009(-2)	1.78686(-3)
FROM 3 TO 4	5.64191(-2)	6.99061(-2)	5.64191(-2)
FROM 4 TO 4	1.80676(-1)	1.41749(-1)	1.71616(-1)
FROM 1 TO 5	2.09026(-3)	4.62224(-3)	2.14524(-3)
FROM 2 TO 5	4.62731(-4)	6.87550(-3)	3.83732(-4)
FROM 3 TO 5	0.00000(-0)	1.23346(-2)	0.00000(-0)
FROM 4 TO 5	2.78330(-2)	5.63396(-2)	2.78330(-2)
FROM 5 TO 5	2.56359(-1)	1.91525(-1)	2.57912(-1)
FROM 1 TO 6	3.92817(-4)	5.08358(-4)	3.86840(-4)
FROM 2 TO 6	1.07059(-4)	1.13774(-4)	9.02281(-5)
FROM 3 TO 6	0.00000(-0)	2.45804(-3)	0.00000(-0)
FROM 4 TO 6	0.00000(-0)	1.26653(-2)	0.00000(-0)
FROM 5 TO 6	4.88148(-2)	7.99251(-2)	4.67188(-2)
FROM 6 TO 6	2.33307(-1)	2.02225(-1)	2.34703(-1)
FROM 1 TO 7	0.00000(-0)	3.00015(-4)	0.00000(-0)
FROM 2 TO 7	0.00000(-0)	6.79639(-4)	0.00000(-0)
FROM 3 TO 7	0.00000(-0)	1.47602(-3)	0.00000(-0)
FROM 4 TO 7	0.00000(-0)	7.41895(-3)	0.00000(-0)
FROM 5 TO 7	0.00000(-0)	4.57886(-2)	0.00000(-0)
FROM 6 TO 7	1.08064(-1)	1.46702(-1)	1.06603(-1)
FROM 7 TO 7	2.45931(-1)	2.22781(-1)	2.47263(-1)
FROM 1 TO 8	0.00000(-0)	1.78854(-4)	0.00000(-0)
FROM 2 TO 8	0.00000(-0)	4.08671(-4)	0.00000(-0)
FROM 3 TO 8	0.00000(-0)	8.90752(-4)	0.00000(-0)
FROM 4 TO 8	0.00000(-0)	4.50111(-3)	0.00000(-0)

NOTE NUMBER IN PARENTHESES INDICATES THE POWER OF 10 BY WHICH THE GIVEN VALUE IS TO BE MULTIPLIED.

TABLE A-6(CONTINUED)
VALUES OF THE TOTAL SCATTERING CROSS-SECTION FOR 18 GROUPS

GROUP	SIGMA S (1/CM) GRAPHITE REG. 1 AND 5	SIGMA S (1/CM) FUEL REG. 2 AND 4	SIGMA S (1/CM) GRAPHITE REGION 3
FROM 5 TO 8	0.00000(-0)	2.78243(-2)	0.00000(-0)
FROM 6 TO 8	0.00000(-0)	8.10891(-2)	0.00000(-0)
FROM 7 TO 8	1.15084(-1)	1.71677(-1)	1.13640(-1)
FROM 8 TO 8	2.54432(-1)	1.74121(-1)	2.55954(-1)
FROM 1 TO 9	0.00000(-0)	1.07234(-4)	0.00000(-0)
FROM 2 TO 9	0.00000(-0)	2.46426(-4)	0.00000(-0)
FROM 3 TO 9	0.00000(-0)	5.38374(-4)	0.00000(-0)
FROM 4 TO 9	0.00000(-0)	2.73058(-3)	0.00000(-0)
FROM 5 TO 9	0.00000(-0)	1.69001(-2)	0.00000(-0)
FROM 6 TO 9	0.00000(-0)	4.92600(-2)	0.00000(-0)
FROM 7 TO 9	0.00000(-0)	9.67055(-2)	0.00000(-0)
FROM 8 TO 9	1.18731(-1)	1.90547(-1)	1.17209(-1)
FROM 9 TO 9	2.49940(-1)	2.72987(-1)	2.51500(-1)
FROM 2 TO 10	0.00000(-0)	1.49252(-4)	0.00000(-0)
FROM 3 TO 10	0.00000(-0)	3.26556(-4)	0.00000(-0)
FROM 4 TO 10	0.00000(-0)	1.66030(-3)	0.00000(-0)
FROM 5 TO 10	0.00000(-0)	1.02846(-2)	0.00000(-0)
FROM 6 TO 10	0.00000(-0)	2.99806(-2)	0.00000(-0)
FROM 7 TO 10	0.00000(-0)	5.88598(-2)	0.00000(-0)
FROM 8 TO 10	0.00000(-0)	1.10210(-1)	0.00000(-0)
FROM 9 TO 10	1.16811(-1)	2.08711(-1)	1.15233(-1)
FROM 10 TO 10	2.52671(-1)	1.67039(-1)	2.54247(-1)
FROM 3 TO 11	0.00000(-0)	1.95501(-4)	0.00000(-0)
FROM 4 TO 11	0.00000(-0)	9.95483(-4)	0.00000(-0)
FROM 5 TO 11	0.00000(-0)	6.16971(-3)	0.00000(-0)
FROM 6 TO 11	0.00000(-0)	1.79866(-2)	0.00000(-0)
FROM 7 TO 11	0.00000(-0)	3.53136(-2)	0.00000(-0)
FROM 8 TO 11	0.00000(-0)	6.61233(-2)	0.00000(-0)
FROM 9 TO 11	0.00000(-0)	1.23482(-1)	0.00000(-0)
FROM 10 TO 11	1.18091(-1)	2.18606(-1)	1.16503(-1)
FROM 11 TO 11	2.54747(-1)	1.86686(-1)	2.56316(-1)
FROM 4 TO 12	0.00000(-0)	6.07499(-4)	0.00000(-0)

NOTE NUMBER IN PARENTHESES INDICATES THE POWER OF 10 BY WHICH THE GIVEN VALUE IS TO BE MULTIPLIED.

TABLE A-6(CONTINUED)
VALUES OF THE TOTAL SCATTERING CROSS-SECTION FOR 18 GROUPS

GROUP	SIGMA S (1/CM) GRAPHITE REG. 1 AND 5	SIGMA S (1/CM) FUEL REG. 2 AND 4	SIGMA S (1/CM) GRAPHITE REGION 3
FROM 5 TO 12	0.00000(-0)	3.76643(-3)	0.00000(-0)
FROM 6 TO 12	0.00000(-0)	1.09808(-2)	0.00000(-0)
FROM 7 TO 12	0.00000(-0)	2.15594(-2)	0.00000(-0)
FROM 8 TO 12	0.00000(-0)	4.03698(-2)	0.00000(-0)
FROM 9 TO 12	0.00000(-0)	7.53899(-2)	0.00000(-0)
FROM 10 TO 12	0.00000(-0)	1.31674(-1)	0.00000(-0)
FROM 11 TO 12	1.19023(-1)	2.30215(-1)	1.17444(-1)
FROM 12 TO 12	2.56700(-1)	1.94328(-1)	2.57521(-1)
FROM 5 TO 13	0.00000(-0)	2.27647(-3)	0.00000(-0)
FROM 6 TO 13	0.00000(-0)	6.63709(-3)	0.00000(-0)
FROM 7 TO 13	0.00000(-0)	1.30313(-2)	0.00000(-0)
FROM 8 TO 13	0.00000(-0)	2.44013(-2)	0.00000(-0)
FROM 9 TO 13	0.00000(-0)	4.55693(-2)	0.00000(-0)
FROM 10 TO 13	0.00000(-0)	7.95909(-2)	0.00000(-0)
FROM 11 TO 13	0.00000(-0)	1.36850(-1)	0.00000(-0)
FROM 12 TO 13	1.18791(-1)	2.40694(-1)	1.17966(-1)
FROM 13 TO 13	2.57314(-1)	1.99820(-1)	2.58124(-1)
FROM 6 TO 14	0.00000(-0)	6.51449(-3)	0.00000(-0)
FROM 7 TO 14	0.00000(-0)	1.27907(-2)	0.00000(-0)
FROM 8 TO 14	0.00000(-0)	2.39510(-2)	0.00000(-0)
FROM 9 TO 14	0.00000(-0)	4.47287(-2)	0.00000(-0)
FROM 10 TO 14	0.00000(-0)	7.81236(-2)	0.00000(-0)
FROM 11 TO 14	0.00000(-0)	1.34328(-1)	0.00000(-0)
FROM 12 TO 14	0.00000(-0)	2.31363(-1)	0.00000(-0)
FROM 13 TO 14	1.19059(-1)	3.90856(-1)	1.18247(-1)
FROM 14 TO 14	3.17211(-1)	3.21039(-1)	3.18534(-1)
FROM 7 TO 15	0.00000(-0)	4.65979(-3)	0.00000(-0)
FROM 8 TO 15	0.00000(-0)	8.72568(-3)	0.00000(-0)
FROM 9 TO 15	0.00000(-0)	1.62953(-2)	0.00000(-0)
FROM 10 TO 15	0.00000(-0)	2.84618(-2)	0.00000(-0)

NOTE NUMBER IN PARENTHESES INDICATES THE POWER OF 10 BY WHICH THE GIVEN VALUE IS TO BE MULTIPLIED.

TABLE A-6(CONTINUED)
VALUES OF THE TOTAL SCATTERING
CROSS-SECTION FOR 18 GROUPS

GROUP	SIGMA S (1/CM) GRAPHITE REG. 1 AND 5	SIGMA S (1/CM) FUEL REG. 2 AND 4	SIGMA S (1/CM) GRAPHITE REGION 3
FROM 11 TO 15	0.00000(-0)	4.89381(-2)	0.00000(-0)
FROM 12 TO 15	0.00000(-0)	8.42902(-2)	0.00000(-0)
FROM 13 TO 15	0.00000(-0)	1.40782(-1)	0.00000(-0)
FROM 14 TO 15	6.00051(-2)	3.15045(-1)	5.86778(-2)
FROM 15 TO 15	3.17686(-1)	3.24190(-1)	3.19007(-1)
FROM 8 TO 16	0.00000(-0)	4.41453(-3)	0.00000(-0)
FROM 9 TO 16	0.00000(-0)	8.24424(-3)	0.00000(-0)
FROM 10 TO 16	0.00000(-0)	1.43996(-2)	0.00000(-0)
FROM 11 TO 16	0.00000(-0)	2.47591(-2)	0.00000(-0)
FROM 12 TO 16	0.00000(-0)	4.26447(-2)	0.00000(-0)
FROM 13 TO 16	0.00000(-0)	7.12258(-2)	0.00000(-0)
FROM 14 TO 16	0.00000(-0)	1.58284(-1)	0.00000(-0)
FROM 15 TO 16	6.00922(-2)	4.28848(-1)	5.87692(-2)
FROM 16 TO 16	3.47573(-1)	4.89256(-1)	3.49149(-1)
FROM 9 TO 17	0.00000(-0)	1.27500(-3)	0.00000(-0)
FROM 10 TO 17	0.00000(-0)	2.22695(-3)	0.00000(-0)
FROM 11 TO 17	0.00000(-0)	3.82909(-0)	0.00000(-0)
FROM 12 TO 17	0.00000(-0)	6.59516(-3)	0.00000(-0)
FROM 13 TO 17	0.00000(-0)	1.10153(-2)	0.00000(-0)
FROM 14 TO 17	0.00000(-0)	2.44792(-2)	0.00000(-0)
FROM 15 TO 17	0.00000(-0)	6.59962(-2)	0.00000(-0)
FROM 16 TO 17	3.04048(-2)	3.34482(-1)	2.88290(-2)
FROM 17 TO 17	3.64078(-1)	6.62588(-1)	3.65784(-1)
FROM 10 TO 18	0.00000(-0)	2.50141(-5)	0.00000(-0)
FROM 11 TO 18	0.00000(-0)	4.30100(-5)	0.00000(-0)
FROM 12 TO 18	0.00000(-0)	7.40797(-5)	0.00000(-0)
FROM 13 TO 18	0.00000(-0)	1.23729(-4)	0.00000(-0)
FROM 14 TO 18	0.00000(-0)	2.74961(-4)	0.00000(-0)
FROM 15 TO 18	0.00000(-0)	7.41299(-4)	0.00000(-0)
FROM 16 TO 18	0.00000(-0)	3.74469(-3)	0.00000(-0)
FROM 17 TO 18	1.38991(-2)	1.71589(-1)	1.21929(-2)

NOTE NUMBER IN PARENTHESES INDICATES THE POWER OF 10 BY WHICH THE GIVEN VALUE IS TO BE MULTIPLIED.

TABLE A-7
AVERAGE INVERSE SPEED
FOR 18 GROUPS

GROUP NUMBER	1/V (SEC/CM) GRAPHITE REG. 1 AND 5	1/V (SEC/CM) FUEL REG. 2 AND 4	1/V (SEC/CM) GRAPHITE REGION 3
1	2.76516(-10)	2.69235(-10)	2.72153(-10)
2	3.34239(-10)	3.41406(-10)	3.38431(-10)
3	4.38438(-10)	4.33819(-10)	4.39308(-10)
4	7.63897(-10)	7.30522(-10)	7.59417(-10)
5	1.35426(- 9)	1.33199(- 9)	1.34820(- 9)
6	1.93397(- 9)	1.93249(- 9)	1.93213(- 9)
7	2.47999(- 9)	2.48889(- 9)	2.47783(- 9)
8	3.18853(- 9)	3.17777(- 9)	3.18564(- 9)
9	4.09336(- 9)	4.10976(- 9)	4.08945(- 9)
10	5.25631(- 9)	5.24689(- 9)	5.25136(- 9)
11	6.74941(- 9)	6.73959(- 9)	6.74308(- 9)
12	8.66281(- 9)	8.65765(- 9)	8.65859(- 9)
13	1.11235(- 8)	1.11186(- 8)	1.11182(- 8)
14	1.65739(- 8)	1.65555(- 8)	1.65352(- 8)
15	2.73271(- 8)	2.72937(- 8)	2.72633(- 8)
16	6.34061(- 8)	6.30796(- 8)	6.28346(- 8)
17	4.90212(- 7)	4.77779(- 7)	4.74673(- 7)
18	5.05351(- 6)	4.90765(- 6)	5.05351(- 6)

NOTE NUMBER IN PARENTHESES INDICATES THE POWER OF 10 BY WHICH THE GIVEN VALUE IS TO BE MULTIPLIED.

TABLE A-8
AVERAGE ENERGY
FOR 18 GROUPS

GROUP NUMBER	E (MEV) GRAPHITE REG. 1 AND 5	E (MEV) FUEL REG. 2 AND 4	E (MEV) GRAPHITE REGION 3
1	6.89044(- 0)	7.32742(- 0)	7.15225(- 0)
2	4.76849(- 0)	4.56614(- 0)	4.65050(- 0)
3	2.76865(- 0)	2.83051(- 0)	2.75700(- 0)
4	1.02578(- 0)	1.12520(- 0)	1.03842(- 0)
5	3.04352(- 1)	3.14496(- 1)	3.07130(- 1)
6	1.42451(- 1)	1.42671(- 1)	1.42724(- 1)
7	8.66308(- 2)	8.60053(- 2)	8.67827(- 2)
8	5.24064(- 2)	5.27636(- 2)	5.25023(- 2)
9	3.17984(- 2)	3.15414(- 2)	3.18598(- 2)
10	1.92843(- 2)	1.93540(- 2)	1.93209(- 2)
11	1.16959(- 2)	1.17303(- 2)	1.17181(- 2)
12	7.09988(- 3)	7.10841(- 3)	7.10686(- 3)
13	4.30612(- 3)	4.30993(- 3)	4.31025(- 3)
14	2.03142(- 3)	2.03609(- 3)	2.04120(- 3)
15	7.47242(- 4)	7.49105(- 4)	7.50832(- 4)
16	1.65793(- 4)	1.67736(- 4)	1.69125(- 4)
17	6.25036(- 6)	6.71803(- 6)	6.87922(- 6)
18	4.73735(- 8)	5.50230(- 8)	4.73735(- 8)

NOTE NUMBER IN PARENTHESES INDICATES THE POWER OF 10 BY WHICH THE GIVEN VALUE IS TO BE MULTIPLIED.

LIST OF REFERENCES

Arg 63 Argonne National Laboratory, *Reactor Physics Constants*, *U. S. Atomic Energy Commission Report No.* ANL-5800, Second Edition (1963).

Ave 58a R. Avery, "Theory of Coupled Reactors," *Proceedings of the Second United Nations International Conference on the Peaceful Uses of Atomic Energy*, Geneva, P/1858 (1958).

Ave 58b R. Avery, *et al.*, "Coupled Fast-Thermal Power Breeder Critical Experiment," *Proceedings of the Second International Conference on the Peaceful Uses of Atomic Energy*, Geneva, P/632 (1958).

Bal 59 G. C. Baldwin, "Kinetics of a Reactor Composed of Two Loosely Coupled Cores," *Nuclear Science and Engineering 6*, 320-327 (1959).

Bal 62 D. C. Baller, *The FAIM Code, a Multigroup, One-Dimensional Diffusion Equation Code*, *U. S. Atomic Energy Commission Report No.* NAA-Sr-7137 (1962).

Boy 64 A. R. Boynton and R. E. Uhrig, "Evaluation of Two-Region-Reactor Parameters by Random Noise Measurements," *Nuclear Science and Engineering*, *18*, 220-229 (1964).

But 64 L. D. Butterfield, Reactor Supervisor, Nuclear Engineering Department, University of Florida Personal Communication (1964).

But 65 L. D. Butterfield, "Pulsed Neutron Measurements in the University of Florida Training Reactor," Unpublished M.S.E. Thesis, University of Florida (1965).

Cha 61 R. H. Chastain, "Transfer Function of the University of Florida Training Reactor," Unpublished M.S.E. Thesis, University of Florida (1961).

Coc 65a R. G. Cockrell, "A Description of the SAIM Code, a Multigroup, One-Dimensional Diffusion Equation Code," Nuclear Engineering Department Internal Report (1965).

Coc 65b R. G. Cockrell, "A Description of CØUPKIN, a Code for Computing Coupled Kinetics Parameters," Nuclear Engineering Department Internal Report (1965).

Dou 61 D. E. Dougherty and C. N. Shen, "The Space-Time Neutron Kinetic Equations Obtained by the Semidirect Variational Method," U. S. Atomic Energy Commission Report No. KAPL-2000-16, Section IV (1961).

Dun 58 J. M. Duncan, *University of Florida Training Reactor Hazards Summary Report*, *Bulletin Series No. 99, Vol. XII, No. 10*, Florida Engineering and Industrial Experiment Station (1958).

Gla 52 S. Glasstone and M. C. Edlund, *The Elements of Nuclear Reactor Theory*, D. Van *Nostrand Company, Inc., Princeton, N. J.* (1952).

Hen 55 A. F. Henry, "Computation of Parameters Appearing in the Reactor Kinetics Equations," U. S. Atomic Energy Commission Report No. WAPD-142 (1955).

Hil 52 F. B. Hildebrand, *Methods of Applied Mathematics*, Prentice-Hall, *Inc., Englewood Cliffs, N. J. (19*52).

Joa 61 G. D. Joanou and J. S. Dudek, "GAM-I: A Consistent P_1 Multigroup Code for the Calculation of Fast Neutron Spectra and Multigroup Constants," U. S. Atomic Energy Commission Report No. GA-1850 (1961).

Kap 52 W. Kaplan, *Advanced Calculus*, Addison-Wesley Publishing *Company, Inc., Rea*ding, Mass. (1952).

Kap 62 S. Kaplan, R. Ewen, N.J. Curlee and S. Margolis, "Space-Time Kinetics," *Naval Reactors Physics Handbook*, Section 5.4 *(1962)*.

Kav 64 S. R. Kavipurapu, "Energy and Spatially Dependent Impulse Response and Transfer Functions of Nuclear Systems," Ph.D. Dissertation, University of Florida (1964).

Klo 62 H. Klose, *et al.*, *Proceedings of the Brookhaven Conference on Neutron Thermalization*, U. S. Atomic Energy Commission Report No. BNL-719, Vol. III (1962).

Kyl 65 C. D. Kylstra and R. E. Uhrig, "Spatially Dependent Transfer Function for Nuclear Systems," *Nuclear Science and Engineering* *22*, 191-205 (1965).

Lal 61 G. Lalande, *Industries Atomiques* *516* (1961).

Lan 60 L. D. Landau and E. M. Lifshitz, *Mechanics*, Addison-Wesley Publishing Company, Inc., Reading, Mass. (1960).

Len 56 D. H. Lennox and C. N. Kelber, "Summary Report on the Hazards of the Argonaut Reactor," U. S. Atomic Energy Commission Report No. ANL-5647 (1956).

Meg 60 R. V. Meghreblian and D. K. Holmes, *Reactor Analysis*, McGraw-Hill Book Company, Inc., New York, N. Y. (1960).

Mil 49 W. E. Milne, *Numerical Calculus*, Princeton University Press, Princeton, N. J. (1960).

Mor 53 P. M. Morse and H. Feshbach, *Methods of Theoretical Physics, Part I*, McGraw-Hill Book Company, Inc., New York, N. Y. (1953).

Oha 65 M. J. Ohanian, Assistant Professor, Nuclear Engineering Department, University of Florida, Personal Communication (1965).

Par 63 B. M. Parlett, "NU EIG4-Eigenvalues of Complex Matrices," A.E.C. Computing and Applied Mathematics Center, Courant Institute of Mathematical Sciences, New York University, New York,(1963).

Per 52 Sam Perlis, *Theory of Matrices*, Addison-Wesley Publishing Company, Inc., Reading, Mass. (1952).

Per 60 R. Perez-Belles, *et al.*, "Pulsed-Neutron-Source Measurements at the Bulk Shielding Facility," *Neutron Physics Annual Progress Report for the Period Ending September 1, 1960*, Oak Ridge National Laboratory (1960).

Per 62 R. B. Perez, "Lectures on Perturbation Theory, Reactor Kinetics and Pulsed Neutron Techniques," Department of Nuclear Engineering, University of Florida, Gainesville, Florida, Unpublished notes written in (1962).

Per 65 R. B. Perez and R. S. Booth, "Excitation of Neutron Waves by Modulated and Pulsed Sources," *Proceedings of the Symposium on Pulsed Neutron Research Sponsored by the International Atomic Energy Agency*, Karlsruhe, Germany (1965).

Ros 61 D. J. Rose and M. Clark, Jr., *Plasmas and Controlled Fission*, John Wiley and Sons, Inc., New York, N. Y. (1961).

Sag 64 M. Sagot, *et al.*, *Proceedings of the Symposium on Exponential and Critical Experiments*, International Atomic Energy Agency *3* (1964).

Sal 64 S. Salah, "Neutron Spectrum Measurements in Heterogeneous Media," Ph.D. Dissertation, University of Florida (1964).

Sea 64 R. L. Seale, *Coupled Core Reactors*, U. S. Atomic Energy Commission Report No. LAMS-2967 (1964).

Sel 59 D. S. Selengut, "Variational Analysis of Multi-Dimensional Systems," U. S. Atomic Energy Commission Report No. HW-59126, 89-124 (1959).

Shu 60 R. H. Shudde and J. Dyer, "TEMPEST, a Neutron Thermalization Code," North American Aviation Program Description (1960).

Shu 61 M. A. Shultz, *Control of Nuclear Reactors and Power Plants*, McGraw-Hill Book Company, Inc., New York, N. Y. (1961).

Sjö 56 N. Sjöstrand, "Measurements of a Subcritical Reactor Using a Pulsed Neutron Source," Arkiv for Fysik 11:233 (1956).

Spi 59 M. R. Spiegel, *Vector Analysis*, Schaum Publishing Company, New York, N. Y. (1959).

Sta 62 E. Starr and G. A. Price, *Proceedings of the Brookhaven Conference on Neutron Thermalization*, U. S. Atomic Energy Commission Report No. BNL-719, Vol. III (1962).

Ste 58 J. C. Stewart, "Interaction of Weakly Coupled Reactor Systems, with Application to the Convergatron," *Proceedings of the Second International Conference on the Peaceful Uses of Atomic Energy*, Geneva, P/632 (1958).

Tho 61 C. A. Thompson, "Neutron Flux Calculations for a Graphite Moderated Twenty Per Cent Enriched Reactor," Unpublished M.S.E. Thesis, University of Florida (1961).

Tob 62 M. L. Tobias and T. B. Fowler, "The Twenty Grand Program for the Numerical Solution of Few-Group Neutron Diffusion Equations in Two Dimensions," U. S. Atomic Energy Commission Report No. ORNL-3200 (1962).

Wei 58 A. M. Weinberg and E. P. Wigner, *The Physical Theory of Neutron Chain Reactors*, The University of Chicago Press, Chicago, Ill. (1958).

Wyl 60 C. R. Wylie, Jr., Advanced *Engineering Mathematics*, McGraw-Hill Book Company, Inc., New York, N. Y., Second Edition (1960).

BIOGRAPHICAL SKETCH

Robert Gifford Cockrell was born in Birmingham, Alabama on August 21, 1937. His parents are Mr. and Mrs. Charles Wilbur Cockrell. The author married the former Bobbye June Hawkins of Sparta, Tennessee on June 6, 1959. He received the degree of Bachelor of Science in Engineering Physics (with Special Distinction) from the University of Oklahoma in June of 1962 and the degree of Master of Science in Engineering from the University of Florida in June of 1963.

During three years of his graduate work the author held an Atomic Energy Commission Special Fellowship in Nuclear Science and Engineering. He is a Registered Professional Engineer-in-Training in the State of Oklahoma and a student member of the American Nuclear Society.

This dissertation was prepared under the direction of the chairman of the candidate's supervisory committee and has been approved by all members of that committee. It was submitted to the Dean of the College of Engineering and to the Graduate Council, and was approved as partial fulfillment of the requirements for the degree of Doctor of Philosophy.

August 14, 1965

R Martin
Dean, College of Engineering

Dean, Graduate School

Supervisory Committee:

Chairman

G R Dalton (per THP)

RG Selfridge